PETROLOGY AND GEOCHEMISTRY OF THE MELANGE ZONE AND SOUTHERN AMPHIBOLITE BELT ROCKS FROM GANTAR AREA, ALLAI-KOHISTAN, HAZARA, N.PAKISTAN.

Thesis presented for the degree
of Master of Philosophy at the
University of Peshawar.

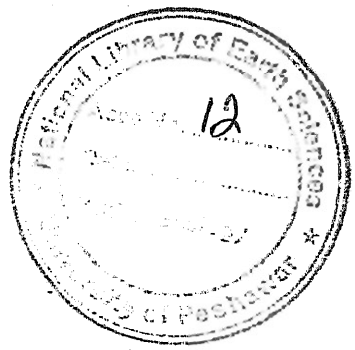

BY

Mohammad Zahid Khan

National Centre of Excellence in Geology
University of Peshawar

September, 1991.

CONTENTS

ACKNOWLEDGEMENTS

The author wishes to express his profound gratitude to Dr. Majid (Chairman and Professor department of geology) and Dr. S. Hamidullah (Assistant professor in NCE geology), the thesis advisors for their valuable suggestions, useful discussion of various problems, critical review of manuscript and supervision of thesis.

Due regards are extended to Dr. Qasim Jan (Director and Professor in NCE geology), for his kind advises, fruitful discussions, providing concerned literature and financial assistance in the field.

Mr. Anwar Hussain and Nasir Munawar Aziz, under graduate students in the Department of Geology, are gratefully acknowledged for providing assistance in many ways, particularly in helping the typing of final manuscript.

A note of thanks is also extended to Mr. Fazal Ahmad for drafting various figures and maps.

LIST OF FIGURES

LIST OF TABLES

ABSTRACT

Petrographic and geochemical study was performed for the Kohistan Island arc (KIA) rocks, Main Mantle Thrust (MMT) melange zone and Indian plate rocks at Gantar and Kalalota, Allai Kohistan, Hazara, in order to envisage the petrogenetic history of these rocks. Field and petrographic data show that the KIA is composed of amphibolites (mainly epidote amphibolites) together with hornblende pegmatite. The melange zone includes blue schist, green schist, meta-gabbro/norite, ultramafic and pillow lavas while the Indo-Pak plate comprises quartz-muscovite-chlorite-carbonate schist, quartz-actinolite schist, calcareous schist, graphitic schist and siliceous marble.

Amphibolites of the Kohistan arc are derived mainly from the basic magma of non-alkaline characters (transitional between tholeiitic and calc-alkaline) through crystallization differentiation of ferro-magnesium minerals with plagioclase. This protolithic material was then subjected to a metamorphism of amphibolites facies followed by retrogression into epidote amphibolite facies and green schist facies.

Mineral chemistry of amphibolites reflects maximum metamorphic temperature i.e.600 C for tschermakitic hornblende and 500 C for the actinolite under a metamorphic PH2O of 4-5Kb. The hornblende pegmatite appears to be of possible metasomatic origin.

Lavas occurring North East of the Gantar and Kalalota show fractionation trend controlled by ferro-magmesium minerals and plagioclase similar to those shown by amphibolites, however, these lavas indicate tholeiitic affinities rather than transitional character displayed by amphibolites.

The gabbro-noritic rocks together with ultramafic rocks from Shergarh Sar area indicate character of ophiolitic cumulates and a fractionation history controlled by olivine, pyroxene and plagioclase.

The green schist indicate a probable igneous parentage and its glaucophane together with that of the blue schist reflect a maximum PH2O of 7Kb whereas the actinolite of green schist encompasses a PH2O of 5Kb. A blue schist facies metamorphism followed by retrogression into green schist facies are suggested for these rocks.

It is also concluded that the mafic/ ultramafic rocks, meta-gabbro/norites, blue schist, pillow lavas and other basic rocks (metamorphosed to green schist) envision the normal ophiolitic sequence being offset by intensive multiple episodes of tectonic deformations (subducting and obducting environment).

CHAPTER 1 INTRODUCTION

General

The Kohistan Island arc in Northern Pakistan is one of the world-wide known geological features and is considered as a fossil island arc, of possible early Cretaceous age (Tahirkheli, 1979). The general rock sequence from North towards South established in Kohistan is (a) Chalt ophiolitic Melange, (b) Yasin group, (c) Rakaposhi volcanic complex, (d) Ghizar molasses, (e) Ladakh intrusive, (f) Dir group, (g) Kalam group, (h) Jeshai diorites, (i) the Chilas complex, (j) the Southern amphibolite belt,(k) Garnet granulites, (l) the Jijal complex and (m) the Melange zone rocks (blue schist) along MMT (see Jan and Tahirkheli, 1979; Coward et al., 1982 ; Bard et al., 1980).

The southern amphibolite belt also known as the Kamila amphibolite comprises a great variety of rocks including dunite, peridotite, pyroxenite, hornblendites, metapillows, olivine-gabbro, norites, diorites , tonalites, trondhjemites, granites, hornblende-pegmatites, granitic pegmatites, aplite and different types of veins in addition to amphibolites. The southern amphibolite extends for more than 350 km from Nanga parbat (East) towards Afghanistan (west). The belt attains a maximum width about 50 km in Indus valley (Jan, 1991; Hamidullah and Hussain, 1991 in press).

Lithologically and structurally the amphibolite belt is a complex sequence, in which, in addition to compositionally highly varied types of rocks, it also reflects the history of multiple episodes of metamorphism and deformation (Bard, 1983; Coward et

al., 1982, 1986). Earlier workers like Jan (1979, 1988, 1991), on the basis of field, petrographic character and preliminary chemical data, the amphibolite is considered as (a) mainly massive homogeneous with local banding , indicating igneous plutonic character (b) chemical character corresponding to basic plutonic and volcanic tholeiitic to calc-alkaline character (c) metamorphic episodes indicating those of amphibolite facies, epidote amphibolite facies and upper green schist facies. (d) A possible metasomatic origin for hornblendites, (e) Intrusive character of the diorites, meta -gabbros, granitic rocks, dykes, veins, and occurrence of pillow-lavas and (g) the presence of kaolinite (clay mineral) forming after the alteration of granites in the amphibolites belt .

THE MELANGE ZONE:

The melange zone rocks along the main mantle thrust (MMT) have also been investigated by several workers (Desio and Shams, 1980 ; Shah, 1986; Jan, 1988, 1991). In Allai-Kohistan across the Indus S-E of Jijal and 30 km NE of Shangla, Majid and Shah (1985) have found a thick melange zone separating, amphibolites of the Kohistan arc from gneiss of the Indian plate. The melange consist of ultramafic and volcanic rocks, greenschist, metagraywackes, limestone and chert. The melange at Shangla-Mingora has been divided by Kazmi et al. (1984) from South to North into, (a) Mingora ophiolite melange, b) The Charbagh green schist melange and (c) The Shangla blue schist melange.

The talc carbonate schist contains emerald in Mingora, Chro-

mite and asbestose at various other localities.

THE INDO-PAKISTAN PLATE

South of MMT are the Salkhalas series of Indian subcontinent, have been placed as the oldest unit of the Lesser Himalayas by Tahirkhali (1979) and comprises dominantly of pelitic schist together with graphitic schist. It has type section in Kashmir and has not been found in direct association with the MMT, nevertheless, several thick graphitic patches occur in the close vicinity of MMT. However, Salkhalas has been found in direct contact with MMT in the study area at Narsuk, Allai Kohistan (Fig.1). Recently Tahirkhali (1991 in press) divided Salkhalas into two fold divisions Rattu formation (upper Salkhalas) and Burgiwala formation (lower Salkhalas).

The Gantar and Kalalota (thesis area) Allai Kohistan, is lying east of river Indus, covering about 30 Km area between latitude 34° 50′N to 34° 53′N and longitude 73° 5′E to 73° 10′E (Topo-sheet No:43F/1). It is bounded by main Allai khwar, and is easily accessible from the Karakuram high way by an unmetalled road (about 30 Km long) from Thakot to Bana. Khargarai is the highest peak with an elevation 8000 feet, followed by Palang peak (Fig.1).

1.2 TECTONIC SETTING:

Northern Pakistan is the junction point among the best known mountain chains of the world, namely, the Himalaya, Karakoram and Hindukush.The Indus suture, which separates the Indian plate from the Eurasian plate Gansser (1980) is further divided westwards in

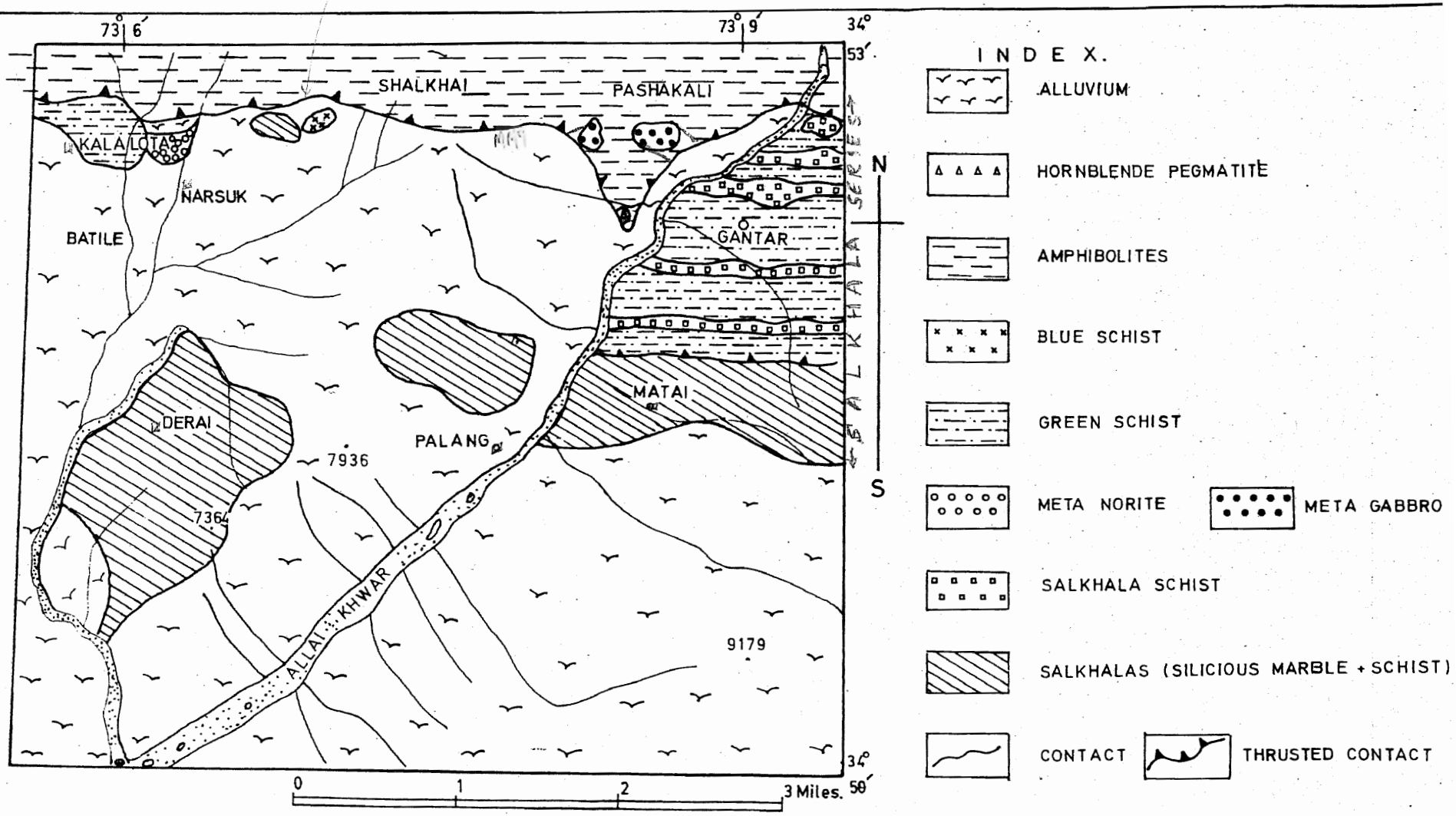

Fig:- 1. GEOLOGICAL MAP OF GANTAR, KALALOTA AND SURROUNDING AREA OF ALLAI KOHISTAN.

the Northern Pakistan into two (Fig.2), Northern megashear or main Karakoram thrust (MKT) and main Mantle thrust (MMT) or the southern suture zone. (Tahirkheli, 1979; Bard et al,.1980; Bard, 1983).

The MKT marks the boundary between the Kohistan sequence and the Asian continent (Fig. 2, after Searle et al,. 1989). Whereas MMT separates the Cretaceous Kohistan Arc from the Indian plate which contains a wide variety of rocks ranging from Late Precambrian pelites and Cambrian granites (Lefort et al,. 1980) to Paleozoic-Mesozoic sediments (Coward et al., 1986).

The MMT extends from Ladakh through Northern Pakistan to Eastern Afghanistan, covering about 1000km distance and making a sharp loop around the Nanga Parbat called Nanga Parbat Haramoosh syntaxes (see Fig.2). This suture is expressed as intensively deformed and display parallel schistosity. (coward et al., 1986). The Kohistan sequence is sandwich between the two major maga-sheares (i.e MMT and MKT), is considered as separating the crust and the mantle of an obducted Island Arc. (Bard et al., 1980) Jan and Kempe (1973), Tahirkhali(1979), Klootwijk (1979) and Hamidullah and Jan (1987) envisage a calc-alkaline character, typical of continental orogenic belt and Island Arc to the rocks of Kohistan sequence.

1.3 PREVIOUS WORK:

A few years back very little was known about the geology of Allai Kohistan Hazara, because of inaccessibility of the area. It was the mid-seventies when the first group started work on the mentioned area.

of workers?

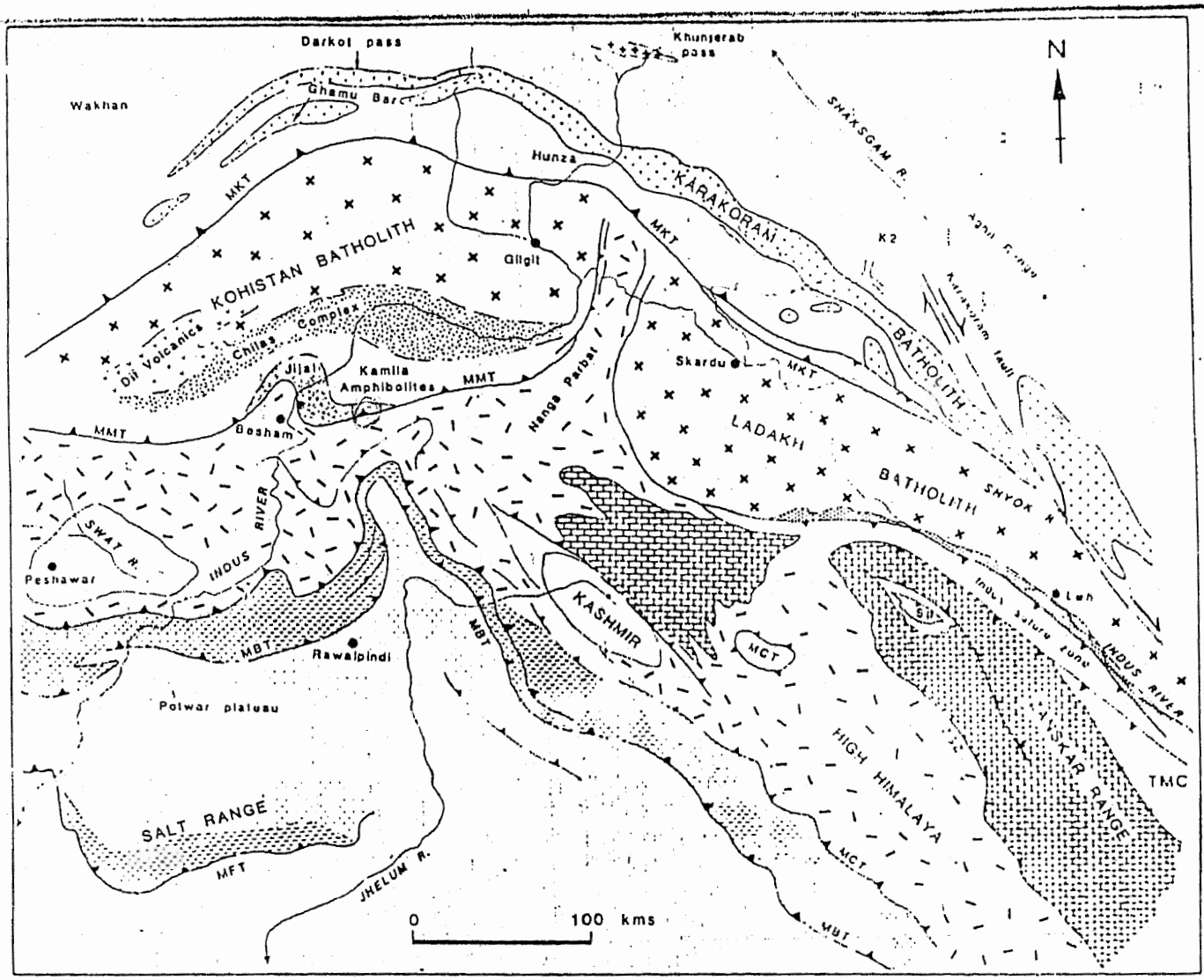

Figure 2. Geologic sketch map of the western Himalaya and Karakoram. The Baltoro and Biafo Glaciers are shown south and west of K2. MKT = Main Karakoram Thrust; MMT = Main Mantle Thrust; MCT = Main Central Thrust; MBT = Main Boundary Thrust; MFT = Main Frontal Thrust; ZSZ = Zanskar Shear Zone; TMC = Tso Morari complex; Sp = Spontang Ophiolite. Phanerozoic sedimentary rocks of the Indian continental margin in the Zanskar Range (bricks) lie structurally above the High Himalayan gneisses and granites (stipple). The Kohistan-Ladakh batholith (large crosses) is bounded along the south by the Indus suture zone and MMT and along the north by the Shyok suture zone or the MKT. The composite Karakoram batholith is shown in small crosses and the Khunjerab pass granite plutons is shown with larger crosses in the far north.

Hamidullah et al. (1977) and Yosafzai et al.(1977) presented a preliminary account on the petrography and field relationship of different rocks units of the Shergar Sar area and the surrounding area in Allai Kohistan.

Ashraf et al. (1900) marked the Main Mantle Thrust and presented general lithologic description of the rocks, separating the salkhalas and Southern granitic gniess of Indian plate from the melange zone and the arc amphibolites. Baluch et al.(1982) distinguished the various types of amphibolites of Shergarh Sar area.

Shah (1986) presented a detailed petrographic and geochemical study on amphibolites and melange of Allai Kohistan. He classified amphibolites into epidote amphibolite and garnet amphibolite, and ultramafic rocks of melange zone into clinopyroxenite, peridotite and serpentinite together with pillow lava, green schist and blue schist. Based on petrographic character and petrochemistry Shah (1986) and Shah et al. (1990 in press) considered the amphibolites as the product of arc relatec tholeiitic magma, latter on subjected to metamorphism of an amphibolite facies. In addition Shah (1986) considered the ultramafics and volcanic rocks of oceanic character (ophiolites) of the Tethyen crust trapped in the Main Mantle Thrust melange environment. He considered subducting and obducting environment responsible for the development of melange zone.

1.4 PRESENT SCOPE:

The present work was carried out to extend the investigation at Gantar and Kalalota towards SE of the Shergarh sar area. The study is aimed to prepare a detail geological map and perform the petrographic study, mineral and rock chemistry of the amphibolite and melange zone rocks, in order to establish the petrogenic model including pressure -temperature estimation, affinity, tectonic description and fractionation history of these rocks.

CHAPTER:2

Field Relations/Petrography

2.1 Field Relations

The thesis area can be broadly divided into three petro-tectonic units, with stratigraphic succession from North to South, as follows:

a) The Kohistan arc sequence

b) The Indus Suture melange zone

c) The Indo-Pakistan Subcontinent Plate (Salkhalas)

The Kohistan arc sequence consists of the following lithologies:

(a) amphibolites (b) epidote amphibolites and (c) hornblende pegmatite.

most are volcanics?

The Melange zone includes (a) green schist (b) blue schist (d) meta-gabbro/norites.

Salkhalas

The Salkhalas comprises of (a) quartz-muscovite-chlorite-carbon-ate schist (b) quartz-actinolite schist (c) calcareous schist (d) graphitic schist and (e) siliceous marble.

Amphibolites

The Amphibolites are well exposed just North of Pashakal, Gantar, Shalkhai and Kalalota village, and are extended in East-West direction. These are the dominant rocks in the area, and can hardly be distinguished from the associated gabrroic rocks.The gabbroic rocks were found at Gantar, and differentiated on the basis of petrography (see Section 2.2a). Amphibolites and

gabrro/norites are homogeneous and massive but local banding and foliation are not uncommon. Fractures filling discordant quartzo-feldspathic veins and sporadic slickensides of epidote, indicating minor faulting,are common in the area. Small to large patches of hornblende pegmatite, at places, containing porphyroblasts of hornblende, can also be observed in these amphibolite. Iron leaching on the weathered surface of amphibolite is also common feature of these rocks.

(b) MMT melange zone rocks

The melange zone can be identified by abundant occurrence of green schist, blue schist, chert as well as the ultramafic rocks including pyroxinite, serpentinite and peridotite (see Shah, 1986). Green schist are the most voluminous rocks in the area and are well-exposed at the Gantar, Metai and kalalota area, lying directly in contact with arc amphibolite in the North and the salkhalas graphitic schist and siliceous marble in the South. Small outcrop and patches of graphitic schist and other schistose rocks of the Salkhalas are exposed at various places within the green schist manifesting tectonic emplacement. The green schist is highly fractured, jointed, foliated and weathered on the surface. Layers of carbonaceous material, quartzo-feldspathic/calcite veins, minor folds (tygmatic folds), faults and buddinage structure are conspicuous in the melange zone.

A small outcrop of blue schist near MMT , assosciated with Salkhalas, occur at Narsuk village in the area.

↑

not shown in the map!

(c) Indo-Pakistan Plate

The Indo-Pakistan plate rocks (Salkhalas) contain various groups of schistose rocks .The contact of the Salkhalas with the melange zone and amphibolites are highly sheared and dislocated, reflecting tectonic emplacement in the area. Large pieces of Salkhalas including graphitic schist and calcareous schist etc, are present in the green schist. At Kalalota the Salkhalas has been found in direct contact with the arc amphibolites. These schistose rocks are highly fractured, jointed and weathered with tight folding, concordant and discordant calcite veins. The crushed and mylonised graphitic schist usually intermingled with the calcareous schist, indicating intense deformation.

2.2 Petrography

The petrography of these rocks in the Northern part of Allai Kohistan has been studied by (Hamidullah et al., 1977; Yousafzai et al., 1977 ; Baluch et al., 1982 and Shah, 1986). During the present study seventy five representative samples were selected for petrographic investigation. The modal composition are represented in the table 3.1. The major megascopic and microscopic features are as follows.

2.2A.
2.1 The Kohistan arc sequence

The Kohistan sequence consists of the following lithologies; (i) amphibolites (ii) epidote amphibolites and (iii) hornblende pegmatite.

(i) Amphibolites

Megascopic Features:

In handspecimen, the amphibolites are medium to course grained, greenish gray to dark gray rocks. Amphibole imparts dark gray color to these rocks. Amphibole, plagioclase, and quartz grains can easily be identified in the handspecimen. The grain size of these rocks generally varies from 0.5mm to 5mm. Some specimen exhibits preferred orientation of grains and others show clear banding of alternate white and dark minerals.

Under microscope the amphibolites are medium to course grained rocks with inequigranular, xenoblastic to subideoblastic texture.Preferred orientation can also be noticed in these sections. While in some sections quartzo-feldspathic veins cross-cut the original fabric.

Amphibolites consist of hornblende, plagioclase, quartz, epidote, chlorite, actinolite, sphene and opaque ores, while rutile and carbonates occur in some sections (see Table 2.1).

Hornblende and plagioclase are the dominant minerals. Amphibole is generally pleochroic from brownish green to pale green but rarely greenish to bluish green and non pleochroic. The former type is tschermakite and tschermakitic hornblende in composition whereas the latter one is magnesio-hornblende and actinolitic in composition (see Section 3.1a). The grains of these amphibole are anhedral to subhedral and medium to course grained. These crystals poikiloitically enclose a considerable high number of quartz grains adopting a sieve structure . Amphibole is generally intergrown with plagioclase.

The textural relationship shows that actinolitic hornblende has developed at the margins of the tschermakitic hornblende.

Plagioclase with anorthite content (An% 16), occurs as anhedral to subhedral, medium to course grained, and commonly intergrown with hornblende. It has partially or completely altered to epidote and sericite, imparting cloudy appearance to the rock. Belbs of quartz are the common inclusion in plagioclase.

Epidote occurs as fine grained aggregate, grown after plagioclase and some grains intruding the host rocks, are also observed.

Quartz occurs as anhedral minute grains, relatively larger grains as well as granular aggregates. Undulating extinction, indicating intense deformation is noticed in many of quartz grains.

Sphene and rutile occur in traces associated with opaque ores. These have, probably, developed at the expense of TiO_2, released from ilmenite and calcium from plagioclase.

Traces of chlorite and carbonates are also found in certain rocks.

TABLE 2.1 Modal composition of amphibolites and hornblende pegmatite based on visual estimation.

MIN	Amp1	Amp5	Amp 55	Amp60	Amp62	Amp63	HBP6	HBP9
Hb	45	35	40	30	45	35	40	65
Act	0	0	5	5	0	0	5	5
Pg	40	40	40	45	37	40	20	30
Qtz	8	15	00	00	10	10	30	5
Chl	00	5	5	5	0	7	00	00
Epd	3	2	7	3	4	6	1	1
Ore	2	3	3	12	4	2	3	3
Sph	T	00	00	00	00	00	00	1
Rut	T	00	00	00	00	00	00	00
Cor	T	00	00	00	00	00	00	00

AMP= Amphibolites.

HBP= Hornblende-Pegmatite.

(ii) Epidote Amphibolites:

Megascopic features:

Megascopically these are medium to coarse grained, greenish gray to light green rocks. Epidote, Hornblende and plagioclase are the most recognizable minerals in hand specimen. Epidote grains give green tint to these rocks. Most of the grains are varying from 2mm-4mm in size. The rock is generally homogeneous (massive) but rarely foliated. Minor epidote veins are also common.

In thin section the epidote amphibolites are medium to coarse grained, granoblastic to inequigranular and xenoblastic to hypidioblastic in texture. In granoblastic texture a mosaic of equidimensional grains is observed. Some rocks show well defined fabric and others are massive.

The dominant minerals are hornblende, plagioclase, epidote, actinolite and quartz while chlorite, opaque ore, biotite and muscovite are accessories. Traces of sphene and apatite are also noticed in these rocks.(see Table 2.2)

Hornblende and plagioclase are generally similar to as described in amphibolite. The polygonal grains of hornblende are more sieved and corroded in epidote amphibolite. Kink banding, however, so far not seen in the plagioclase of amphibolites, is also noticed in the epidote amphibolites.

Epidote ranges from epidote to zoisite, occur as anhedral to subhedral grains but some occur as prismatic or columnar aggregates, all intergrown with green hornblende. The epidote sur-

rounds either partially or wholly altered grains of plagioclase. Secondary epidote veins are conspicuously present.

Quartz is found intersecting between the hornblendes and epidote crystals through out the section. The individual grains exhibit undulating extinction and occasionally , display deformation lamella . Opaque ores and sphene are generally associated and occur as disseminated grains in the rock.

Biotite occurs along the cleavages and fractures of hornblendes whereas minute flakes of chlorite, muscovite and traces of apatite are also observed in these rocks.

Epidote amphibolites of similar mineralogical composition have also been reported by Arif et al. (1983) from Khawaza Khela area, Swat Shah (1986) from Shergarh area, Allai Kohistan , Hussain and Hamidullah (1991) from Mahak, Swat and Jan (1988,1991) from Kohistan island arc, Northern Pakistan.

This reference is Hamidullah et al (1991)

Hamidullah, S., Hussain, I. & Rouber, I.

The epidote amphibalite simply loses rocks which are the same as plagioclase amphibalite but with more epidote — i.e more retrogressed portion of the plag — amphibalite.

TABLE 2.2

MODAL COMPOSITION OF EPIDOTE AMPHIBOLITE BASED ON VISUAL ESTIMATION

MIN	A1k3	A1K4	A15K6	A15K7	A15K8
Hb	30	60	50	10	40
Pg	40	20	25	45	30
Epd	15	15	23	10	21
Qtz	6	4	12	15	5
Ore	4	1	5	2	2
Biotite	0	0	3	0	0
Mvt	0	0	2	0	0
Chl	5	0	0	3	2
Sphene	0	T	T	0	0
Apt	0	T	T	0	0

(III) HORNBLENDE-PEGMATITE

Megascopic features:

Sporadic patches of hornblende pegmatite are embedded in the amphibolites with well developed large crystals of hornblende ranging in size from 1-5cm, along with feldspars and occasionally quartz can be seen in hand specimen. The large hornblende crystals are generally lying parallel to the general orientation of banding in pegmatite.

Under the microscope hornblende, plagioclase, quartz, actinolite, epidote, biotite, sphene and ore are observed. Compositionally tschermakitic hornblende (Table 2.1) is dominant mineral having subhedral to anhedral grains, with poikilitic inclusion of quartz.The corroded margins of hornblende reflects fibrous amphibole. Biotite and epidote are grown along the cleavages of hornblende.

Plagioclase (An% 16) has vigorously altered to epidote imparting cloudy appearance to the rocks. Quartz occur both interstitially as well as inclusion in hornblende.

Magnetite and ilmenite are disseminated throughout the rocks. Traces of sphene associated with magnetite are also present.

2.2 B Melange zone

The following lithologies are noticed in the MMT melange zone;

(i) Meta-gabbro/norites

The meta-gabbro is a medium to course grained massive rock in which pyroxene, plagioclase and hornblende can be identified in handspecimen. The microscopic study reveals that it is an inequigranular, xenoblastic to subideoblastic rock, containing , plagioclase, clinopyroxene, orthopyroxene, quartz and hornblende in decreasing order of abundance (Table 2.3). Beside these minerals biotite, muscovite, epidote, talc, actinolite and opaque minerals are also present.

Plagioclase (Labradorite) is the most abundant mineral, when fresh, exhibits excellent twinning, while some grains display deformation lamella. Partial alteration into saussuratized material, containing epidote and white mica, is commonly noticed.

The clinopyroxene are mostly diopsidic in composition,occurs both as anhedral and prismatic grains, commonly intergrown with orthopyroxene. Pale green to brownish pleochroic hornblende develop at the expense of Clinopyroxene and plagioclase. The inclusion of quartz are generally associated with clinopyroxene. When fresh, clinopyroxene grains appear to be homogeneous under the microscope and no exsolution phenomena or variation in color was observed.

The orthopyroxene (hypersthene to ferro-hypersthene) occurs as anhedral to subhedral grains, pleochroic from brown-green to pale green and usually associated with clinopyroxene. Some grains

are steatized into the cluster of talc , suggesting alteration in orthopyroxene. The altered grains are less pleochroic probably reflecting low iron content in the orthopyroxene. The development of hornblende and some biotite at the expense of orthopyroxene and plagioclase is also noticed. Corona structure having core of plagioclase, a middle rim of hornblende and outer margin of orthopyroxene is in accord with this interpretation. Fibrous amphibole forming after the ferromagnesium mineral is noticed, indicating retrogression and shearing of metagabbro at shallow level.

Corona-bearing metagabbro of almost similar composition have also been described by Bartholom (1958, 1960) Jan et al.(1984) from the Lowville Quadrangle and Kohistan island arc, Northern Pakistan, respectively.

The quartz metagabbro is similar to metagabbro except for th presence of quartz and bluish green hornblende. The alteration of hornblende into uralitic fibrous amphibole is in high proportion in latter type.

The meta-quartz norite is also petrographically similar to metagabbro except for the high content of fresh plagioclase (An% 69) and high proportion of strongly pleochroic orthopyroxene.

TABLE 2.3

MODEL COMPOSITION OF GABBRO-NORITIC ROCKS BASED ON VISUAL ESTIMATION

MIN	GB2	GB51	GB8	GB59	GB-N 53
Pg	47	55	52	50	43
CPX	15	10	7	10	5
OPX	0	0	13	5	25
Qtz	15	15	2	5	10
Hb	5	5	10	20	3
Act	10	10	3	7	0
Bio	0	0	3	0	2
Mus	T	T	0	0	2
Epd	2	2	3	1	0
Ore	2	3	5	2	3
Sphene	T	T	0	0	0
Talc	0	0	0	2	0

GB= Gabbro.

GB-N= Gabbro-Norite.

(ii) Green schist:

Megascopic features:

In hand specimen, the green schist is a homogeneous (massive) , fine to medium grained and greenish gray to light green rocks, exhibiting occasionally schistosity, banding and compositional layering. Quartzo-feldspathic / calcic veins together with minor folds and crenulations are abundant in these rocks; the latter indicating intense deformation. Chlorite, epidote, calcite, quartz and plagioclase can be identified in hand specimen. Surface alteration has resulted the development of secondary epidote veins, whereas intense deformation has given rise to talcosic material.

Under the microscope the green schist is fine to medium grained rock, with well developed fabric and foliation and texturally it is inequigranular to porphyroblastic rock. Lenticular and spindle shaped patches surrounded by fine grained schistose matrix, occurs, showing cataclastic deformation . Compositional layering and banding defining tight microfolding and schistosity, is very well displayed in these rocks (See also Higyons, 1971 and Shah,1986).

Green schist composed of green minerals like chlorite, actinolite, epidote along with cloudy plagioclase (albite). Quartz, graphite? and muscovite are also abundant . Biotite, apatite, tourmaline, calcite , hornblende, sphene and opaque minerals present as accessories. (Table 2.4)

Actinolite (Magnesio-hornblende) is one of the most abundant mineral, appear in green schist as prismatic crystals, acicular

needles and flakes, both randomly oriented as well as follow the general fabric. The actinolite needles and quartz grains sometimes present in the form of lenses, wrapped in chlorite-muscovite and graphite bands, also scattered throughout the section. In some sections the brown green hornblende also exists, reflecting transformation into actinolite.

Chlorite (Repidolite to clinochlore) is the second abundant mineral in the rock commonly intergrown with muscovite and graphitic material. It also occur in the form of bands associated with graphite, muscovite and epidote. Chlorite is pleochroic from pale green to green color, occasionally exhibit anomalous pinkish brown birefringence.

Albite occurs in the form of anhedral to subhedral grains displaying carlsbad twinning and is altered to epidote. Epidote occurs in the form of fine grain aggregates and is generally associated with chlorite-actinolite but also emerge as independent bands.

Quartzo-feldspathic material is found in the form of bands , patches, fine grain aggregates and equigranular grains. Quartz veins cross cutting the fabric of the rocks are also present.

Muscovite is usually found as minor tabular patches and bands, associated with chlorite and fine grained sericite. In some section yellowish brown pleochroic biotite, with fasicular bundle structure, is also observed .

Among the opaque minerals magnetite is abundant and is generally associated with sphene. Traces of tourmaline , apatite and sphene are also present.

In the banded variety of green schist the following bands are recognized:

(i) muscovite-chlorite veins (ii) epidote-chlorite vein (iii) graphite-chlorite vein (iv) quartz-feldspathic-actinolite bands (v)calcite-sericite veins.

In the glaucophane bearing green schist, glaucophane is pleochroic from brown to blue, cropping as columnar crystals and flakes, intergrown with epidote and chlorite. The glaucophane may have developed at deep levels at the expense of preexisting ferromagnesium minerals and some Na-bearing phase like plagioclase.

Aegirine has been chemically analyzed in these rocks. chlorite and epidote associated with albite , probably developed after glaucophane and coexisting plagioclase.

(iii) Blue schist

Megascopic features:

A sample collected from the village Narsuk, comprises actinolite, and glaucophane as megacrysts in handspecimen. The rock is homogeneous and massive and its fractures, when present, are filled with epidote veins. Variation in grain size from fine to medium and in color from bluish green to yellowish green (on weathered surface) can be observed in handspecimen.

In thin section blue schist is cloudy and flaky in appearance, equigranular fine to medium grained schistose rock. Glaucophane is the most abundant mineral in the rock. It appears in the form of flakes and fasicular bundles. Individual crystals are

pleochroic from faint blue to purple at core and dark blue to dark purple at margins. Glaucophane is closely associated with muscovite, actinolite and exist as flakes and needles respectively.

TABLE 2.4 Modal composition of green schist and blue schist based on visual estimation.

Min	ALK10	ALK16	ALK34	ALK47	ALK48	Alk64
ACT	10	20	10	8	10	10
CHL	30	10	10	20	20	00
EPD	15	10	30	15	15	T
Pg	15	30	20	20	20	0
Grph	5	3	5	3	00	0
Gl	0	0	0	15	20	50
Qtz	10	10	10	10	10	0
Hb	0	5	T	2	0	0
Mus	10	10	10	5	5	25
Bio	T	00	00	0	0	0
Calc	2	00	00	T	T	0
Ore	3	2	5	2	T	T
Sph	1	0	0	0	0	5
Apt	T	T	0	0	0	0
Tour	0	T	0	0	0	0
Sap	0	0	0	0	0	10

A1K10-A1K48 = Green schist.

A1K64 = Blue schist.

2.2 C Indo-Pakistan Plate

Associated with green schist in the South and Salkhalas in the North, are the variety of schistose rocks which share lithological characters both with the rocks of Indian plate (i.e Salkhalas) and those of melange zone.

Using the nomenclature of Winkler (1976) the following rock types are distinguished.

(i) Quartz- muscovite- chlorite- carbonates schist

Quartz-muscovite-chlorite-carbonates schist is a fine to medium grained, light gray rock with soapy luster. Quartz, calcite, mica and chlorite can be recognized in handspecimen. Compositional layering with tight folding is a conspicuous feature of this rock.

In thin section, it is a fine to medium grained rock, with prominent compositional bands. These bands are closely folded and exhibits lenticular texture. The various bands recognized, contain: (i) muscovite- epidote-graphite bands (ii) epidote-chlorite bands (iii) actinolite-epidote bands (vi) chlorite-muscovite-carbonates bands (v) sericite rich carbonates bands (iv) quartz-feldspathic bands. Cataclasis reflects a mortar texture, is also noticed in some section .

(ii) Quartz- actinolite schist

Megascopic features:

These rocks are exposed near Metai along with green schist. Megascopically these appear similar to green schist, schistosity

and compositional layers with porphyroblast of quartz are well-defined.

In thin section the rock comprises of quartz, actinolite, graphite, epidote, muscovite, sericite, chlorite,ores and carbonates in decreasing order of abundance. Quartz is the most abundant mineral, occurring crystals of uniform size as porphyroblast , wrapped in various ribbons and matrix.

Actinolite emerges as long needles parallel to the schistosity of these rocks and is associated with chlorite or muscovite bands. Beside these bands, numerous others assemblages are as follows: (i) Actinolite- graphite- epidote- bands (ii) Chlorite- sericite epidote bands (iii) Quartz- feldspathic bands (vi) Chlorite bands. Magnetite is generally associated with carbonates.

Intense microfoiding and crenulations reflect, in contrast to compositional layering, tectonic deformation in the rock.

(iii) Calcareous schist

Calcareous schist are fine to medium rock with distinct schistosity and compositional layering, rarely massive, dark gray to dirty green in color, with secondary quartz and calcite veins. Crenulation and small tygmatic folds are common in these rock. Quartz, calcite and graphite can be differentiated in handspecimen.

Under the microscope these are fine to medium grained rock, subgranular to inequigranular in texture, with prominent bands and lenses. Carbonates, quartz, actinolite, plagioclase, sericite, graphite, epidote, chlorite, ore and tourmaline occur in decreasing order of abundance in these rock.

Actinolite, graphite, sericite, epidote and at places quartz present as various distinct compositional folded bands, occasionally kinked. quartz also exists as individual grains, reflecting undulating extinction, wrapped in these bands. Plagioclase is partially altered to epidote appear cloudy. Minor veins of epidote are also noticed.

Carbonates occur in fined grained clusters or aggregates, associated with quartz and plagioclase. Among the carbonates siderite and calcite are common. some secondary calcite veins also crosscut the primary rock.

(iv) Graphitic schist

Graphitic schist appears to be schistose rock, dark gray to blackish gray in color, containing crenulation and fractured. It is highly weathered (rusty) and very soft rock with greasy luster due to presence of graphite. Quartz veins crosscutting the graphitic schist, are also common. Graphite, albite, actinolite, chlorite, quartz, muscovite, biotite, carbonates, epidote and ore are the important minerals in the graphitic schist.

The various bands noticed in the graphitic schist are (i) graphite- sericite- actinolite bands (ii) graphite- actinolite bands (iii) calcite-bands and (vi) albite- actinolite assemblages bands are identified. In addition to these bands sericite (muscovite), biotite, fine grained epidote and shattered calcite with sieved structure, are also disseminated through out the rock.

(v) Siliceous marble

Megascopic features.

The siliceous marble is a fine to medium grained rock, exhibiting sugary or crystalline equigranular texture. It is massive and compact, light to dark gray in color, however, it imparts brown-yellowish color on weathered surface. Calcite, quartz and occasionally graphite can be distinguished in hand-specimen. Secondary concordant and discordant calcite veins are commonly noticed in these marbles.

In thin section, rhombic calcite, chlorite, quartz, epidote, graphite, actinolite, traces of ore and sericite are identified. kink bandings and bookshelf structure are also observed in the rock . Calcite is the most abundant mineral ranging from 50 to 90 %. Quartz grains are embedded in the tight rhomb of calcite. The mixture of chlorite and graphite are disseminated in this rock. Sericite, epidote and actinolite occur along the cleavages and to the fabric of the rhombic pattern of calcite.

TABLE 2.5 Modal composition of different schistose rocks

Min.	M14	M19	Alk24	Alk31	Alk18	Alk70
CO2	30	30	12	10	T	90
Pg	40	30	8	T	T	00
Corb+Grp	0	8	8	T	45	00
Mus	T	2	T	5	15	T
Ore	T	5	T	2	T	0
Qtz	20	15	25	50	10	2
Seri	5	2	10	3	5	3
Act	T	8	25	30	15	0
Tour	0	T	0	0	0	0
Chl	0	0	T	T	0	0
Epd	0	0	T	T	0	0

AlK14–AlK24 = Calcareous schist.

AlK31 = Quartz–actinolite schist.

AlK18 = Graphitic schist.

AlK70 = Siliceous marble.

CHAPTER:3 MINERAL CHEMISTRY

3.1 Calcic-amphibole

Calcic-amphibole is one of the dominant constituents of amphibolites and hornblende pegmatites at Kala-lota and Gantar in Allai Kohistan. As mentioned earlier in (Chapter 2.2), considerable color and texture variation from core to margin has been noticed in these amphiboles, which must be reflecting variation in chemical composition (Miyashiro, 1973). To ascertain such assumptions and also, if possible to determine the environment of growth and pressure-temperature condition of crystallization for these amphiboles at least 50 spots were analyzed on different crystals from different rock types. Nineteen representative analysis from various rock types shown in (Table 3.1A), are utilized for plotting on various diagrams and pressure-temperature determination.

Mineral formulae were calculated on the basis of 23 oxygen for all the amphiboles analysis following the procedure of Deer et al. (1962), while the ferrous and ferric iron were computed, following the method of (Robinson, 1982). Calcic amphiboles including tschermakite, tschermakitic-hornblende, ferro-tschermakitic-hornblende, magnesio-hornblende, actinolitic-hornblende and actinolite, classified after Leake (1978) nomenclature (Fig. 3.1 c), follow a straight linear trend with no scatter. On AlIV+NaM4 vs A+AFT plot of Papike et.al.,(1974) data indicates a charge balance

Table: 3.1A. Representative analyses of calcic-amphiboles

File name A:AMP2.RCC

Sample	F.TS.A	FR.TS6	TS.HB6	MG.HB6	TS.HB6	TS.HB6	TS.HB6	TS.HB6	MG.HB6	TS.HB6	TS.58	TS58	T658	TS58	TS.HB5
Group #	1.00	2.00	5.00	6.00	7.00	8.00	9.00	10.00	11.00	12.00	13.00	14.00	15.00	16.00	17.00
Qual	7	7	7	7	7	7	7	7	7	7	7	7	7	7	7
Key	1	1	1	1	5	5	5	5	5	5	3	3	3	3	3
Ref	8	8	8	8	8	8	8	8	8	8	8	8	8	8	8
SiO_2	43.59	40.70	43.86	45.00	43.45	43.70	43.96	43.09	41.43	44.30	37.72	42.45	42.27	43.28	43.82
TiO_2	0.90	2.90	0.42	0.32	1.13	1.11	1.15	1.20	1.03	1.30	2.11	0.46	0.41	0.51	0.86
AL_2O_3	13.66	15.30	14.21	12.96	11.03	10.70	9.97	10.28	11.58	11.76	16.24	15.59	14.82	14.97	13.76
FE_2O_3	0.44	0.33	2.67	4.89	11.67	12.22	11.34	12.00	11.34	11.00	15.89	8.45	9.00	9.45	8.11
FEO	16.30	15.10	12.70	11.84	8.10	8.20	8.94	8.18	8.09	6.76	3.87	9.80	9.33	8.67	8.87
MNO	0.17	0.23	0.22	0.26	0.40	0.32	0.28	0.23	0.46	0.34	0.13	0.20	0.12	0.11	0.07
MGO	8.63	8.44	9.72	10.04	10.82	11.10	10.94	11.04	11.11	10.72	9.62	9.38	10.11	10.31	10.44
CAO	11.90	11.72	11.60	11.29	11.01	11.26	11.08	11.22	11.22	11.29	10.54	11.35	11.62	11.75	11.15
NA_2O	2.03	2.08	1.94	1.95	1.78	1.80	1.80	1.66	2.21	1.63	1.91	1.86	1.47	1.50	1.56
K_2O	0.00	0.00	0.00	0.00	0.00	0.00	0.00	0.00	0.51	0.00	0.00	0.00	0.00	0.00	0.00
Total	97.62	96.80	97.34	98.35	99.39	100.41	99.46	98.90	98.98	101.10	98.23	99.54	99.65	100.55	98.67
SI	6.458	6.112	6.463	6.551	6.324	6.311	6.411	6.320	6.113	6.328	5.548	6.141	6.120	6.175	6.341
TI	0.101	0.327	0.047	0.035	0.124	0.121	0.126	0.132	0.114	0.140	0.233	0.050	0.045	0.055	0.094
AL	2.396	2.708	2.468	2.224	1.892	1.821	1.714	1.777	2.014	1.980	2.815	2.658	2.529	2.518	2.350
FE_3	0.050	0.038	0.296	0.536	1.278	1.328	1.244	1.324	1.258	1.182	1.759	0.919	0.981	1.014	0.883
FE_2	2.029	1.896	1.565	1.441	0.986	0.990	1.090	1.003	0.998	1.046	0.476	1.185	1.130	1.034	1.073
MN	0.021	0.029	0.027	0.032	0.049	0.039	0.035	0.029	0.057	0.041	0.035	0.025	0.015	0.013	0.009
MG	1.914	1.889	2.134	2.178	2.347	2.389	2.378	2.413	2.443	2.282	2.152	2.022	2.181	2.192	2.251
CA	1.897	1.886	1.831	1.761	1.717	1.742	1.731	1.763	1.774	1.728	1.661	1.759	1.803	1.796	1.730
NA	0.586	0.606	0.554	0.550	0.502	0.504	0.509	0.472	0.632	0.451	0.545	0.522	0.553	0.415	0.438
K	0.000	0.000	0.000	0.000	0.000	0.000	0.000	0.000	0.096	0.000	0.000	0.000	0.000	0.000	0.000
AL_4	1.542	1.888	1.537	1.449	1.676	1.689	1.589	1.680	1.887	1.672	2.452	1.859	1.880	1.825	1.659
AL_6	0.854	0.820	0.931	0.775	0.216	0.133	0.125	0.097	0.127	0.307	0.363	0.799	0.650	0.693	0.691
Mg#	0.485	0.499	0.577	0.602	0.704	0.707	0.686	0.706	0.710	0.686	0.819	0.630	0.659	0.677	0.677
T-Site	8.000	8.000	8.000	8.000	8.000	8.000	8.000	8.000	8.000	8.000	8.000	8.000	8.000	8.000	8.000
C-Site	4.998	4.999	5.000	4.998	4.999	4.999	4.998	4.998	4.998	4.998	4.999	5.000	5.001	5.001	5.000
B-Site	2.000	2.000	2.000	2.000	2.000	2.000	2.000	2.000	2.000	2.000	2.000	2.000	2.000	2.000	2.000
A-Site	0.483	0.491	0.386	0.311	0.219	0.246	0.240	0.235	0.502	0.179	0.205	0.281	0.356	0.212	0.168
Na-A	0.103	0.114	0.169	0.239	0.283	0.258	0.269	0.237	0.226	0.272	0.339	0.241	0.197	0.203	0.270
Na-A	0.483	0.491	0.386	0.311	0.219	0.246	0.240	0.235	0.406	0.179	0.205	0.281	0.356	0.212	0.168
FeO*	16.70	15.40	15.10	16.24	18.60	19.20	19.15	18.98	18.30	18.66	18.17	17.40	17.43	17.17	16.17
Mg#	0.370	0.384	0.422	0.412	0.398	0.396	0.393	0.398	0.408	0.395	0.380	0.380	0.397	0.405	0.423
den	2.83	2.85	2.79	2.77	2.76	2.77	2.77	2.77	2.77	2.77	2.74	2.77	2.77	2.76	2.75

Table: 3.1A Continued

File name A:AMF2.ROC

Sample	TS53	ACT.7	ACT.H8	MG.HB7
Group #	18.00	20.00	21.00	22.00
Qual	7	7	7	7
Key	3	3	3	3
Ref	8	8	8	8
SiO_2	43.21	54.06	52.74	51.10
TiO_2	0.59	0.00	1.50	0.36
AL_2O_3	16.03	8.90	9.13	9.70
FE_2O_3	4.33	0.11	1.44	0.11
FEO	11.71	13.80	12.40	13.14
MNO	0.10	0.14	0.11	0.05
MGO	9.58	10.20	11.90	11.44
CAO	11.48	11.60	10.93	11.78
NA_2O	2.26	1.00	0.75	1.52
Total	99.29	99.81	100.90	99.70
SI	6.243	7.571	7.301	7.213
TI	0.064	0.000	0.156	0.091
AL	2.730	1.469	1.490	1.614
FE_3	0.471	0.012	0.150	0.012
FE_2	1.415	1.616	1.435	1.551
MN	0.012	0.017	0.013	0.006
MG	2.063	2.128	2.455	2.406
CA	1.777	1.740	1.621	1.781
NA	0.633	0.272	0.201	0.416
AL_4	1.757	0.429	0.699	0.787
AL_6	0.973	1.040	0.791	0.827
Mg#	0.593	0.568	0.631	0.608
T-Site	8.000	8.000	8.000	8.000
C-Site	4.998	4.813	5.001	4.393
B-Site	2.000	2.000	1.823	2.000
A-Site	0.410	0.012	0.000	0.197
Na-B	0.223	0.260	0.201	0.219
Na-A	0.410	0.012	0.000	0.197
FeO#	15.61	13.90	13.70	13.24
Mg#	0.411	0.454	0.497	0.495
den	2.78	2.74	2.75	2.76

on the basis of calculated oxygen. (Fig.3.1 a-b). The actinolite and the actinolitic-hornblende, however show a little deflection than the trend of other amphibolites on this plot, indicating relatively low Al4+NaM4 components. One of these analysis show less cations < 2 in the B- site(see Table 3.1A), while the discrepancy in the others can be related probably, to a bit over estimation of SiO2 . The difference is however, not as high to discard these data. Maximum concentration of the data are plotted in the field of tschermakitic-hornblende and occupy a position between the hornblende, tschermakite and actinolite on the plots of Deer et al. (1966) and Giret et al. (1980) respectively (Fig.3.1d,e). On the basis of the manipulation of data using various plots an over all substitutions of Ca+Na+Fe2 +Mn+Al4 vs Si+Ti+Mg+Fe3 +Al6 is suggested. This type of general replacement for the amphiboles from all the rock types is supported by the linear negative variation of the data between the groups of elements (Fig.3.1a). Fig. 3.1F display such a general substitution encompasses the tschermakitic type substitution (Si+Mg Al+Al) of (Miyashiro, 1973).

COMPOSITIONAL VARIATION IN CALCIC-AMPHIBOLES

Several authors have proposed a miscibility gap between hornblendic composition (i.e tschermakite, tschermakitic-hornblende, pargasite, pargasitic-hornblende) and actinolite (see Miyashiro, 1958; Shido, 1958; Shido and Miyashiro, 1959; cooper and Lover

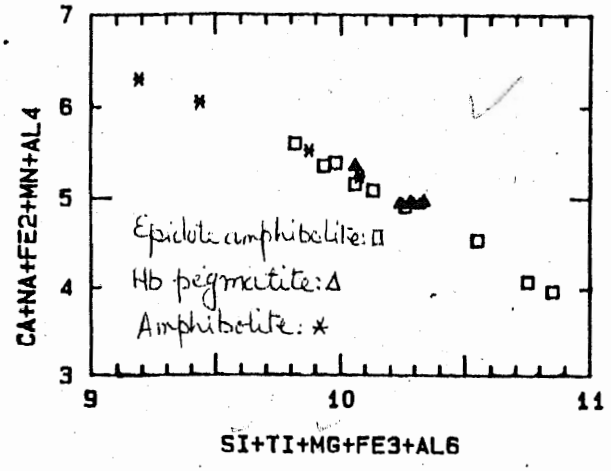

3.1 a

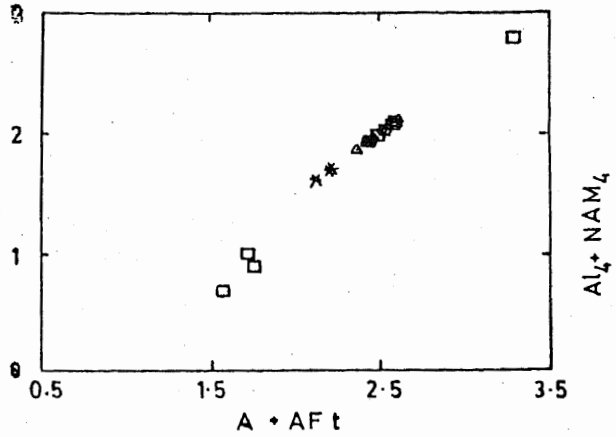

3.1 b

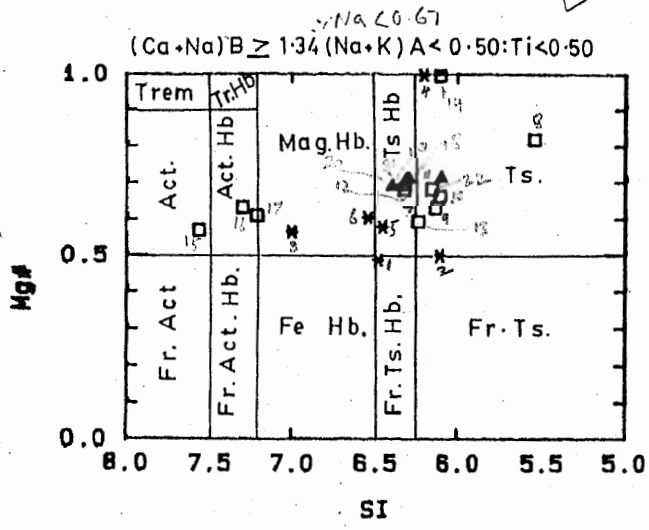

3.1 c

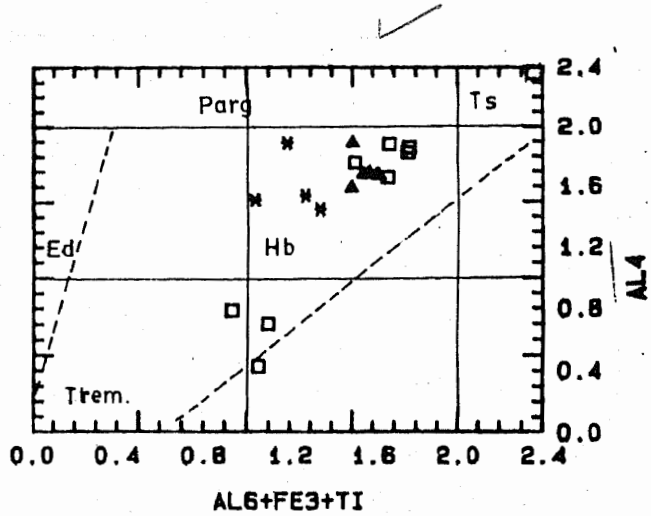

3.1 d

Fig. 3.1 a. CA+NA+FE2+MN+AL4 VS SI+TI+MG+FE3+AL6 Plot of amphiboles from the amphibolites of Gantar and kalalota area, Allai Kohistan.

Fig. 3.2 b. The ionic charge balance plot of Gantar calcic amphibole showing substitution between A+AFT and AL4+NAM4. (after Papike, 1974) Symbols as Fig. 3.1 A.

Fig. 3.1 c. Compositional fields for Gantar amphibole on the classification diagram of Leake (1978). Key as Fig. 3.1 A.

Fig. 3.1 d. Chemical variation of the studied amphiboles on AL6+FE3+TI VS AL4 plot adopted from Dear et al., (1966). Key as Fig. 3.1 A.

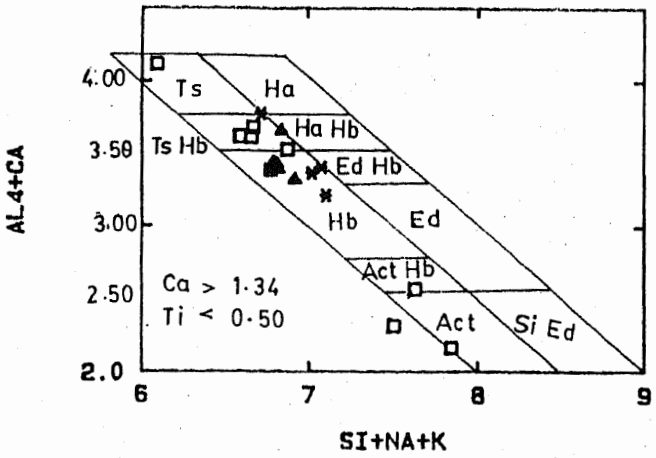

3.1e

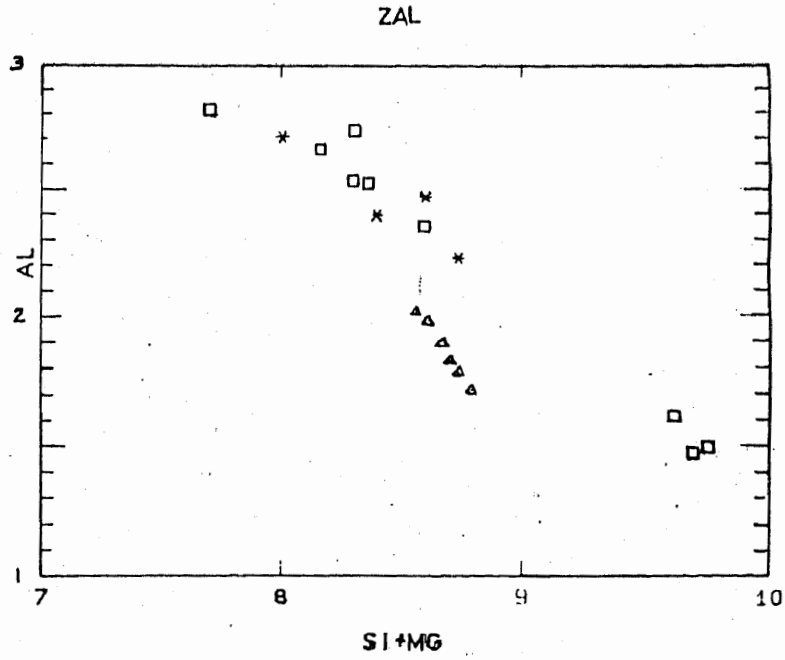

3.1f

Fig. 3.1 e. CA+AL4 VS SI+NA+K plot of the studied amphiboles in the field of data from non-orogenic complexes after Giret et al., (1980). Symbols as in Fig. 3.1 A.

Fig. 3.1 f. Si+Mg VS total Al plot of the studied amphiboles, indicating the degree of tschermakitic substitution after Miyashiro (1973).

ing, 1970; Cooper,1972 and Misch and Rice, 1975) . While others have favored a continuous solid solution series between the two end members (Robinson and Spear, 1982 and Kamineni,1986). The present data of calcic-amphibole of Allai Kohistan also straddle the miscibility gap between the two end members of amphibole. The generation of five amphiboles including two end members i.e actinolite and tschermakite, the middle members tschermakitic-hornblende, magnesio-hornblende and actinolitic-hornblende in the calcic-amphibole and almost positive correlation between Al4 and A-site in epidote amphibolite, do suggest a strong clue for the probable continuous compositional variation in the calcic-amphiboles (Fig. 3.1,g). Moreover the occurrence of fibrous actinolite around the tschermakitic-hornblende crystals, reflects the episodic generation of two amphiboles end members under the retrogressive metamorphic condition from amphibolite grade to that of greenschist.

The actinolite analysis from the epidote -amphibolites, which seem to be representative compositions having been resulted from the retrogressional transformation of the hornblendic composition, fall in the miscibility gap defined by Misch and Rice (1975), on Al4 vs Al, and Al vs estimated temperature respectively (Fig.3.1 h,i). It has been proposed by Kamineni (1986) that the continuity of composition and its lack, is more likely the function of specific physiochemical environment of the reaction (see also Robinson and Spear, 1982). It is therefore, suggested on the basis of present data that if the kinetic of the reaction had allowed and or more data had been obtained, continuous compositional variation would have been obtained in the chemistry of

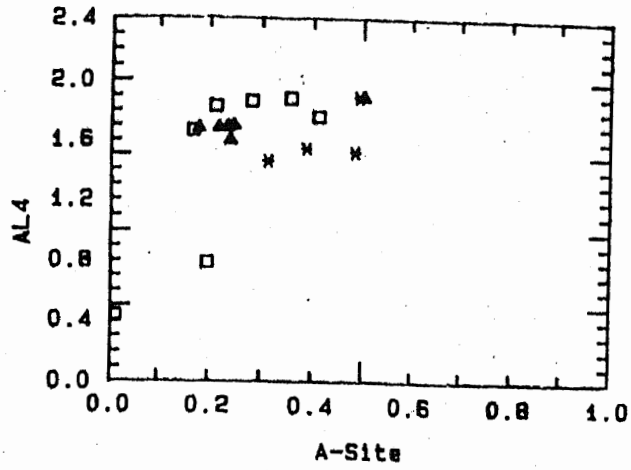

3.1 g

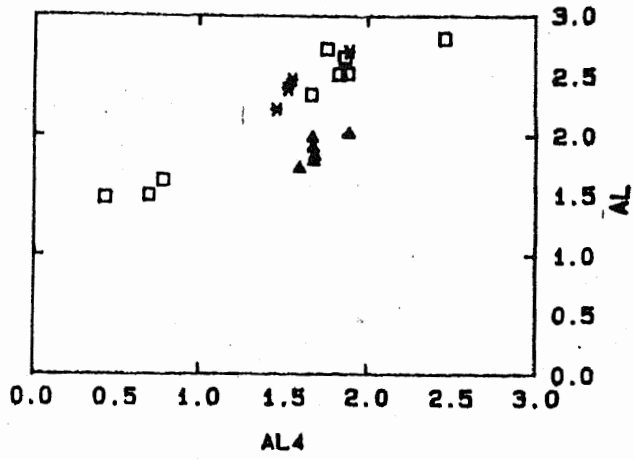

3.1 h

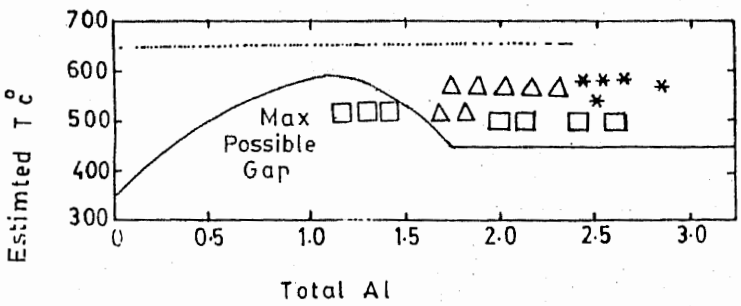

3.I(i)

Fig.3.1 g. A-site vs Al4 gives variation of the analysis amphiboles of the studied area, indicating the degree of edinetic substitution and positive correlation in epidote amphibolite. Key as in Fig.3.1 A.

Fig. 3.1 h. Al vs Al4 plot of the studied calcic amphibole with the data having Al4 < 1 plotting in the field defined as vacant by Misch and Rice (1975). Key as in Fig.3.1 A.

Fig. 3.1 i. Total Al Vs estimated temperature plot of the studied calc. amphibole, actinolites fall in the miscibility gap described by Misch and Rice (1975).

calcic-amphibole under present investigation.

PRESSURE-TEMPERATURE ESTIMATION:

Different methods and parameters were used for pressure-temperature estimation for calcic-amphiboles.

Considering Plyusnina (1982) method based on plagioclase-hornblende geothermobarometry (An% vs ΣAl,Hb), the tschermakitic- hornblende indicates 500°C where as the actinolite reflects 450 °C temperature for their development. On the mole% vs An% plot of plyusnina (1982), the tschermakitic hornblende shows 500 °C temperature and a 4-5 Kb pressure, while the extrapolated curves for actinolite indicate <500 °C temperature for the crystallization, which is in accord with the first estimation. Similarly plyusnina (1982) average wt% Al2O3 parameter suggests 530 °C temperature and 5.5Kb pressure for tschermakitic-hornblende. Al2O3 wt. percentage in amphibole has been considered as directly proportional to the grade of metamorphism (Leak,1965-1971).

Pressure-Temperature were also estimated on the basis of (Rasse, 1974; Spear,1980; Liard and Ilbee, 1981b and Perchuk,1966) see (Table3.1B).

Except temperature obtained on the basis of Perchuk (1966) method, Plyusnina (1982) individual wt.% Al2O3 parameters and pressure estimated for tschermakitic-hornblende in hornblende-pegmatite and actinolite on the basis of Rasse (1974) models, the other methods are consistent with each other (see Table 3.1 B). A generalized assessments of these pressure-temperature estimates

indicates that the tschermakitic-hornblende have probably crystallized at temperature ranges from 500-510 °C, and pressure range 4-5 Kb while the actinolite have grown at temperature ranges from 400 to 450 °C .

As we consider the hornblende and plagioclase having been developed under equilibrium condition, and the methods used for calculating the temperatures of their crystallization imply pairs of hornblende and plagioclase by Plyusnina (1982) Spear (1980) and Perchuck (1966), therefore the estimates obtained seem to be more reliable than those obtained on the individual parameters for temperature .

A general correspondence was noticed when these estimates were checked on the criteria described for the correlation of pressure-temperature condition with TiO2, Na2O, Al4 and Al6. (Leake, 1965-71; Kostyak and Sobolev, 1969; Ernst, 1972 and Rasse, 1974). Similarly the interpretation made about the present data regarding pressure-temperature is also in accord with the garnet zone and biotite zones of Miayshiro, (1973), and Liard and Ilbee(1981), which is equivalent to epidote amphibolite facies and green schist facies environment respectively (Fig.3.1j(i,ii,iii). However the discrepancies observed on the Rasse (1974) diagram for pressure estimates using Al6 Vs. Si for Gantar tschermakitic hornblende is questionable (See Fig.3.1k) , considering Shido and Miyashiro (1959) Engel and Engel (1962) Binns (1965) and Bard (1972) who also proposed that the rather complex dependence of the Al-content upon temperature, pressure and chemical environment makes it difficult to use it as an indicator of metamorphic grade.

Table 3.1B Estimated P-T Chart for Ca- amphibole

Methods	Parameters Used	T Ts-Hb, Mag.Hb	Act.	P Ts-Hb Act.
Plyusnina (1982)	An% Vs EA1Hb	500°C	450°C	
____	Mole An%	500°C	< 500°C	4Kb
____	Wt.%A1203	600°C (530°C)	~~560°C~~ not applicable in this	510°C 5.5Kb
Spear (1980) ------	ln(XAn/XAb)in Pg Vs ln(Ca,M4/Na, M4) in amph. 490 ± 20 °C			
Perchuk (1966)	XCa=Pg(Ca/Ca+Na+K) Pg vs XCa=Amph(Ca/Ca+Na+K)Amph	450°C	400 °C	
Raase (1974)	A16 Vs Si	-	-	4-5Kb -7Kb Amph + Epd-amphibolites 1-2Kb Hb-Pigmatite

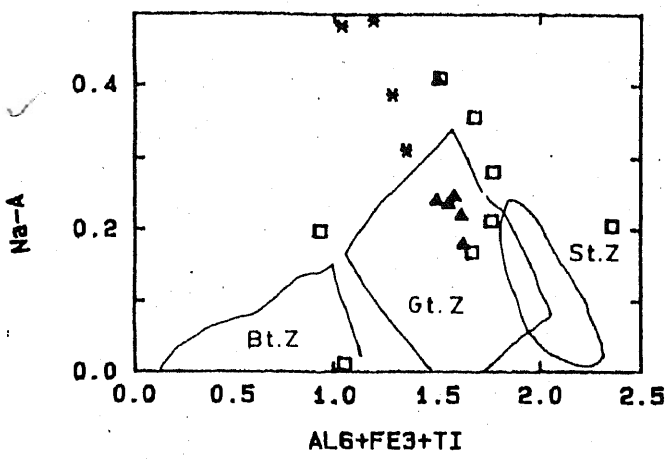

3.1 J(ii)

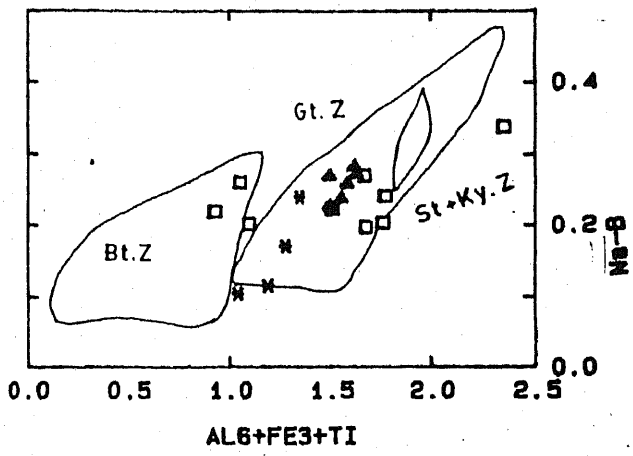

3.1 J (i)

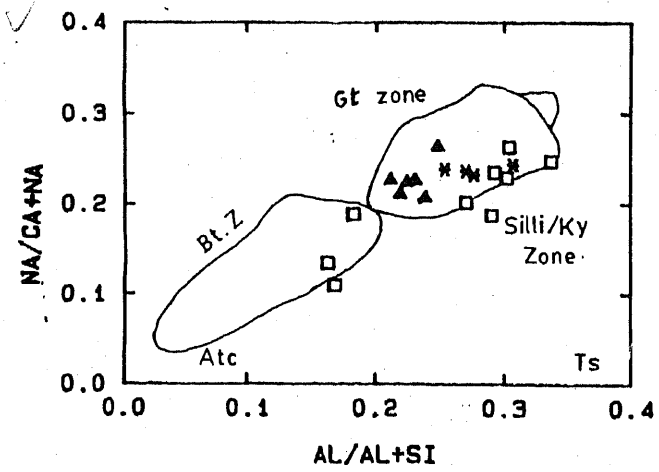

3.1 J (iii)

Fig. 3.1 J. (i-iii) Calcic amphiboles from the studied area on the Na-B, Na-A Vs Al6+ Fe3 +Ti and Al/Al +Si Vs NA/ Ca +Na plot of Liard and Albee (1982b), defined for biotite and garnet Staurolite zone of the green schist and amphibolites.

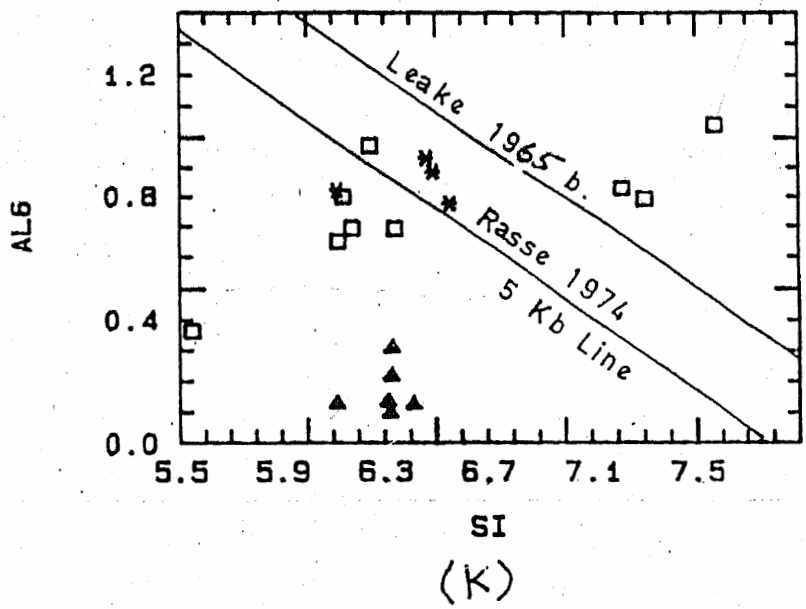

Fig. 3.1 K. Plots of the studied calc. amphiboles on the Al6 Vs Si diagram of Rasse (1974). The maximum Al6 limit of Leake (1965b) is also shown.

3.2 ALKALI AMPHIBOLES

Alkali amphiboles occur in blue schist and green schist rocks at Gantar Metai and Kala Lota as described earlier in (Section 2.2B). Twenty five points were analyzed on glaucophane crystals and representative data is shown in the (Table 3.2A-B). Mineral formulae were calculated on the basis of 23 oxygen, whereas ferric and ferrous iron estimates were computed using the method of (Robinson et al., 1982). These analysis show (Ca+NaB) > 1.34, NaB > 1.34 and (Na+K)A < 0.50 and were named as alkali amphiboles. Only three of these analyses have (Na+K)A > 0.50 and are thus classified as sodic and sodic calcic amphiboles. On the basis of Mg/Mg+Fe^{2+} and Fe3+/Fe3+ +Al6 plots (Fig.3.2 a(i-ii), these data occupy the field of glaucophane ferro-glaucophane, crrosite, eckermanite and richterite (See Leake 1978)

Potassium is generally absent from A-site and FeO/MgO is generally higher in the glaucophane of green schist as compare to that of blue schist.

Zoning, shown by pleochroic colors of these amphiboles in the blue schist and particularly in the green schist (Section 2.2B-iii), is confirmed on the basis of chemical data, where the cores of glaucophane component are surrounded by the margin of crrosite component.

The crrosite content of the glaucophane in green schist is higher than that of the blue schist, whereas magnesio-hornblende and aegirine have developed after glaucophane in the green schist, all reflect retrogression. High Fe3/Fe3+Al6 in the

TABLE 3.2 A REPRESENTATIVE ANALYSES OF AMPHIBOLE FROM BLUESCHISTS

File name A:GLAUCO2.ROC

Sample	GL	GL	GL	CROSS	GL	CROSS	CROSS	ECKERM	CROSS	GL
Group #	2.00	5.00	6.00	7.00	9.00	10.00	11.00	12.00	13.00	10.00
Qual	5	5	5	5	5	5	5	5	5	5
Key	5	5	5	1	5	1	1	8	1	5
Ref	8	8	8	8	8	8	8	8	8	8
SIO_2	56.80	57.21	56.54	54.02	56.92	56.88	56.50	55.32	56.00	56.12
TIO_2	0.02	0.10	0.01	2.65	0.09	0.10	0.02	0.20	0.00	0.03
AL_2O_3	7.80	8.00	8.21	8.12	7.66	7.52	9.74	7.21	8.21	8.60
FE_2O_3	4.56	1.56	5.11	5.45	1.22	5.45	6.78	0.11	6.22	5.00
FEO	9.50	11.50	9.80	9.52	13.60	10.93	8.30	14.04	8.92	10.31
MNO	0.10	0.10	0.09	0.23	0.00	0.09	0.03	0.22	0.07	0.30
MGO	9.20	9.30	9.50	9.33	8.67	9.13	9.10	9.67	9.32	8.80
CAO	1.06	0.90	1.23	1.98	1.90	1.33	0.90	1.77	1.11	1.50
NA_2O	6.06	7.03	6.76	5.80	6.40	6.70	6.20	7.84	6.42	6.30
K_2O	0.00	0.00	0.00	0.00	0.00	0.00	0.40	2.51	0.00	0.00
Total	95.10	95.70	97.25	97.10	96.46	98.13	97.97	98.89	96.27	96.96
SI	8.099	8.132	7.945	7.654	8.110	7.973	7.845	7.891	7.933	7.927
TI	0.002	0.011	0.001	0.282	0.010	0.011	0.002	0.021	0.000	0.003
AL	1.311	1.340	1.360	1.356	1.286	1.242	1.594	1.212	1.371	1.432
FE_3	0.489	0.166	0.540	0.581	0.131	0.574	0.708	0.012	0.663	0.531
FE_2	1.133	1.367	1.152	1.128	1.620	1.281	0.964	1.675	1.057	1.218
MN	0.012	0.012	0.011	0.028	0.000	0.011	0.004	0.027	0.008	0.036
MG	1.955	1.970	1.989	1.970	1.841	1.907	1.883	2.055	1.967	1.852
CA	0.162	0.137	0.185	0.301	0.290	0.200	0.134	0.270	0.168	0.227
NA	1.675	1.937	1.842	1.593	1.768	1.821	1.669	2.168	1.763	1.725
K	0.000	0.000	0.000	0.000	0.000	0.000	0.071	0.457	0.000	0.000
AL_4	0.000	0.000	0.055	0.346	0.000	0.027	0.155	0.109	0.067	0.073
AL_6	1.311	1.340	1.305	1.010	1.286	1.215	1.439	1.103	1.304	1.359
Mg#	0.633	0.590	0.633	0.636	0.532	0.598	0.661	0.551	0.651	0.603
T-Site	8.099	8.132	8.000	8.000	8.110	8.000	8.000	8.000	8.000	8.000
C-Site	4.901	4.866	4.998	4.998	4.888	4.998	4.999	4.893	5.000	4.999
B-Site	1.837	2.000	2.000	1.894	2.000	2.000	1.803	2.000	1.932	1.952
A-Site	0.000	0.074	0.027	0.000	0.058	0.020	0.071	0.895	0.000	0.000
Na-B	1.675	1.863	1.815	1.593	1.710	1.800	1.669	1.730	1.763	1.725
Na-A	0.000	0.074	0.027	0.000	0.058	0.020	0.000	0.438	0.000	0.000
FeO#	13.60	12.90	14.40	14.42	14.70	15.83	14.40	14.14	14.52	14.81
Mg#	0.434	0.450	0.428	0.423	0.401	0.396	0.418	0.437	0.422	0.403
den	2.58	2.59	2.58	2.62	2.62	2.60	2.57	2.62	2.58	2.59

53

2, 5, 6, 7, 9, 10, 11, 12, 13, 14 GBL: 0 7th Nov

TABLE 3.2 B REPRESENTATIVE ANALYSES OF AMPHIBOLE FROM GREEN SCHISTS

File name [illegible]

Sample	MICH47	CROSS4	CROSS	FR.GL	ECKER	CROSS	CROSS
Group #	2.00	3.00	4.00	5.00	6.00	8.00	9.00
Qual	1	1	1	1	1	1	1
Key	6	1	1	3	5	1	1
Ref	8	8	8	8	8	8	8
SiO_2	56.00	55.53	53.85	56.45	54.75	54.43	54.68
TiO_2	0.00	0.00	0.00	0.17	0.07	0.18	0.14
Al_2O_3	7.40	8.53	7.10	10.52	8.03	9.35	4.66
Fe_2O_3	0.11	5.56	2.00	4.33	3.56	6.67	11.34
FeO	18.84	15.23	15.23	12.52	15.77	13.35	10.58
MnO	0.17	0.11	0.14	0.00	0.05	0.14	0.12
MgO	6.66	6.21	6.17	7.23	7.27	6.06	8.56
CaO	5.44	0.65	1.23	0.86	0.57	0.89	2.96
Na_2O	6.73	7.56	7.31	6.77	6.57	6.49	5.06
K_2O	0.00	0.00	0.00	0.00	2.75	0.20	0.00
Total	95.82	99.41	99.65	98.87	99.51	97.76	98.49
Si	7.978	7.856	7.734	7.950	7.833	7.782	7.625
Ti	0.000	0.000	0.000	0.018	0.008	0.019	0.015
Al	1.322	1.407	1.205	1.724	1.354	1.576	0.789
Fe_3	0.013	0.591	0.267	0.453	0.383	0.717	1.230
Fe_2	2.198	1.802	1.834	1.436	1.865	1.596	1.310
Mn	0.022	0.013	0.017	0.000	0.006	0.017	0.015
Mg	1.554	1.309	1.324	1.498	1.550	1.291	1.825
CA	0.883	0.099	0.190	0.131	0.087	0.136	0.454
NA	1.992	2.074	2.041	1.825	1.706	1.799	1.404
K	0.000	0.000	0.000	0.000	0.502	0.036	0.000
AL_4	0.422	0.144	0.246	0.150	0.167	0.218	0.375
AL_6	0.900	1.264	0.959	1.574	1.188	1.358	0.414
T-Site	8.000	8.000	8.000	8.000	8.000	8.000	8.000
C-Site	4.874	4.999	5.000	5.000	4.999	4.998	5.000
B-Site	2.000	2.000	2.000	1.956	1.993	1.935	1.858
A-Site	0.875	0.172	0.231	0.000	0.502	0.036	0.000
Na-B	1.117	1.901	1.810	1.825	1.906	1.799	1.404
Na-A	0.875	0.172	0.231	0.000	0.000	0.000	0.000
Fe##	[illegible]	[illegible]	22.43	16.42	18.75	19.35	21.16
Mg	0.292	0.258	0.238	0.333	0.305	0.262	0.315
Al	[illegible]	[illegible]	[illegible]	2.66	2.63	2.63	[illegible]

16, 17, 18, 19, 20, 22, 23

crrosite content, probably manifest relatively high oxygen fugacity (Jan, 1985). Glaucophane in the blue schist, however lacks alteration except for one evidence of conversion to a clay mineral (saponite). These features can be related to a wider range of metamorphism in the green schist i.e; (higher high pressure and lower low pressure) than that of blue schist. The presence of saponite may be due to the later much low pressure surface alteration as a result of weathering. (See also Wood ,1980).

Coleman and Papike (1968) and Brown (1977) reported a miscibility gap between the sodic amphiboles (glaucophane-reibeckite) and actinolite . However Jan (1985) found composition plotting with in the defined gap , indicating complete solid solution series in these amphiboles. Three magnesio hornblende composition from the green schist of the Allai Kuhistan also plot within the mentioned miscibility gap and thus support the later view(2.2b)

Using Al203 wt % of calcic amphiboles Plyusnina (1982) the magnesio hornblende in the green schist indicate crystallization at temperature 490 ℃ . However temperature less than 450 ℃ and pressure of 4K have also been obtained using the EAlHb Vs. An% of plagioclase (Plyusnina 1982). On the basis of Spear (1980) and Perchuk (1966) methods temperature of 350 ℃ is obtained for these magnesio hornblende, supporting the figures estimated on the basis of the EAlHb Vs An% of (Plyusnina, 1982). On the Rasse (1974) plot the present data for magnesio hornblende plot just below the 5Kb line suggesting a pressure of less than 5Kb which is consistent with the previous result (See Fig.3.c). These data although do not correspond to a particular defined line of

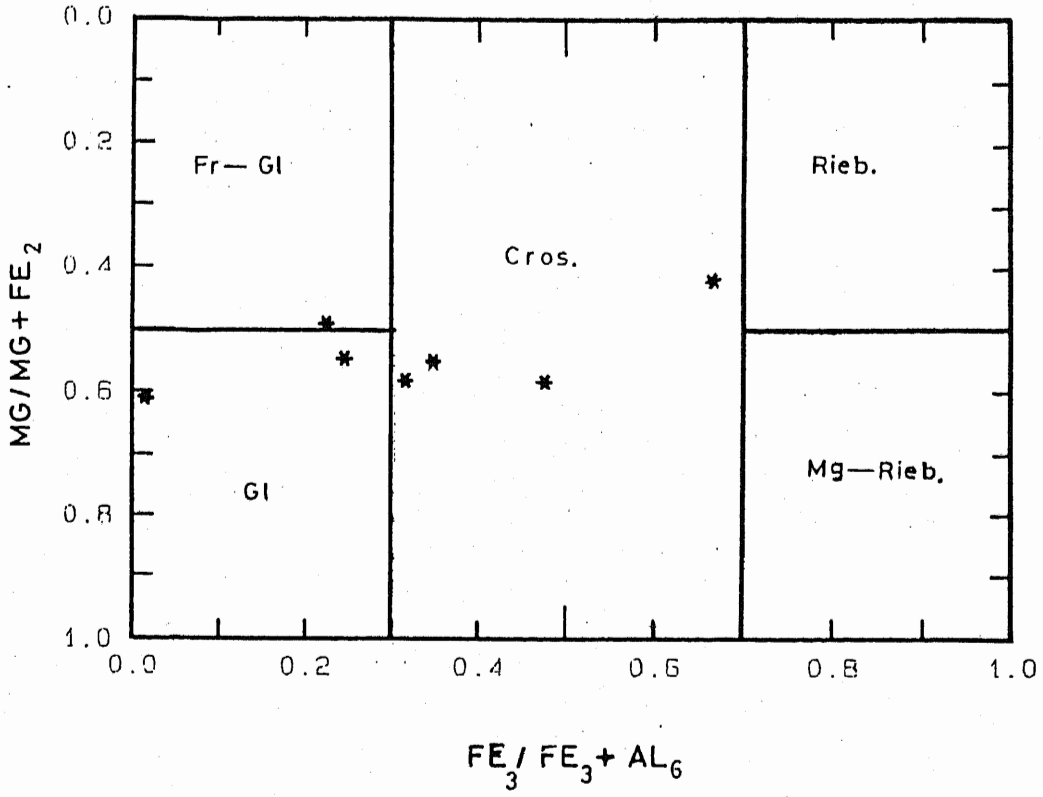

3.2a(i)

Fig. 3.2 a(i). Classification of the sodic amphiboles from green schist, on the Mg/Mg+Fe2 Vs Fe3/ Fe3+Al6 plots of Leake (1978).

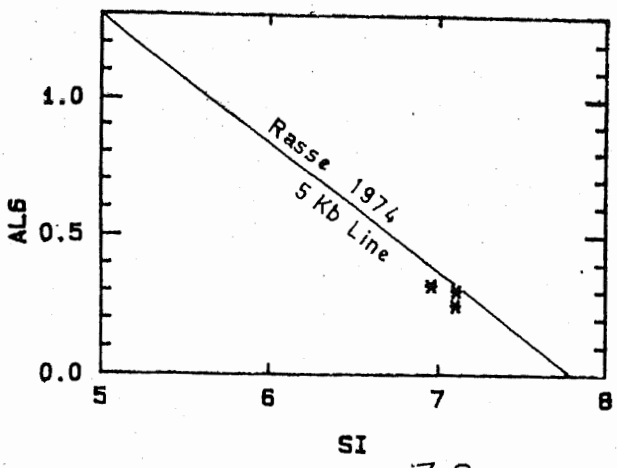

3.2c

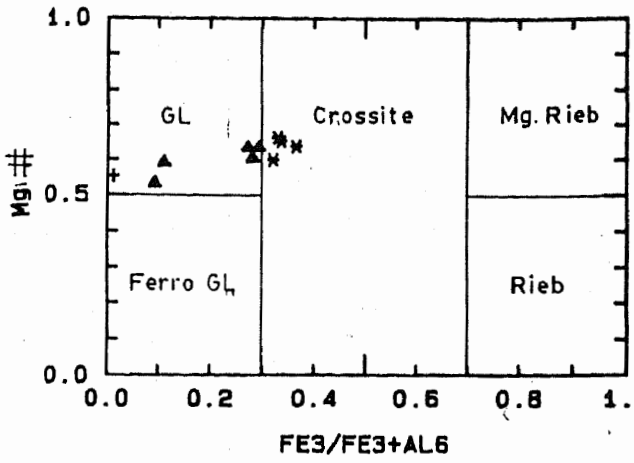

3.2a(ii)

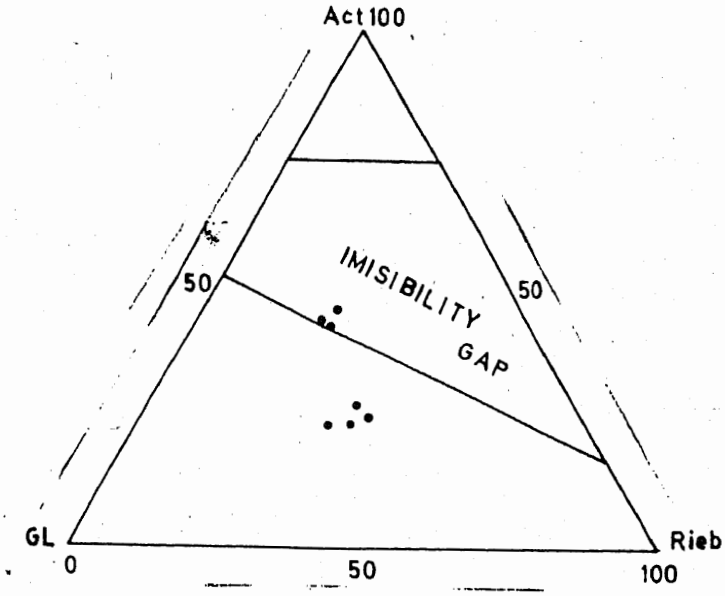

3.2b

Fig. 3.2 a(ii). Classification of the sodic amphiboles from blue schit, on the Mg/Mg+Fe2 Vs Fe3/ Fe3+Al6 plots of Leake (1978).

Fig. 3.2 b. Compositional variations of the Narsuk (Allai-Kohistan) amphibole in terms of actinolite-glucophane-riebeckite components. Area between the lines represents miscibility gap found by Coleman (1967).

Fig. 3.2 c. Plots of the studied calcic amphiboles in green schist on the Al6 Vs Si 5Kb pressure diagram of Rasse (1974).

pressure of Brown (1977, Fig.3.2 d(iii)), however extrapolating the defined line a pressure range of 4-6Kb can be evaluated, which is not drastically different from the previous figures.

The data for the glaucophane both from green schist and blue schist plot above the 5Kb line of Rasse (1974) and also proposed a pressure of 7Kb on the diagram of Brown (1977)(Fig.3.2d-e). The absence of lawsonite, the stability field of glaucophane , the average Si content 6.9 of muscovite (Velde 1968) in the blue schist, also support 7Kb pressure obtained on the basis of the Brown's method.

Two analyses from green schist plot below the 7Kb field of Sanbagawa on NaM4 vs Al4 plot of Brown (1977) probably , indicate the transitional character between blue schist and green schist condition(3.2d(i)). These features also show that the transformation of the blue schist assemblages (Glaucophane, albite, muscovite saponite and quartz) to the green schist assemblages (glaucophane, actinolite, chlorite, albite, epidote, muscovite and quartz) occur during obduction and also glaucophane bearing green schist reflect the signature of the transitional conditions.

can you include it in an assemblage called blue schist association? And if you can because ? in the whole over modal composition then even the some rocks blue schist shows all this transformation. will confirm it.

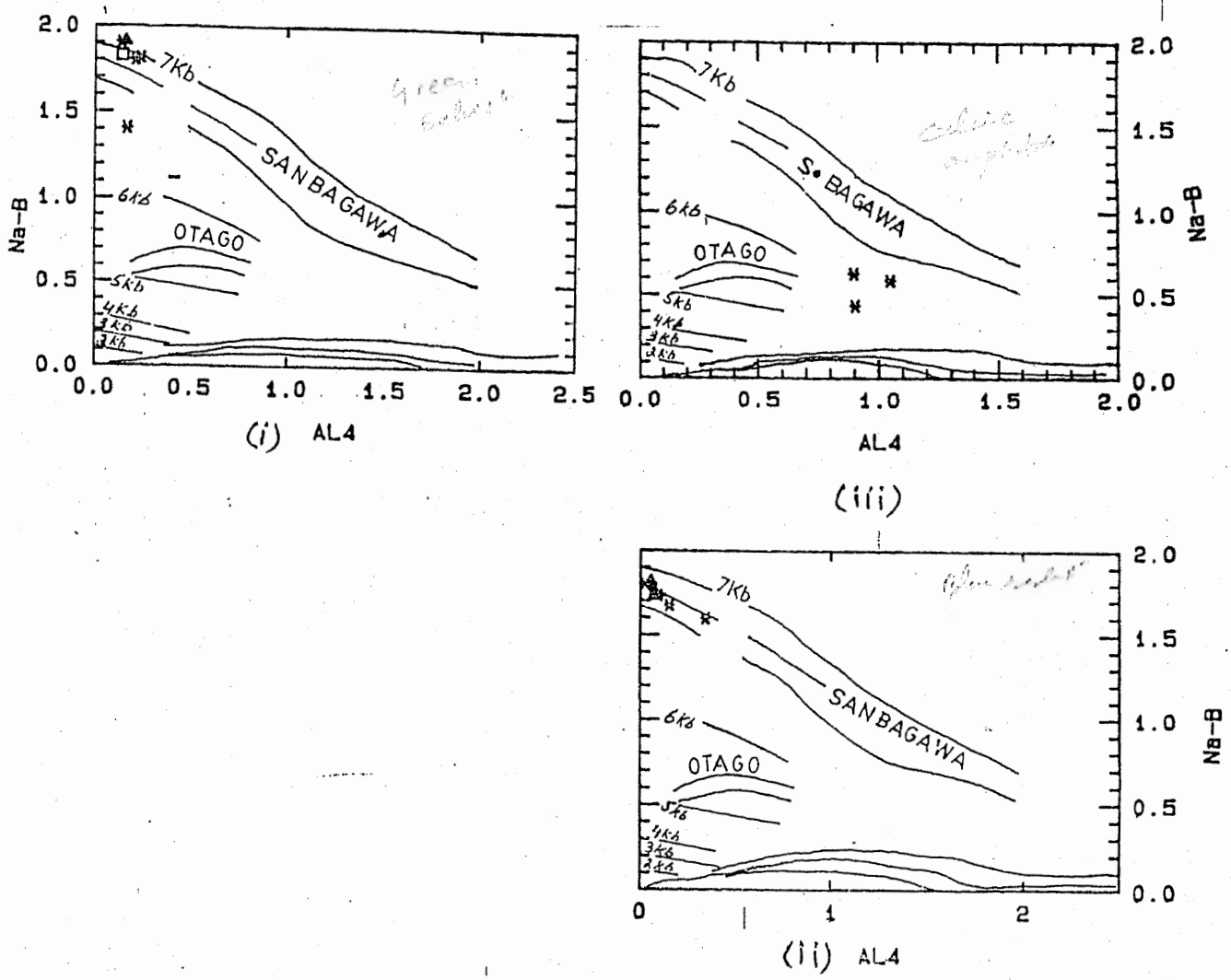

Fig. 3.2 a. Tentative estimates of pressure of calcic. amphiboles of green schist (i), sodic amphiboles of green schist (ii) and blue schist (iii) from studied area on the Na-B Vs Al4 plots of Brown (1977).

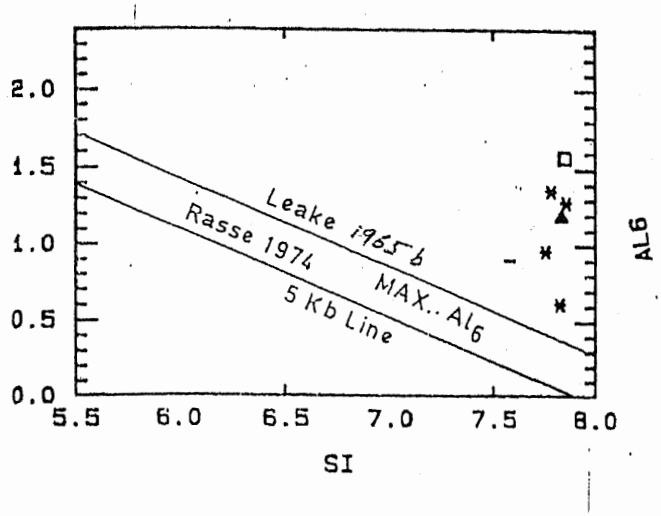

3.2e (i)

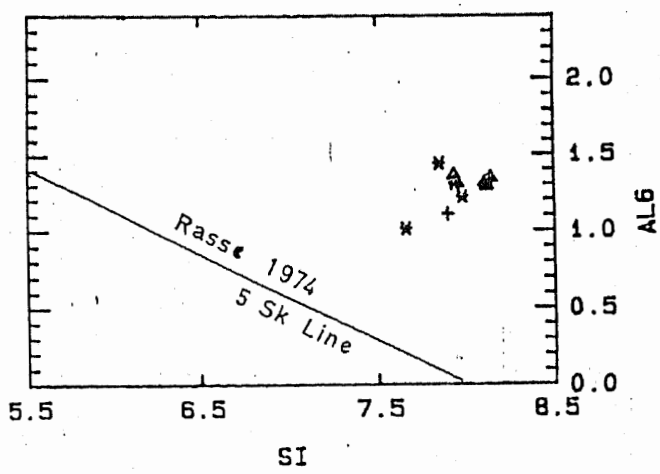

3.2e (ii)

Fig. 3.2 e. Plots of the studied sodic amphiboles of green schist (i) and blue schist (ii) on the Al6 Vs Si diagram of Rasse (1974). The maximum Al6 limit of Leake (1978) is also shown.

3.3 PYROXENE

As mentioned earlier the clinopyroxene and orthopyroxene occur upto 30% in the meta-quartz norite (see Section2.2) Both the ortho and clinopyroxene were analyzed to find out (a) chemical variation relative to petrographic character (b) core to margin elemental variation and (c) assuming these pyroxene as primary igneous to determine magmatic affinity and tectonic setting of the parent magma. Fourteen analysis of orthopyroxene and ten analysis of clinopyroxene of meta-quartz-norite and presented in (Table 3.3 c).

The orthopyroxene is strongly pleochroic, possibly due to high content of Al_2O_3 and other components (Howie, 1965; Davidson and Mathison, 1974 and Jan and Howie, 1980). The enstatite component of orthopyroxene ranges from En57-En50, this range falls with in that, reported for Chilas complex, occurring in the central part of Kohistan (Jan et al., 1984 and Khan et al., 1989).

The clinopyroxene were plotted in the pyroxene quadrilateral (Wo-En-Fs) of (Poldervert and Hess, 1951). The clinopyroxene occur in the field of calcic-pyroxene and the majority of analysis are plotted in the field of diopside except two analysis which were found as augite. (see Fig.3.3 a). The Wo of clinopyroxene ranges from 45-50% except augite, which ranges upto (Wo.40%).

Various cations were potted against each other and based on the relative variation, an overall substitution between Fe+Ca+Al4

TABLE 3.3 C REPRESENTATIVE ANALYSES OF CPX FROM META-NORITE

File name A:MCPX2.ROC

Sample	M53CX4	M53CX1	M53CX1	M53CX2	M53CX4	M53CX5	M53CX1	M53CX1	M53CX1	M53CX1
Group #	1.00	2.00	3.00	4.00	5.00	6.00	8.00	9.00	10.00	11.00
Qual	2	2	2	2	2	2	2	2	2	2
Key	3	3	3	5	3	3	3	5	3	3
Ref	3	3	3	3	3	3	3	3	3	3
SiO_2	50.96	48.91	48.91	51.10	50.95	50.97	50.02	50.10	49.47	50.91
TiO_2	0.26	0.00	0.00	0.29	0.34	0.29	0.07	0.28	0.25	0.00
Al_2O_3	2.84	3.05	3.06	2.81	2.64	2.48	2.88	2.72	2.73	3.04
FEO	9.19	11.78	11.78	12.48	10.95	9.18	13.92	12.96	13.41	13.04
MNO	0.08	0.15	0.15	0.16	2.42	0.08	0.33	0.27	0.10	0.18
MGO	11.58	11.76	11.76	12.30	12.44	11.58	11.58	11.75	11.54	11.58
CAO	19.98	20.51	20.52	17.99	19.79	19.99	21.09	22.20	21.62	21.08
NA_2O	0.62	0.45	0.45	0.48	0.41	0.62	0.42	0.61	0.36	0.42
Total	95.53	96.61	96.63	97.61	99.94	95.19	100.31	100.89	99.48	100.25
		1	2	3	4		5	6		
SI	1.981	1.917	1.916	1.962	1.930	1.989	1.907	1.898	1.901	1.927
TI	0.008	0.000	0.000	0.008	0.010	0.009	0.002	0.008	0.007	0.000
AL	0.130	0.141	0.141	0.127	0.118	0.114	0.129	0.121	0.124	0.136
FE_3	0.061	0.060	0.061	0.033	0.034	0.062	0.084	0.111	0.087	0.041
FE_2	0.360	0.326	0.325	0.434	0.313	0.361	0.359	0.299	0.344	0.372
MN	0.003	0.005	0.005	0.005	0.078	0.003	0.011	0.009	0.003	0.006
MG	0.671	0.687	0.687	0.704	0.702	0.673	0.658	0.663	0.661	0.653
CA	0.832	0.861	0.861	0.740	0.803	0.836	0.861	0.901	0.890	0.855
NA	0.047	0.034	0.034	0.036	0.030	0.047	0.031	0.045	0.027	0.031
AL_4	0.019	0.083	0.084	0.038	0.070	0.011	0.093	0.102	0.099	0.073
AL_6	0.111	0.057	0.057	0.090	0.048	0.103	0.036	0.019	0.025	0.063
$Fe_{3(4)}$	0.000	0.000	0.000	0.000	0.000	0.000	0.027	0.027	0.027	0.027
$Fe_{3(6)}$	0.000	0.000	0.000	0.000	0.000	0.000	0.138	0.138	0.138	0.138
Mg#	0.651	0.678	0.678	0.619	0.691	0.651	0.647	0.689	0.658	0.637
T-Site	2.000	2.000	2.000	2.000	2.000	2.000	2.027	2.027	2.027	2.027
C-Site	1.091	1.135	1.135	1.208	1.184	1.087	1.123	1.083	1.100	1.108
B-Site	0.970	1.000	1.000	0.984	1.000	0.969	1.000	1.000	1.000	0.994
A-Site	0.000	0.030	0.030	0.000	0.017	0.000	0.016	0.029	0.017	0.000
Na-B	0.047	0.004	0.004	0.036	0.013	0.047	0.015	0.016	0.010	0.031
Na-A	0.000	0.030	0.030	0.000	0.017	0.000	0.016	0.029	0.017	0.000
FeOt	9.19	11.78	11.78	12.48	10.95	9.18	13.92	12.96	13.41	13.04
Mg#	0.589	0.531	0.531	0.528	0.563	0.589	0.486	0.507	0.494	0.502
oen	2.76	2.81	2.81	2.80	2.82	2.76	2.84	2.84	2.84	2.82

and Na+Si+Al6+Mg+Ti is proposed for clinopyroxene. This is supported by linear negative trend of the same parameters plotted against each other (Fig. 3.3 b). The sample that is plotted below can be related as analytical error.

On the SiO2 vs Al2O3 plot of Kushiro (1960) and Alz vs TiO2 plot of Lebas (1962) the data also show non-alkaline nature(Fig.3.3c-d). The high but the decreasing Ca content in the clinopyroxene from Allai-Kohistan (Fig. 3.3 a), is also in accord with its non alkaline character (Cornwin et al., 1986; Perfit and Fornari, 1983 and Himmelberg and Ford, 1976). However the behavior of Ca-rich clinopyroxene with fractionation also depends on the order of crystallisation of the clinopyroxene in relation with other Ca-bearing phases like plagioclase (see Hammidullah and Bowes, 1987). The present mineral chemistry, textural character and whole rock chemistry all indicate simultaneous crystallisation of clinopyroxene and plagioclase and thus the Ca-content of clinopyroxene can be therefore, accepted application for the determination of the affinity of the parent magma as non alkaline.

Low PH2O crystallisation favors the early appearance of plagioclase, whereas relatively high PH2O envisage clinopyroxene crystallization in the early stage (Gonly ,1975 and Hammidullah and Bowes, 1987). The simultaneous crystallization of plagioclase and clinopyroxene in the norite of Allai-Kohistan may be therefore related to medium water pressure environment for their fractionation (see Yoder, 1979).

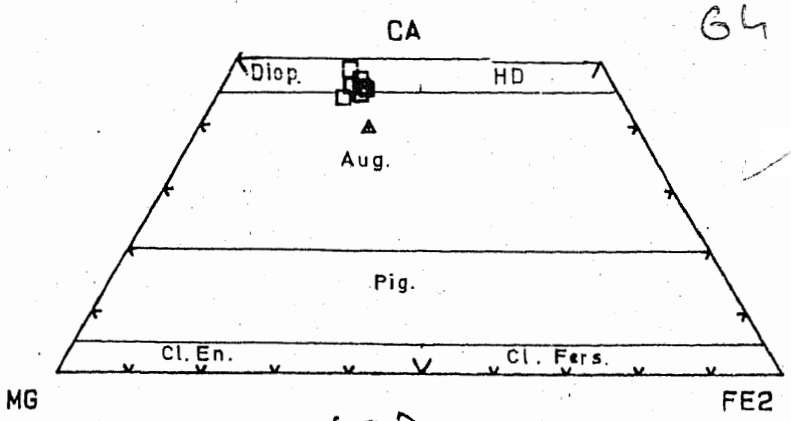

(a)

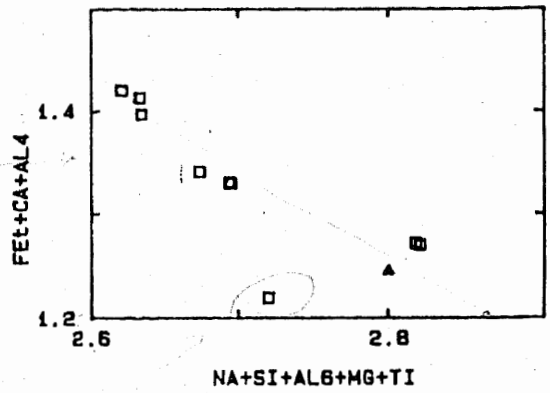

(b)

CPX

Fig.3.3 a Clinopyroxene composition plotted in the pyroxene quadrilateral? of Hess and Poldervart (1951) modified by Morimoto et al., (1986).

Fig.3.3 b. Presumed overall substitute in the clinopyroxene from the meta -norite of Kalalota area between Fet+Ca+ AL4 and Na+ Si+Al6+Mg +Ti.

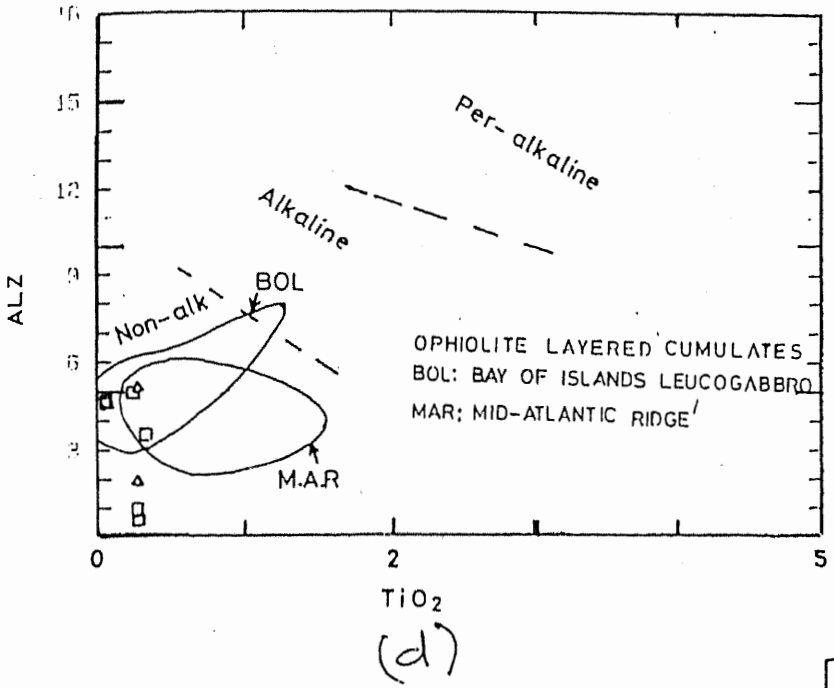

(d)

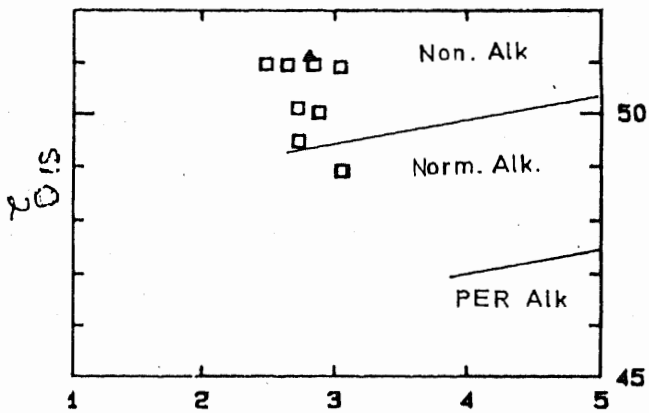

(c)

Fig.3.3 c. SiO2 Vs Al2O3 discrimination diagram for clinopyroxene of metan-orite of studied area after Kushiro (1960).

Fig.3.3 d. Affinity discrimination diagram on the basis of ALZ Vs TiO2 of clinopyroxene of meta-norite of Gantar Allai-Kohistan indicating division line of Lebas (1962) and boundaries (Bol, Mar) after Lucks (1990).

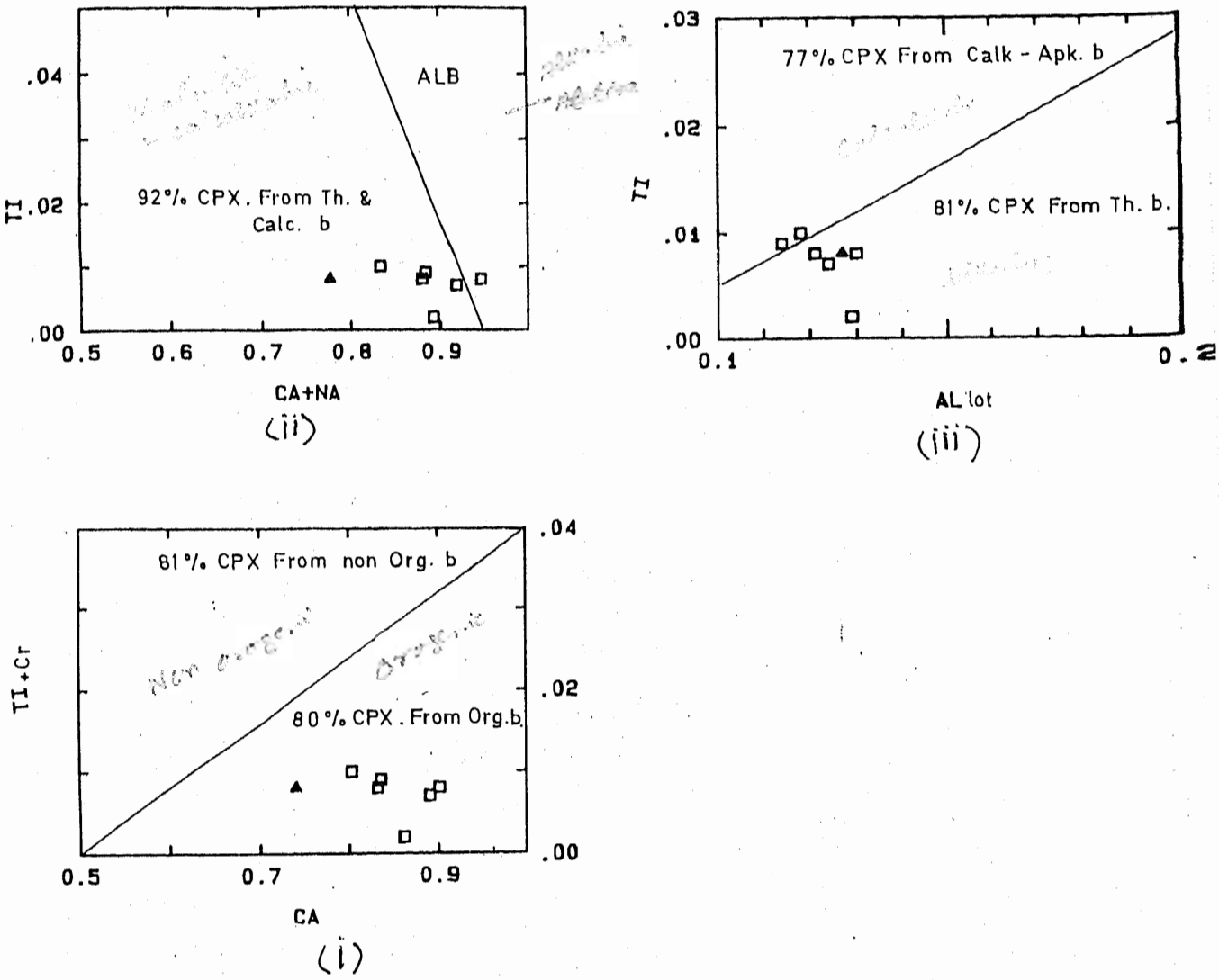

Fig.3.3 (i-iii) Ti+Cr Vs Ca, Ca+Na and tot AL discrimination diagram for the clinopyroxene (meta-norite) of the studied area with the field defined by Leterrier et al., (1982).

Further discrimination of the clinopyroxene has been carried out using Ti +Cr vs Ca+Na, Ca and Ti vs total Al of (Leterrier et al., 1982). These diagrams indicate Clinopyroxene of the study area, to be crystallized from a tholeiitic preceded by calc-alkaline magma, generated under orogenic environments (Fig.3.3 e i-iii). The very low content of cr and Ti in the present data also suggest the orogenic basalt (Island Arc tholeiites).

When plotted on the diagram of Lebas (1962) the data falls within the fields of Bay of islands lecucogabbro and mid-Atlantic ridge of ophiolitic layered cumulates, drawn by Lucks (1990) (Fig.3.3 d). Similarly comparing data plots of ten pyroxene suits of Papike (1982) some of data falls with in the overlapping field between deep sea pyroxene and Island Arc pyroxene. (Fig.3.3 f,i-vi).

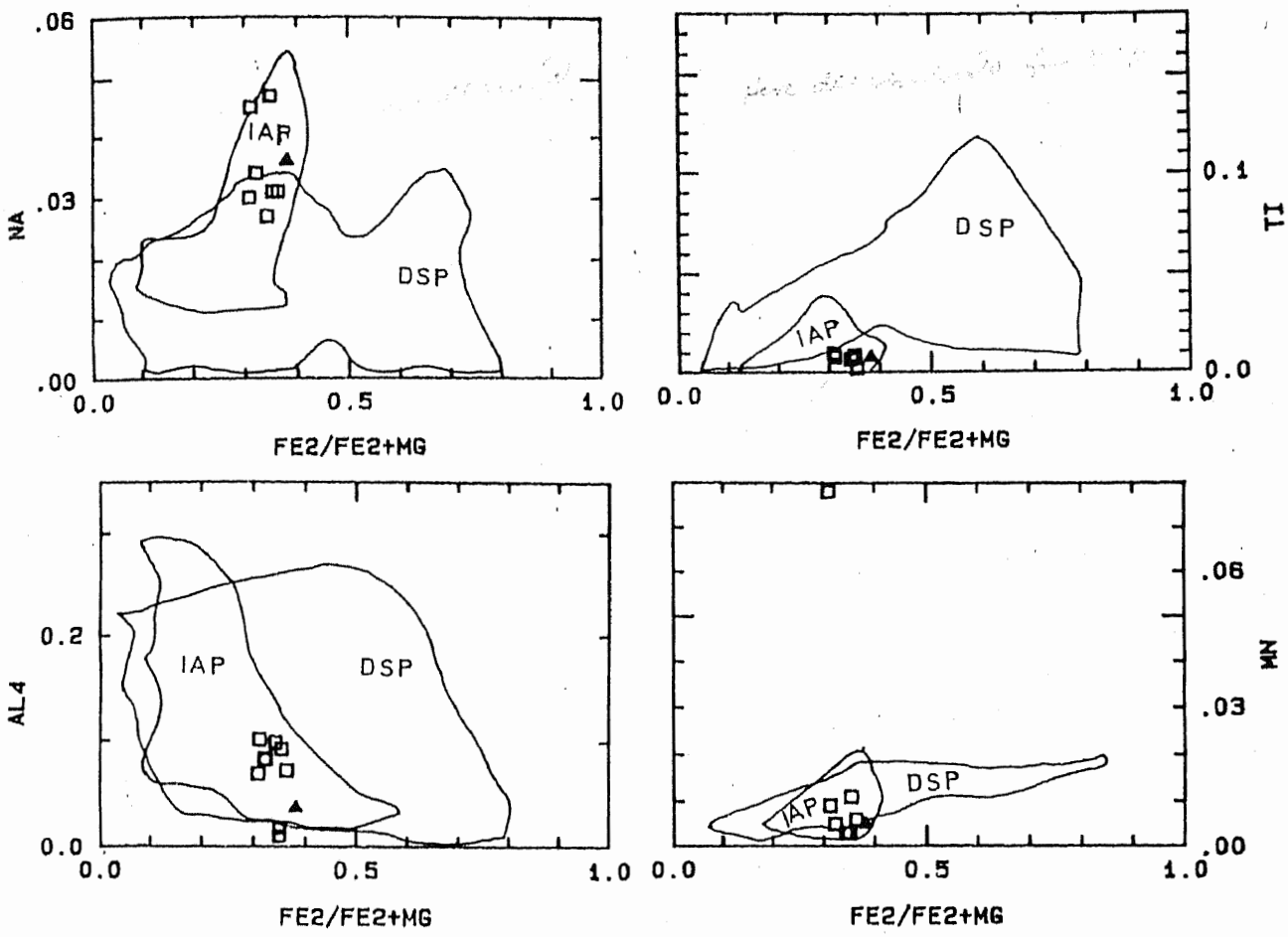

3.3f

Fig. 3.3 e. Clinopyroxene composition from the noritic rocks of Kalalota indicating Island arc + deep sea affinities on the the ten pyroxene suits diagrams of Papike (1982).

6C1

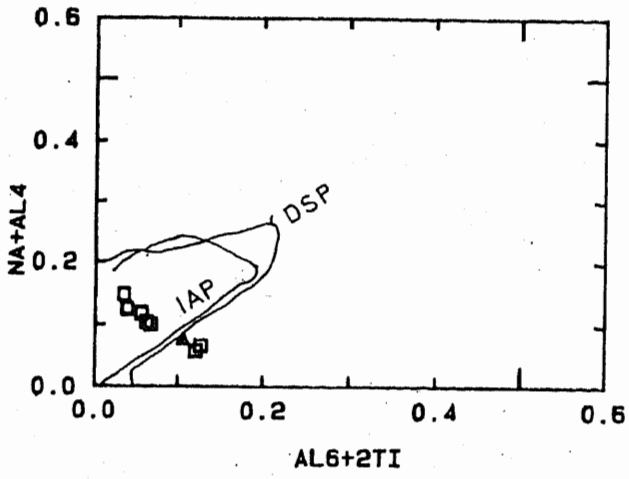
0.6
0.4
0.2
0.0
NA+AL4
DSP
IAP
0.0
0.2
0.4
0.6
AL6+2TI

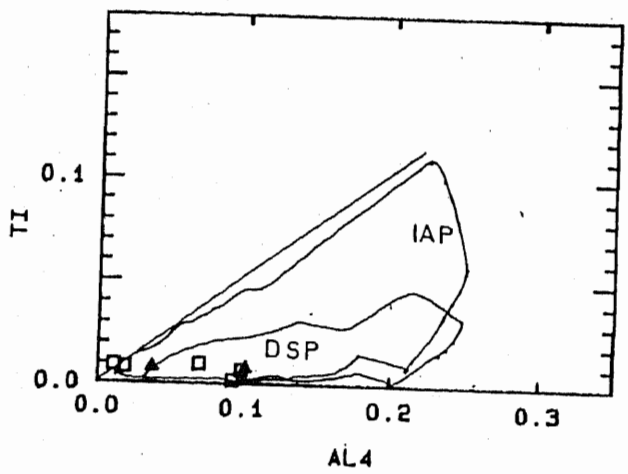
0.1
0.0
TI
IAP
DSP
0.0
0.1
0.2
0.3
AL4

3.3f

CHAPTER 4 PETROCHEMISTRY.

4a - ANALYTICAL TECHNIQUES

Amphibolites, lava, green schist and certain basic rocks along with international standards (BCR,W2,G2,AGV1) were analyzed for major elements. Using molybdenum blue method for SiO2 and alizarine red method for Al2O3 Shapiro (1975) and calorimetric method for TiO2 and P2O5 following by measurements through the use of UV/visible spectrometer. SiO2 was cross checked by Gravimetric method . Minor discrepancies were found in the determination of SiO2.

MgO, MnO, CaO, Fe2O3 (total) , K2O and Na2O were measured by atomic absorption spectrometer using absorption method for former four oxides and flame photometric methods for the latter two oxides. FeO was analyzed by volumetric and calorimetric method (cold titration method, Wilson ,1960). H2O- and ignition loss of some rocks were measured by drying the rocks powder at 120 $^{\circ}$C and 1000 $^{\circ}$C respectively.

4 PETROCHEMISTRY

To elucidate the geochemical pattern magmatic affinities and to investigate the history of evolution resulting from crystallization differentiation, nine samples from amphibolites, seven from lava, nine from basic rocks and five from green schist have been analyzed for major elements. The data together with C.I.P.W norms and are shown in the relevant (Tables 4.1-4).

4.1 AMPHIBOLITES

Amphibolites range in composition from ultrabasic SiO2 < 45%) to intermediate composition (SiO2 52%).

Various diagrams were used to find out the nature of the proto-lithic material for the amphibolites under present investigation. On the SiO2 Vs TiO2 of Tarney (1977) most of the analysis fall in the field, shown for igneous rocks (Fig.4.1a). On the Niggli c vs mg and al- alk of Evans and Leake (1964), the data follow the igneous trend defined for Karro dolorite. (Fig.4.1b-c). Simi-lar features (Fig. 4.1d) are shown by plotting these rocks on a triangular diagram of (leake, 1964). From the manipulation of above mentioned diagrams, their norms, the equal abundance of plagioclase and hornblende and the association of amphibolites with meta gabbro/norite suggest an igneous origin for Gantar and Kalalota amphibolites (see also shah 1986).

On an AFM plot of Irvine and Bargar (1971), except one sample, the rest of the analysis strictly follow the trend of tholeiitic rocks and show iron enrichment affinity. (Fig. 4.1e) When plotted on alkali Vs SiO2 diagram of Schwarzer and Roger (1974) much of the data seems to be scattered in the field of tholeiitic, high alumina basalt or straddle the boundary between the subalkaline and alkaline rocks (4.1f). Similarly on an Al2O3 VS An% , Ol-Ne-Q projection suits of Irvine and Bargar (1971) and Al2O3-FeO-MgO plot of Besson and Fonteilles (1974),

BLE 1 MAJOR ELEMENT AND CIPW NORMS DATA OF AMPHIBOLITES FROM GANTAR

File name A:CZAL20.ROC

Sample	M1	M63	AL20	AL21	AL22	AL23	M7	M58	M59
Group #	1.00	3.00	3.00	3.00	3.00	3.00	4.00	5.00	6.00
Qual	2	2	3	3	3	3	2	2	2
Key	5	5	5	5	5	5	5	5	5
Ref	2	2	3	3	3	3	2	2	2
SiO_2	44.04	52.78	52.89	50.76	44.96	49.06	43.40	42.80	45.46
TiO_2	0.93	0.93	0.78	0.61	0.76	1.19	0.95	0.68	1.46
Al_2O_3	16.20	15.16	15.34	14.00	15.85	15.18	13.02	16.16	18.12
Fe_2O_3	4.37	0.26	6.06	5.29	12.79	8.78	8.95	5.67	6.45
FeO	8.46	6.02	4.87	5.90	1.22	3.18	4.81	7.00	4.42
MnO	0.23	0.27	0.23	0.15	0.17	0.10	0.30	0.25	0.29
MgO	12.50	6.25	6.44	7.76	9.81	8.03	12.02	12.50	6.25
CaO	8.95	9.05	9.03	10.64	13.32	10.67	13.07	10.65	10.65
Na_2O	2.88	5.27	2.05	2.24	1.11	2.09	2.07	2.61	3.15
K_2O	0.50	0.93	0.00	0.04	0.02	0.08	0.21	0.24	0.36
P_2O_5	0.28	0.18	0.18	0.03	0.02	0.05	0.15	0.10	0.28
H_2O+	2.10	3.06	0.00	0.00	0.00	0.00	0.71	2.02	4.40
H_2O-	0.02	0.15	0.00	0.00	0.00	0.00	0.00	0.01	0.04
Total	101.46	100.31	97.87	97.42	100.03	98.41	99.66	100.69	100.73
S.I.	44.220	33.420	34.230	37.470	41.440	37.730	44.240	45.540	31.230
Q	0.000	0.000	9.220	2.400	0.000	0.980	0.000	0.000	0.000
Or	2.950	5.500	0.000	0.240	0.120	0.470	1.240	1.420	2.130
Ab	14.530	35.640	17.350	18.950	9.390	17.690	5.240	7.640	25.920
An	29.800	14.970	32.660	28.030	38.210	31.800	25.620	31.670	34.240
Ne	5.330	4.850	0.000	0.000	0.000	0.000	6.650	7.830	0.400
Di	10.340	23.440	9.000	20.090	22.680	16.930	31.060	16.630	11.230
Hy	0.000	0.000	24.060	23.110	6.630	23.660	0.000	0.000	0.000
Ol	30.250	10.150	0.000	0.000	17.190	0.000	22.790	28.450	14.310
Mt	3.520	0.380	3.310	3.060	3.280	3.900	3.550	3.160	4.290
Il	1.770	1.770	1.480	1.160	1.440	2.260	1.800	1.290	2.770
Ap	0.650	0.420	0.420	0.070	0.050	0.120	0.350	0.230	0.650
FeO#	12.39	6.25	10.32	10.66	12.73	11.08	12.87	12.10	10.23
Mg#	0.534	0.531	0.415	0.452	0.467	0.451	0.515	0.540	0.410
den	2.72	2.57	2.60	2.64	2.66	2.62	2.72	2.73	2.63

Fig 4.1a Plot of SiO2 vs TiO2 of Gantar and Kalalota amphibolites. Boundary between sedimentary and igneous fields after Tarney (1977).

Fig.4.1b-c-d Plots of Niggli c vs mg ,al-alk and 100mg-c-al-alk for the amphibolites of Gantar area. Various trends and fields are after Evans and Leake (1960).

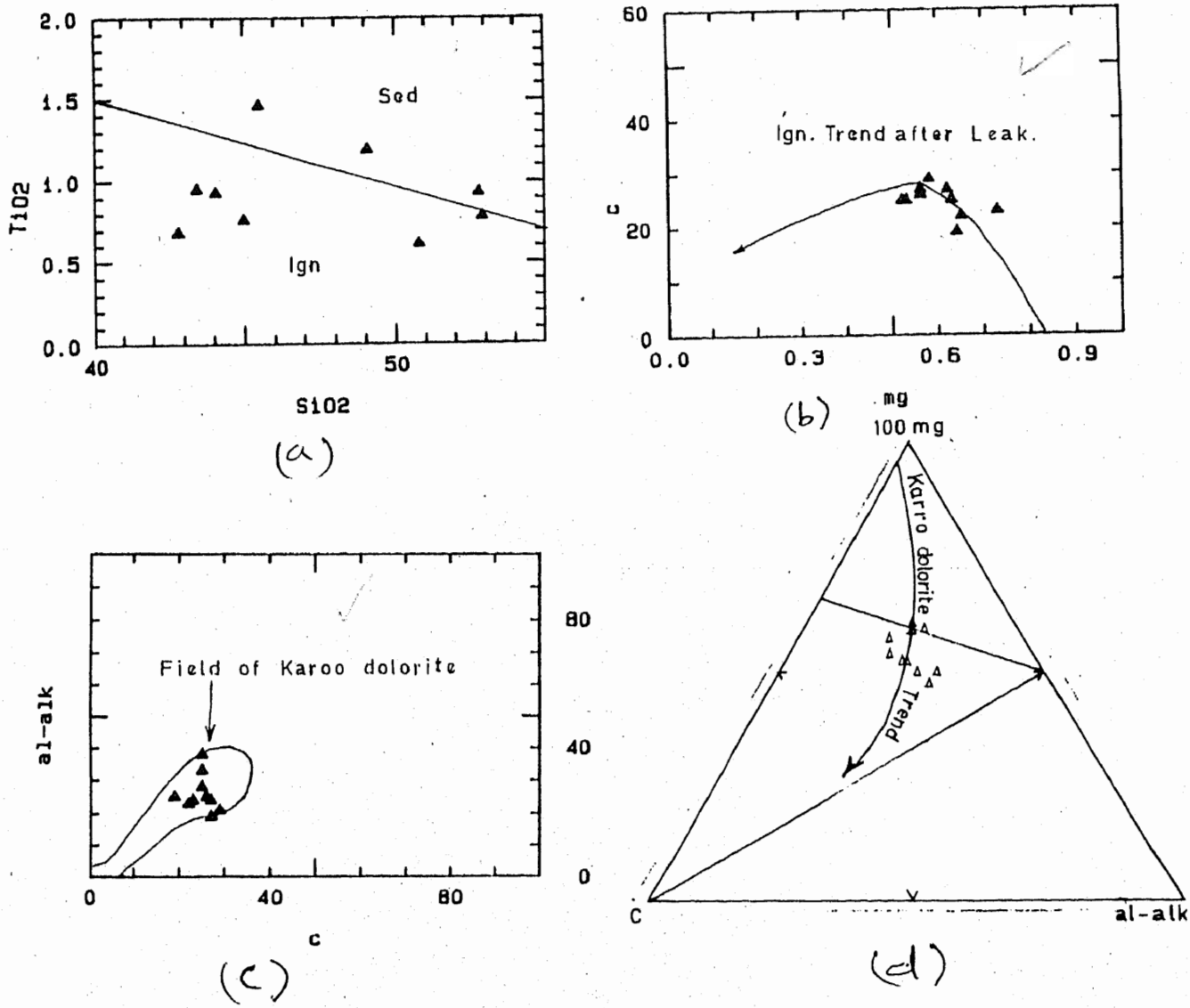

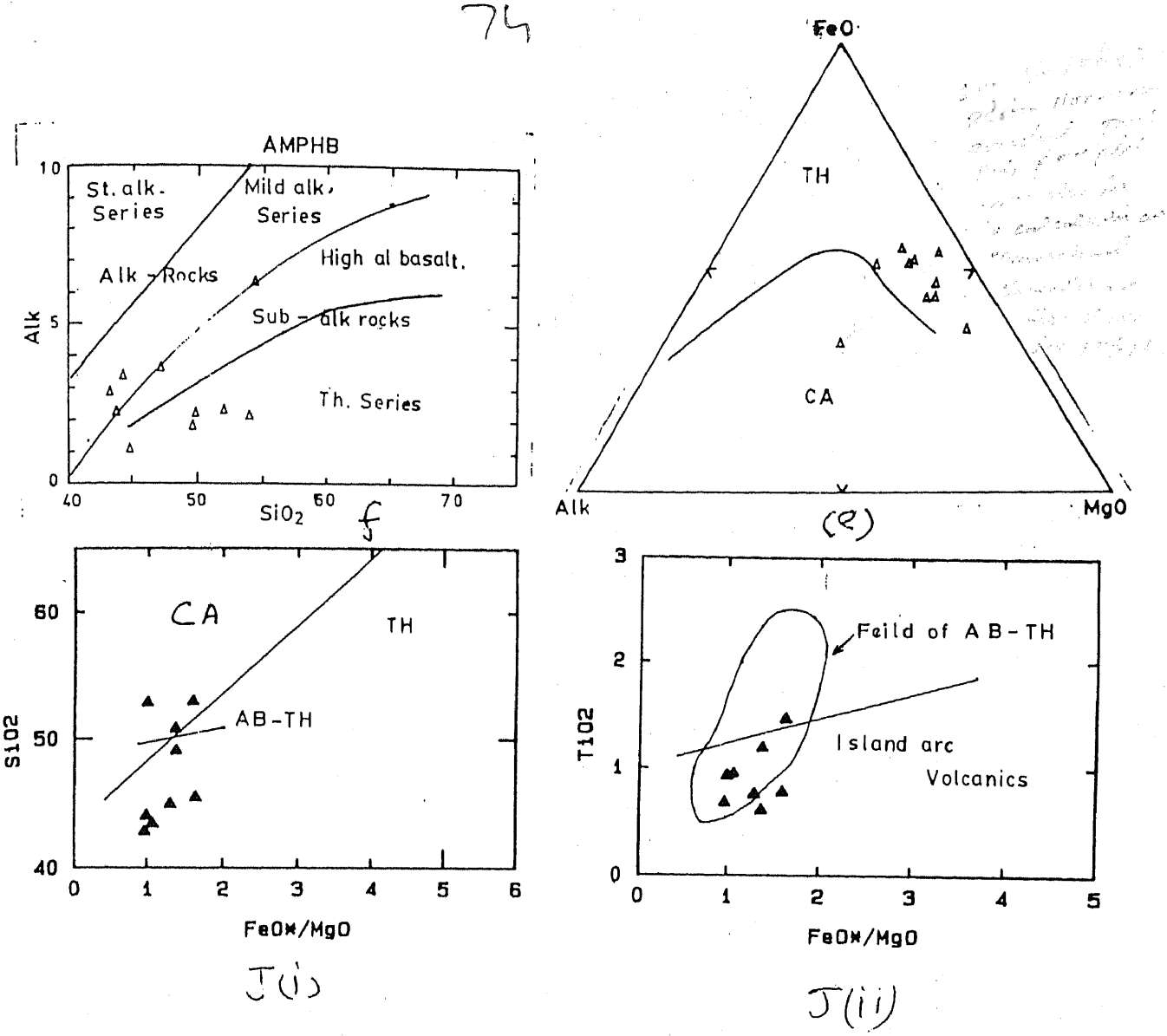

Fig 4.1e AFM plot for the amphibolites of Gantar area. The boundary lines are adopted from Irvine and Bargar (1971).

Fig. 4.1f Alk against SiO2 diagram for gantar amphibolites. Division lines are after Schwarzer and Roger (1974).

Fig.4.1ji-ii-iii. FeO/MgO vs SiO2,TiO2 and Feo plots for amphibolites of Gantar area . AB line and elliptical circle indicates abyssal tholeiitic trends and fields ,and the island arc volcanics are shown below the straight line in F/M -TiO2 plot of Miyashiro (1975).

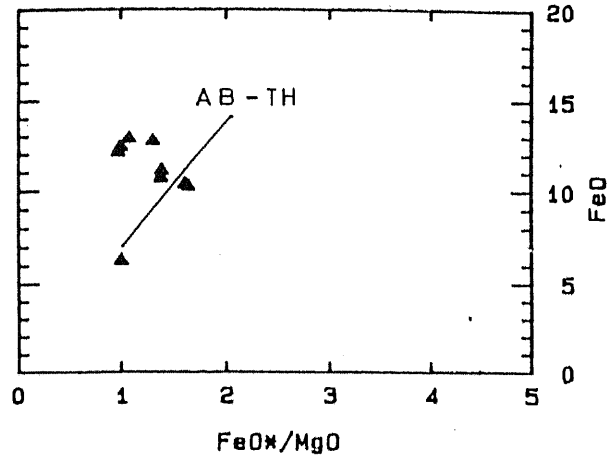

(i)

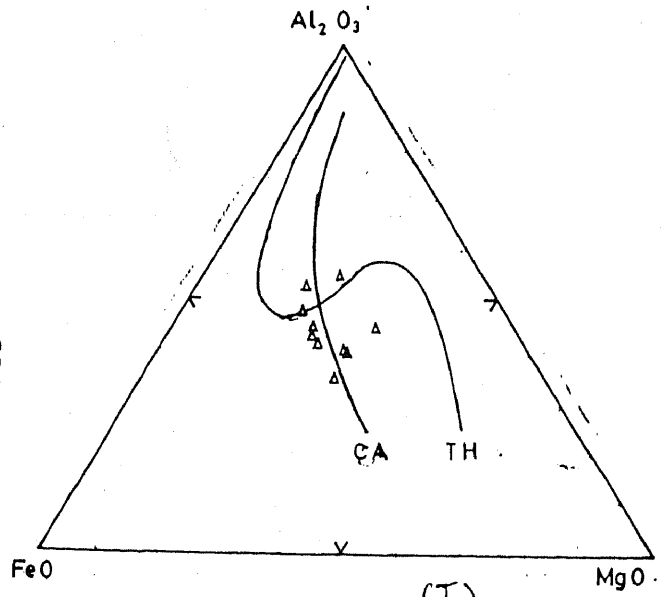

(I)

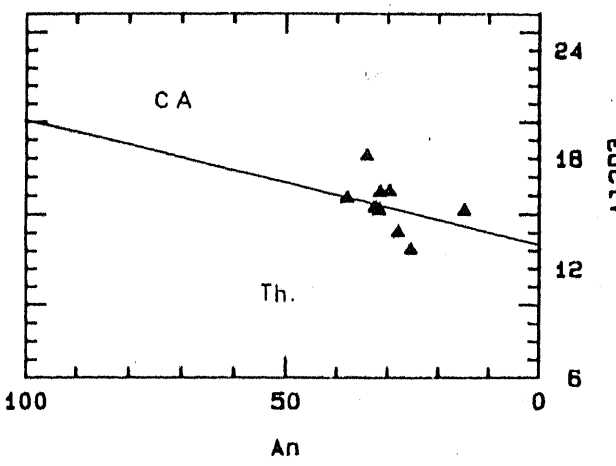

(g)

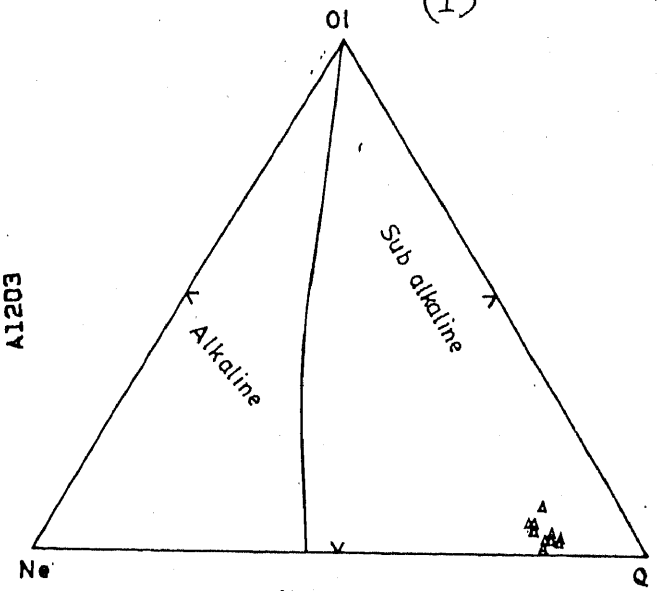

(h)

Fig.4.1g-h Al203 vs An% and Ne-Ol-Q plots for the amphibolites from Gantar area. Fields are after Irvine and Bargar (1971).

Fig. 4.1-i Al203-MgO-FeO triangular diagram for the Gantar amphibolites. trends are adopted from Besson and Fonteilles (1974).

these amphibolites again display both tholeiitic and calc-alkaline character(4.1g-I).

When plotted on FeO/MgO Vs SiO2 , FeO and TiO2 diagrams of Miyashiro (1975), the data follow abyssal tholeiitic trend, and also occur in the overlapping field of abyssal tholeiites and island arc volcanics(Fig.ji-iii).

Oxides Vs S.I plots investigates the fractionation history of the amphibolites, and these oxides were plotted against the solidification index i.e S.I=MgO*100/MgO+FeO+Fe2O3 +Na2O+K2O of Kuno (1972). The popular use of S.I as an index for fractionation in the amphibolites belts rocks has been discussed by Hamidullah and Hussain (1991 in press) in detail.

Continuous positive fractionation trends indicating crystallization differentiation and the control of ferro-magnesium phases like olivine and pyroxene on the liquidus are shown by MgO and FeO Vs S.I plot (Fig 4.1k). The very low FeO* in one of the sample (Table 4.1-A) is because of the considerable low Fe2O3 and can be related to analytical errors.

CaO is generally scattered against S.I with an overall positive trend, whereas Al2O3 shows a positive correlation with S.I in the S.I range of 35-46 and a negative correlation at S.I < 35, both features pointing towards the association of plagioclase with ferro-magnesium minerals during a course of crystallization.

Except one sample (Table 4.1A), SiO2 Vs S.I plot manifests a linear negative trend supporting the dominant role of ferro-magnesium minerals together with calcium-rich plagioclase. The general negative correlation of TiO2 with S.I indicates TiO2

enrichment in the liquids and the scarcity of TiO2 rich phase on the liquidus. The presence of some ilmenite in the norms however, shows that some TiO2 bearing phases were associated with ferromagnesium minerals on the liquidus and the scatter in the TiO2 Vs S.I plot may be reflective of such phenomenon.

Plots of total alkalies and P2O5 against S.I are scattered but a general negative correlation can be visualized. Such plots propose the concentration of these elements in the residual liquids. The scatter may , however, shows that alkali minerals (Na-bearing plagioclase) and apatite have also probably, played a minor role in the evaluation history of these rocks.The presence of apatite and albite in the norms support such a view point.

CMAS PLOTS

To confirm the interpretation obtained on the basis of oxides Vs. S.I plots, the data was also plotted in the CMAS tetrahedron model (O'Hara 1976) and were studied through projection into various planes. For the calculation of CMAS end members wt% oxide were used (see Cox et al., 1979).

A dominant plagioclase fractionation accompanied by pyroxenes and olivine is shown by the plot points of amphibolites lying close to the CAS2 (Pg) apex and with certain samples, showing affinities towards CMS2 (Diop) and M2S(Ol), in a projection from M2S into S-CAS2 - CMS2 plane. Similar interpretations can be drawn on the basis of data plots in a projection from MS (En) into CAS2-M2S-CMS2 (Fig4.1K i-ii). It is difficult to determine which of the two pyroxenes (Ortho or clino pyroxene) was dominant

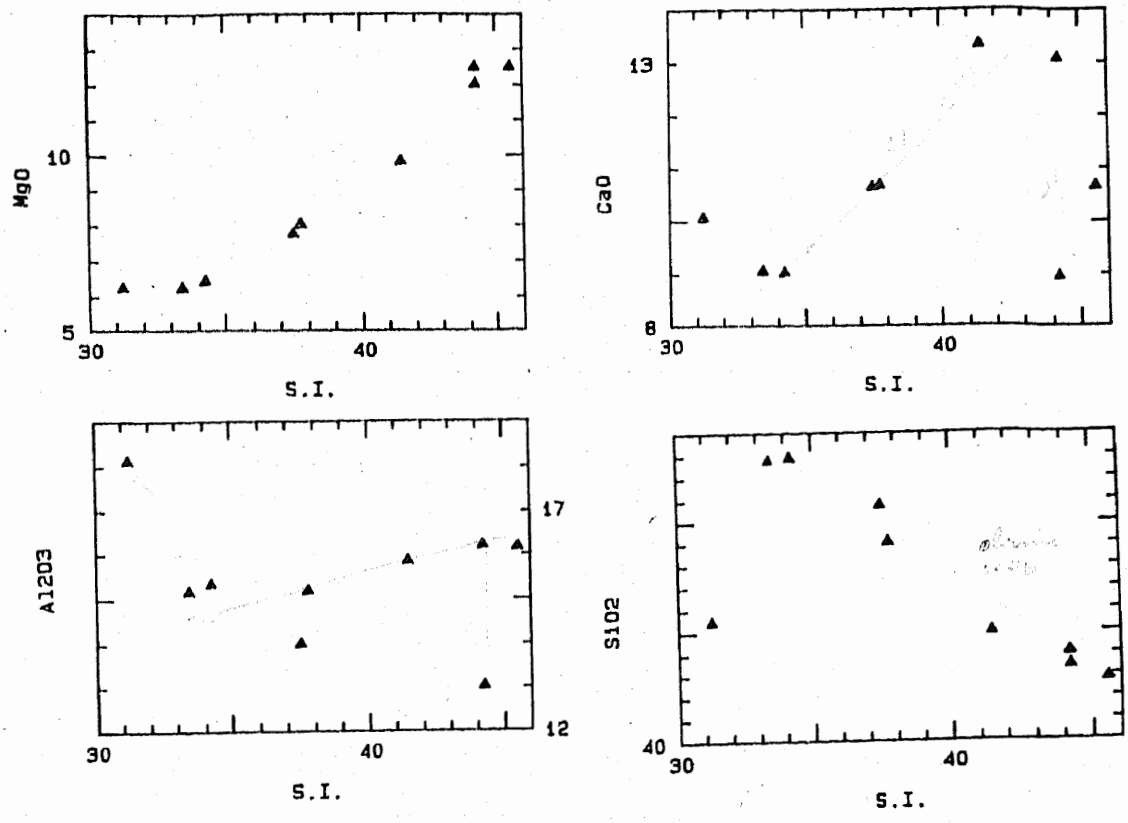

The major oxides against solidification index plots for Gantar and Kalalota amphibolites.

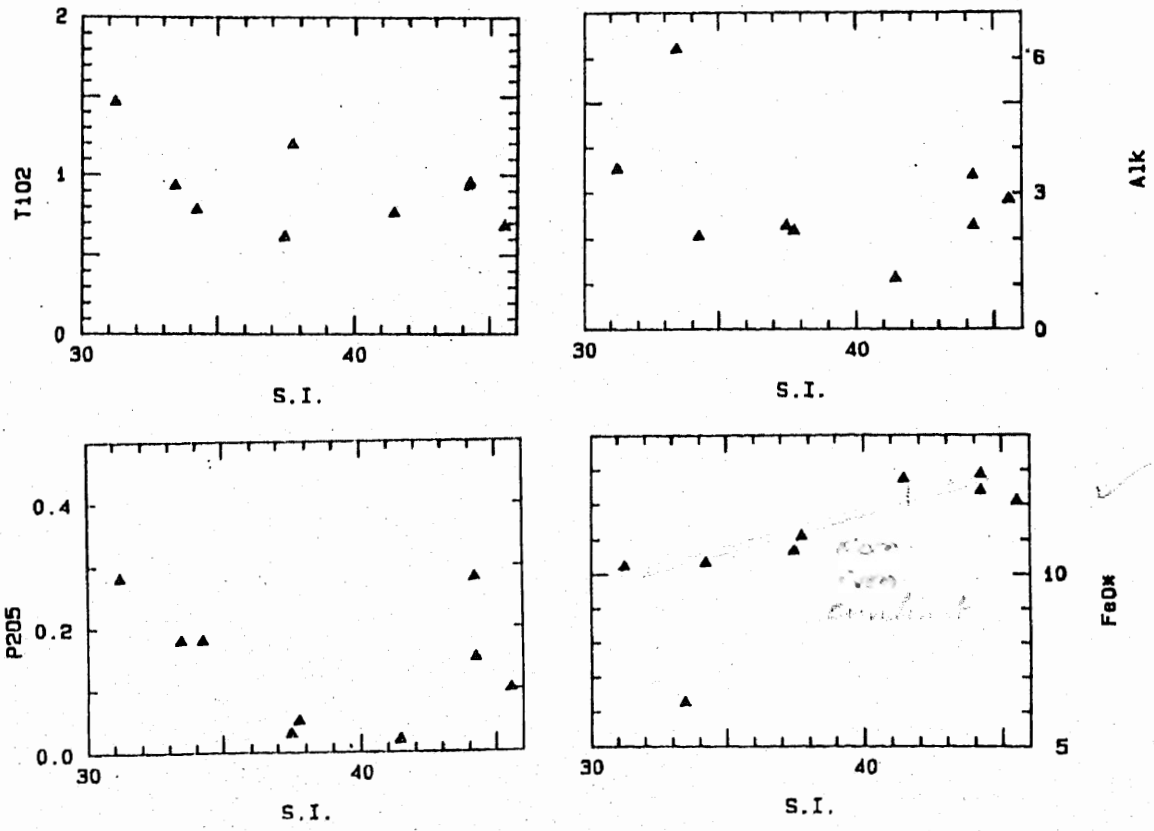

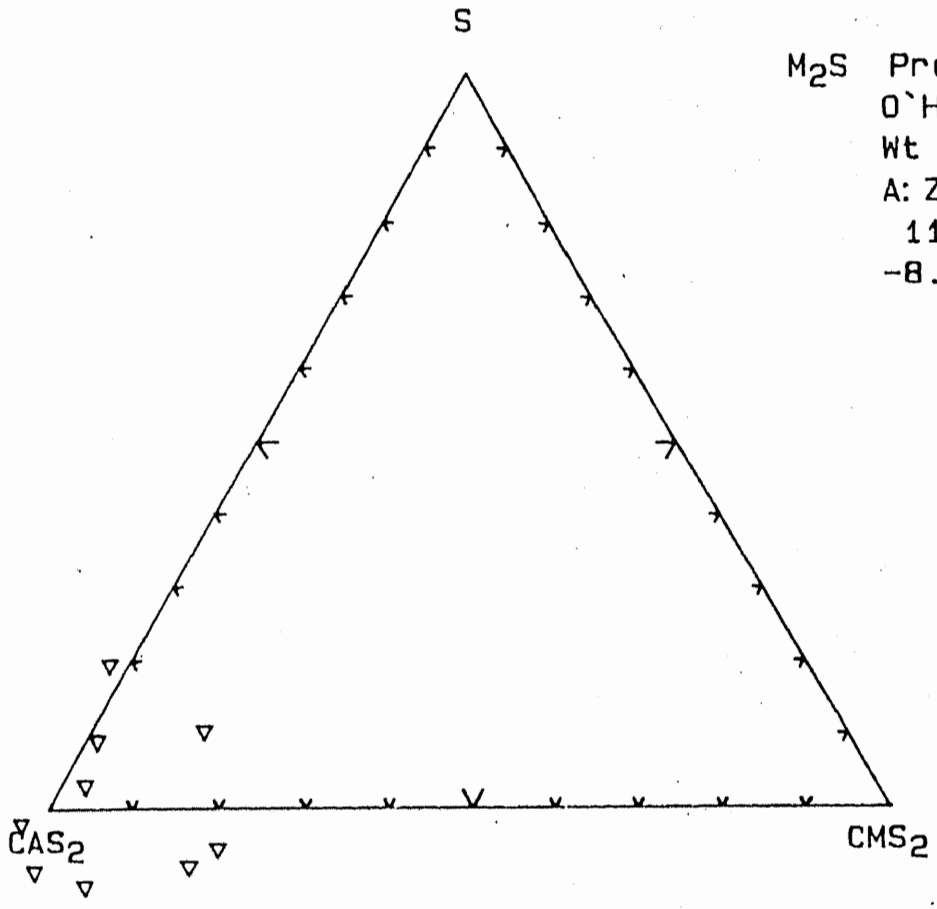

Fig. 4.1- i-ii. CMAS plots of Gantar amphibolites indicating projection from M2S (Ol) and MS(En) planes into S-CAS2(Pg)-CMS2(Diop) and CAS2-M2S-CMS2 planes of O Hara (1976).

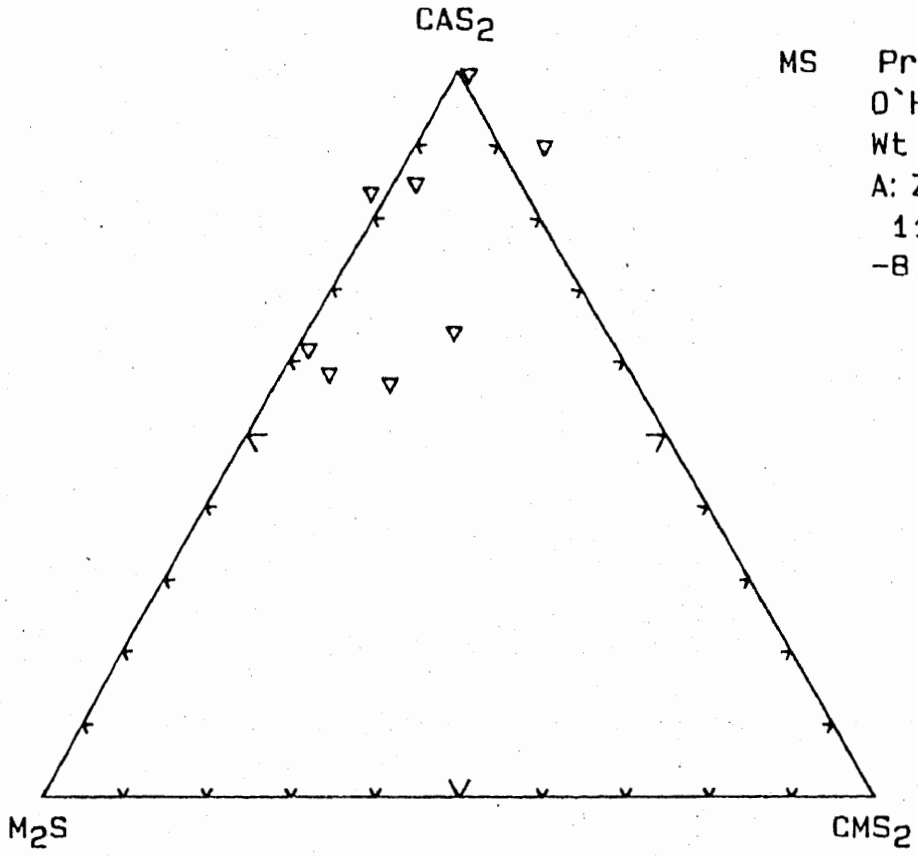

(ii)

pyroxene on the liquidus from the CMAS plots. The presence of hypersthene in the norms, however, shows that orthopyroxene may have played some role in the evaluation history of these rocks.

4.2 Geochemistry of Lavas

Major element data along with C.I.P.W Norms of the selected lavas are presented in (Table 4.2.A), limited chemical variation can be noticed in this data.

On the basis of SiO2 vs alk diagram of Cox et al. (1979) majority of the lavas plot in the field of basalt and basaltic andesite, while some analysis also plot in the field shown for picritic basalt. (see Fig. 4.2 a). Based on the K2O- SiO2 plot of Ewart (1982) the data falls in the field of low -K- thoeiilite (Fig 4.2b). On the alkali vs SiO2, FeO/MgO vs SiO2, Al2O3 vs An% Ol-Ne-O and AFM diagrams (Fig 4.2b- c-d-e-f-g) the lavas exclusively, plot in the field defined for tholeiites rather than calc-alkaline field. on the CaO vs Na2O plot of Vallance (1974), the lavas are classified as non spilitic. (Fig 4.2 h).

To envisage the tectonic set up for the emplacement of these lavas data, were plotted on TiO2 vs FeO/MgO plot of Miayshiro 1975), on which these data show Island arc Volcanic character (4.2 i).

A linear positive correlation trend reflecting fractionation and dominancy of ferromagnesium minerals like olivine, orthopyroxene and clinopyroxene on the liquidus, are shown by MgO vs S.I plot (4.2k). Marked differences in the type and proportion of fractionation phases are revealed by the FeO, SiO2, TiO2, CaO, Al2O3 and Alk. vs S.I plots at S.I values above and below 23. FeOt (FeO and Fe2O3 together and separatly) TiO2 and CaO decreases, while Al2O3, SiO2 and Alk. increases with S.I above 23, indicating the control of clinopyroxene olivine/ orthopyroxene,

TABLE 4.2 THE CHEMICAL ANALYSES AND C.I.P.W NORMS OF LAVAI KOHISTAN

File name A:CZAL23.ROC

Sample	AL13	AL14	AL15	AL16	AL17	AL18	AL19
Group #	2.00	2.00	2.00	2.00	2.00	2.00	2.00
Qual	2	2	2	2	2	2	2
Key	1	1	1	1	1	1	1
Ref	2	2	2	2	2	2	2
SiO_2	52.45	55.31	52.51	47.63	51.11	53.53	52.57
TiO_2	1.60	0.99	1.94	3.38	0.95	1.90	1.33
Al_2O_3	16.20	16.69	14.97	14.06	15.60	16.12	16.81
FeO	12.56	11.95	12.92	15.22	11.16	10.88	8.29
MnO	0.21	0.21	0.20	0.18	0.23	0.24	0.22
MgO	5.66	4.84	5.99	5.34	3.21	3.10	3.47
CaO	10.27	9.43	10.65	6.95	16.36	12.45	13.05
Na_2O	0.74	0.26	0.27	4.88	0.99	1.29	3.03
K_2O	0.03	0.04	0.00	1.30	0.06	0.03	0.03
P_2O_5	0.27	0.27	0.55	1.08	0.33	0.47	1.20
Total	100.00	100.00	100.00	100.00	100.00	100.00	100.00
S.I	29.800	28.260	31.230	19.980	20.800	20.280	23.420
Q	13.170	18.840	16.090	0.000	3.290	14.540	5.770
Or	0.180	0.240	0.000	7.270	0.300	0.180	0.180
Ab	5.750	2.030	2.120	34.330	7.530	10.070	23.520
An	37.490	40.310	36.860	11.980	34.110	35.090	29.590
Ne	0.000	0.000	0.000	2.580	0.000	0.000	0.000
Di	6.360	0.560	7.330	11.490	30.990	15.860	18.820
Hy	21.570	23.610	21.520	0.000	3.140	8.450	6.990
Ol	0.000	0.000	0.000	12.300	0.000	0.000	0.000
Mt	4.310	3.480	4.780	6.810	3.410	3.900	2.320
Il	2.790	1.710	3.420	6.080	1.610	3.320	2.320
Ap	0.580	0.580	1.180	2.360	0.700	1.000	2.550
FeO%	12.56	11.95	12.92	15.22	11.16	10.88	8.29
Mg#	0.338	0.315	0.345	0.285	0.246	0.245	0.322
den	2.70	2.67	2.72	2.73	2.71	2.67	2.63

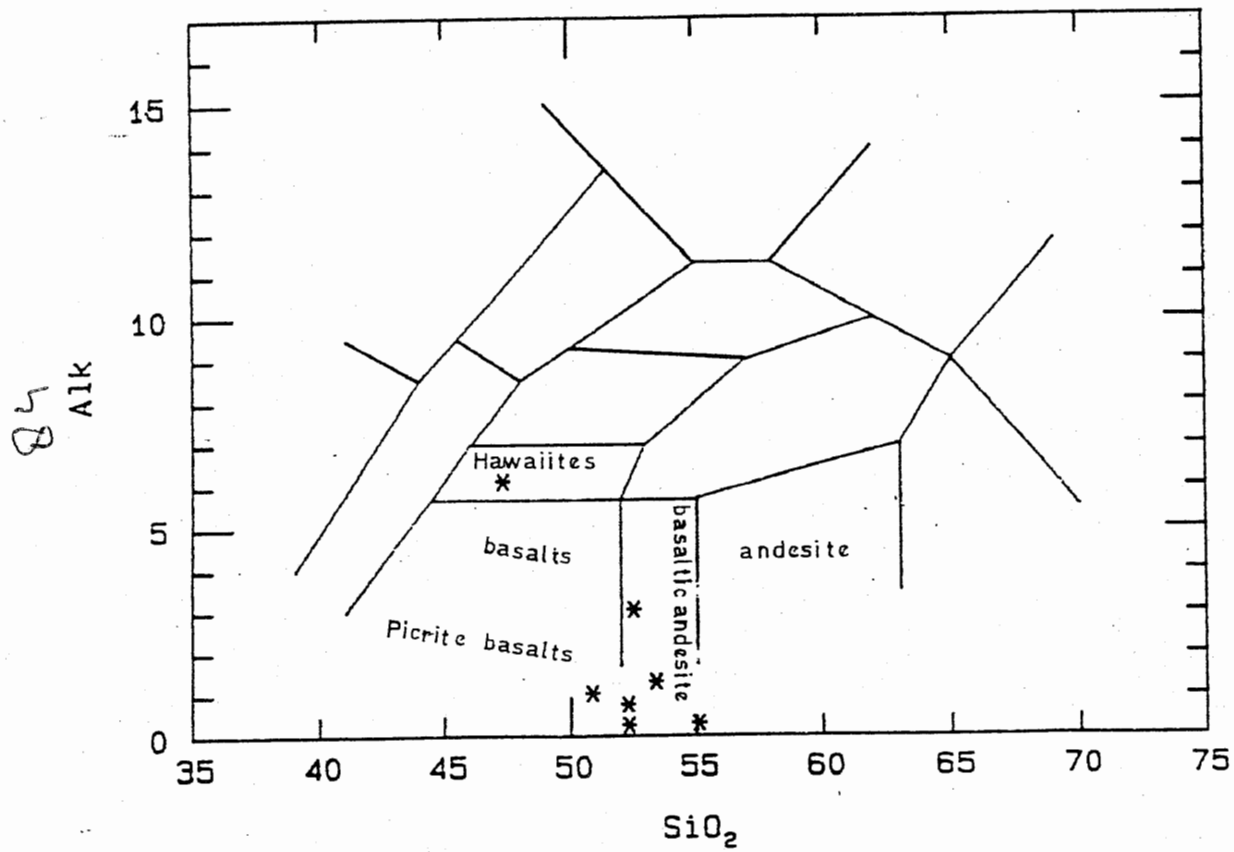

Fig.4.2a. Nomenclature of normal volcanic rocks on the basis of SiO2 vs Na2O+K2O diagram for Allai Kohistan lavas. Boundaries are taken from Cox et al.(1979).

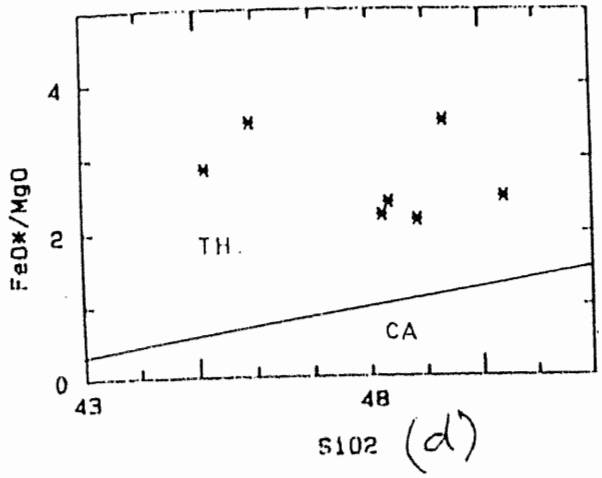

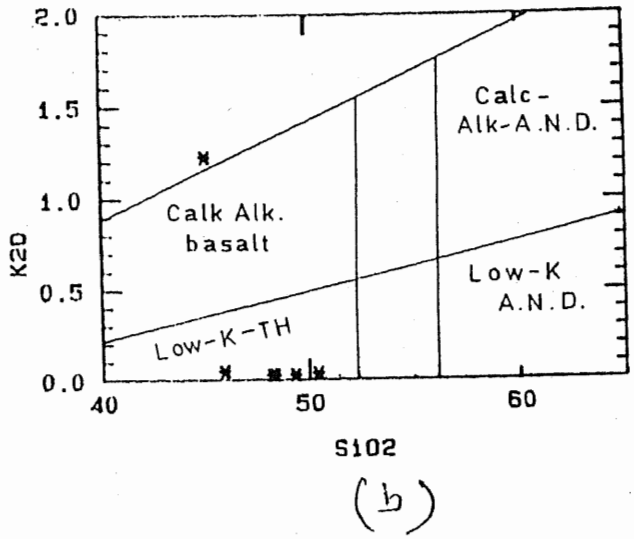

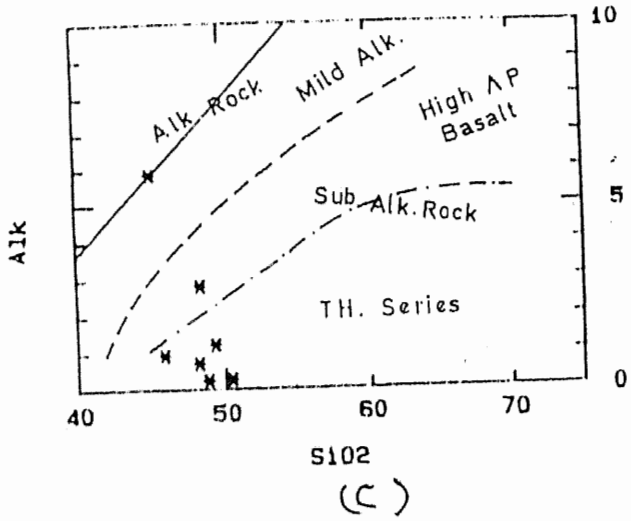

Fig.4.2b. Classification of lavas on the basis of K2O against SiO2 plot for Allai Kohistan lavas, with boundaries from Ewart (1982) modified from Peccerillo and Taylor (1976).

Fig. 4.2c. Alk vs SiO2 plot for Allai Kohistan lavas. Division lines are adopted after Schwarzer and Roger (1974).

Fig.4.2 d. FeO/MgO vs SiO2 plot for the lavas from Allai Kohistan. Boundary are after Miyashiro (1974).

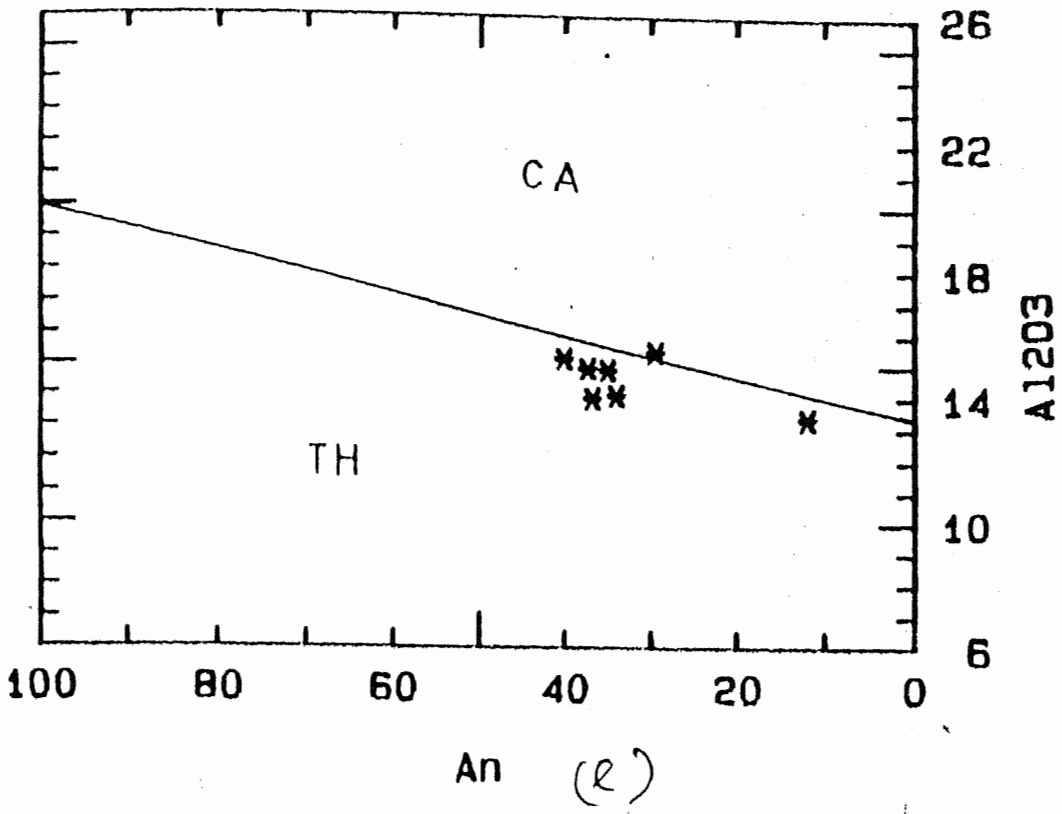

Fig.4.2e,f,g. A1203 vs An% , Ol-Ne-Q and AFM plots for Allai Kohistan lavas, with boundaries from Irvine and Bargar (1971).

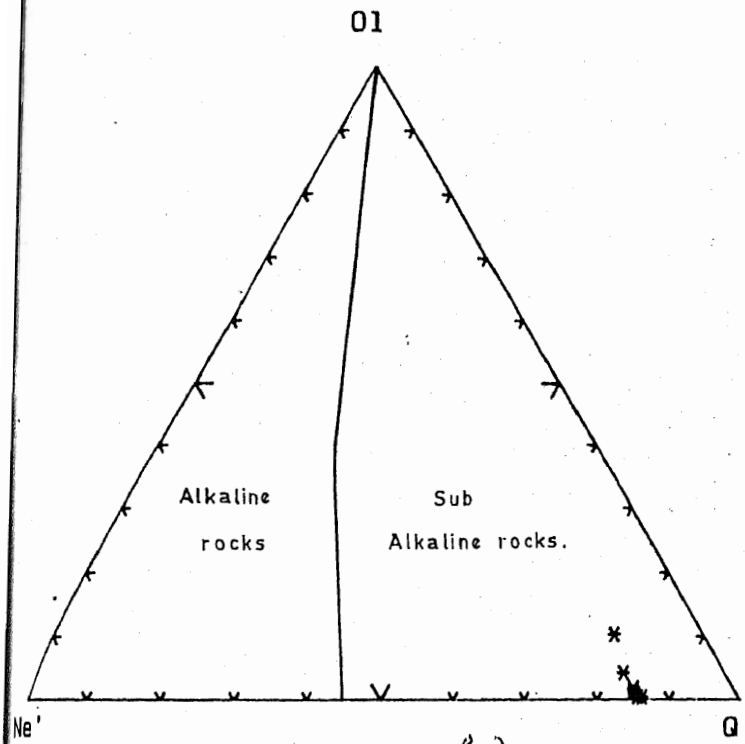

(f)

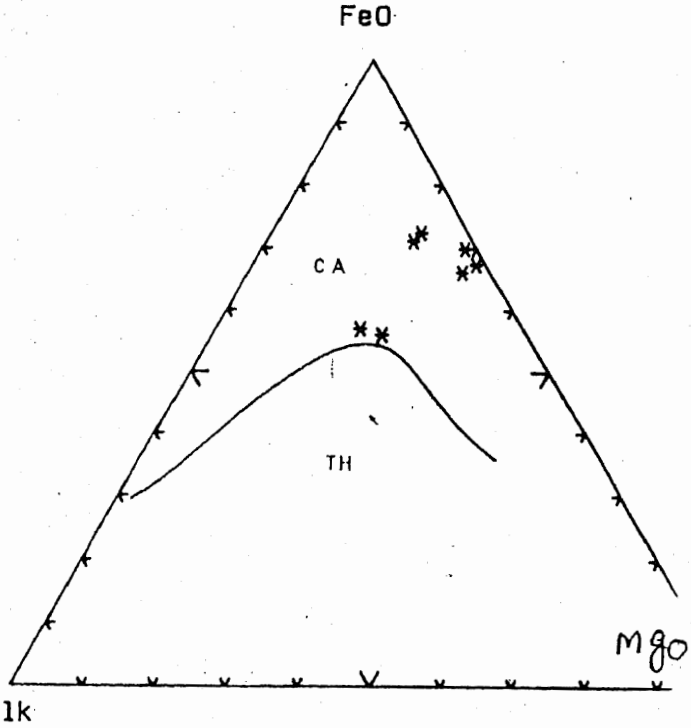

(g)

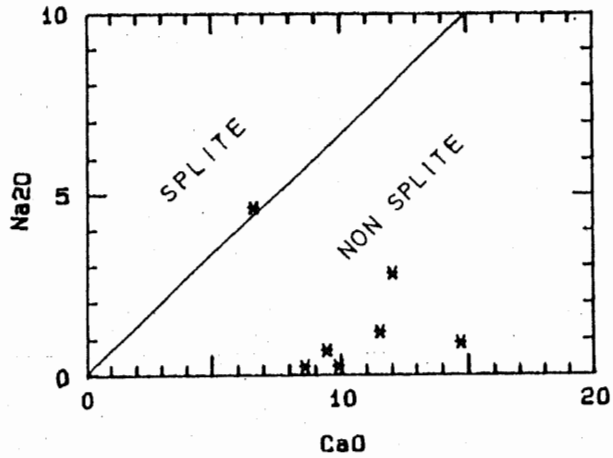
10
5
0
Na2O
SPLITE
NON SPLITE
0
10
20
CaO

(ㄴ)

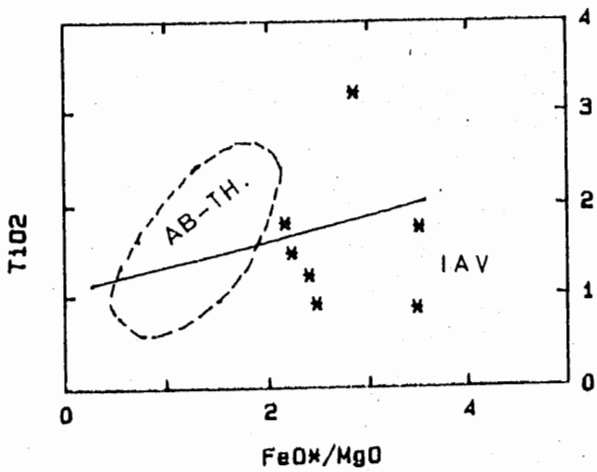
4
3
2
1
0
TiO2
AB-TH.
IAV
0
2
4
FeO*/MgO

(ㄱ)

titano-magnetite/ilmenite in the liquidus. At S.I 23 FeOt (FeO and Fe2O3 together and also separatly behaves similarly) and TiO2 increases suggesting iron enrichment at the latter stage of crystallization. CaO, SiO2 and Al2O3 has been shown a sharp drop reflecting a dominant role of plagioclase crystallization on the liquidus during the last phase of fractionation.

CMAS plots

The data generally plot close to the CAS2 apex in a projection from MS into CAS2-M2S-CMS2 plain, indicating an overall dominant plagioclase fractionation. The general trend like oxide vs S.I. plot, however, can be divided into two parts in this projection A-B and B-C. On the A-B portion of the trend with analysis line towards the CMS2 free side of the M2S-CAS2 join indicates the probable crystallization of a SiO2 under saturated minerals like olivine and/or Spinel. The rest of the A-B trend indicate affinities towards CMS2 indicating some control of cliopyroxene. The B-C portion of the general trend, however follows a sharp bend and much high affinities towards the plagioclase apex, showing the greater control of plagioclase in the later stage of the fractionation. More or less similar interpretation can be obtained from the plot pattern lying along the CMS2-CAS2 join in a projection from M2S to S-M2S-CAS2 plane, indicating the overall dominant role of palgioclase and subordinate clinopyroxene fractionation (Fig. 1 i-ii-iii).

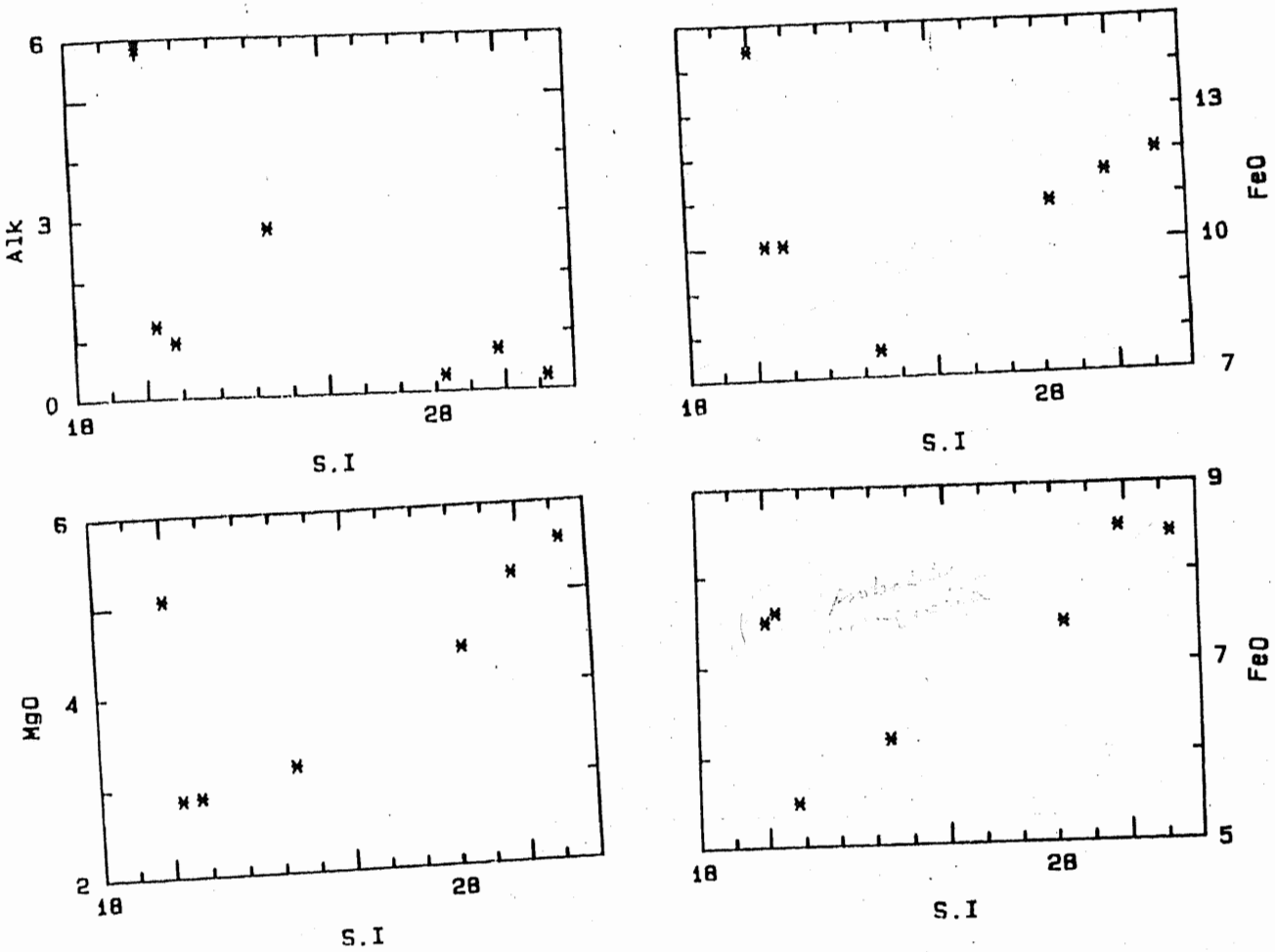

Major oxides Vs. Solidification index

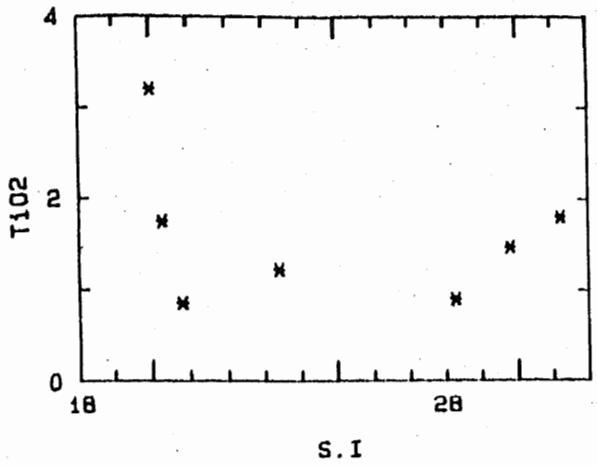
4
2
0
T102
18
28
S.I

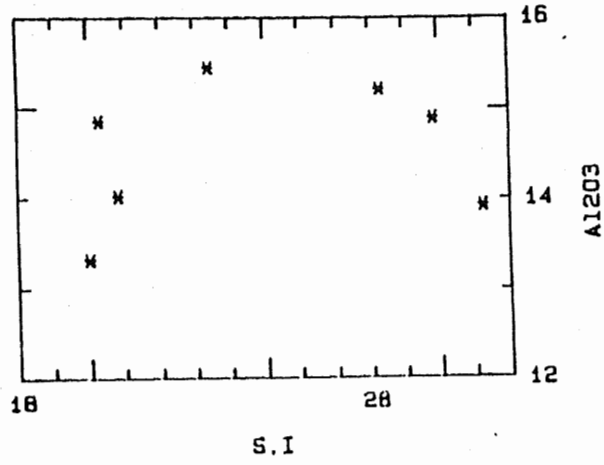
16
14
12
Al203
18
28
S.I

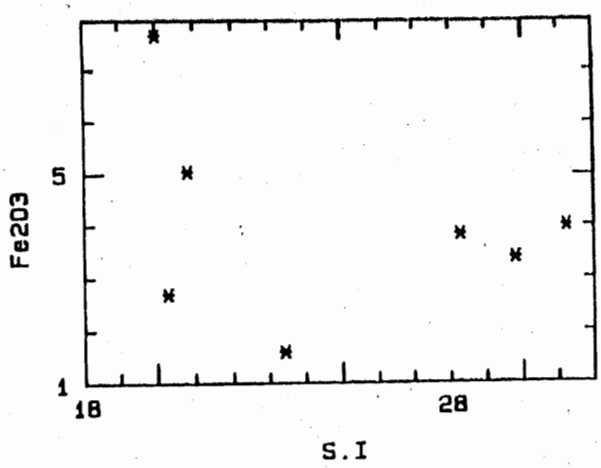
5
1
Fe203
18
28
S.I

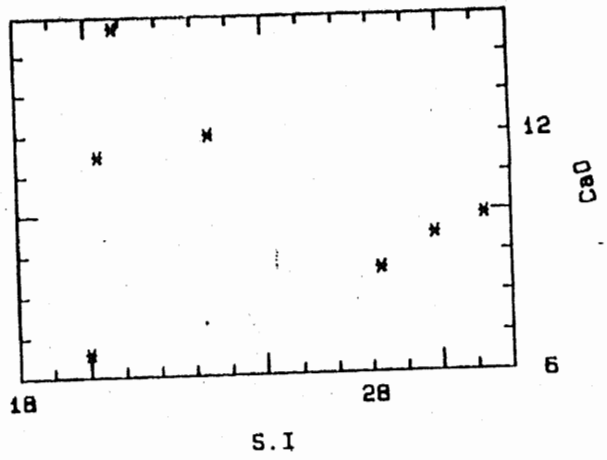
12
6
CaO
18
28
S.I

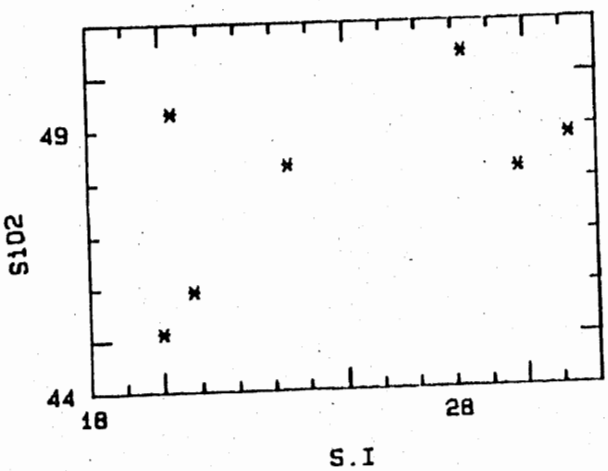
49
44
Si02
18
28
S.I

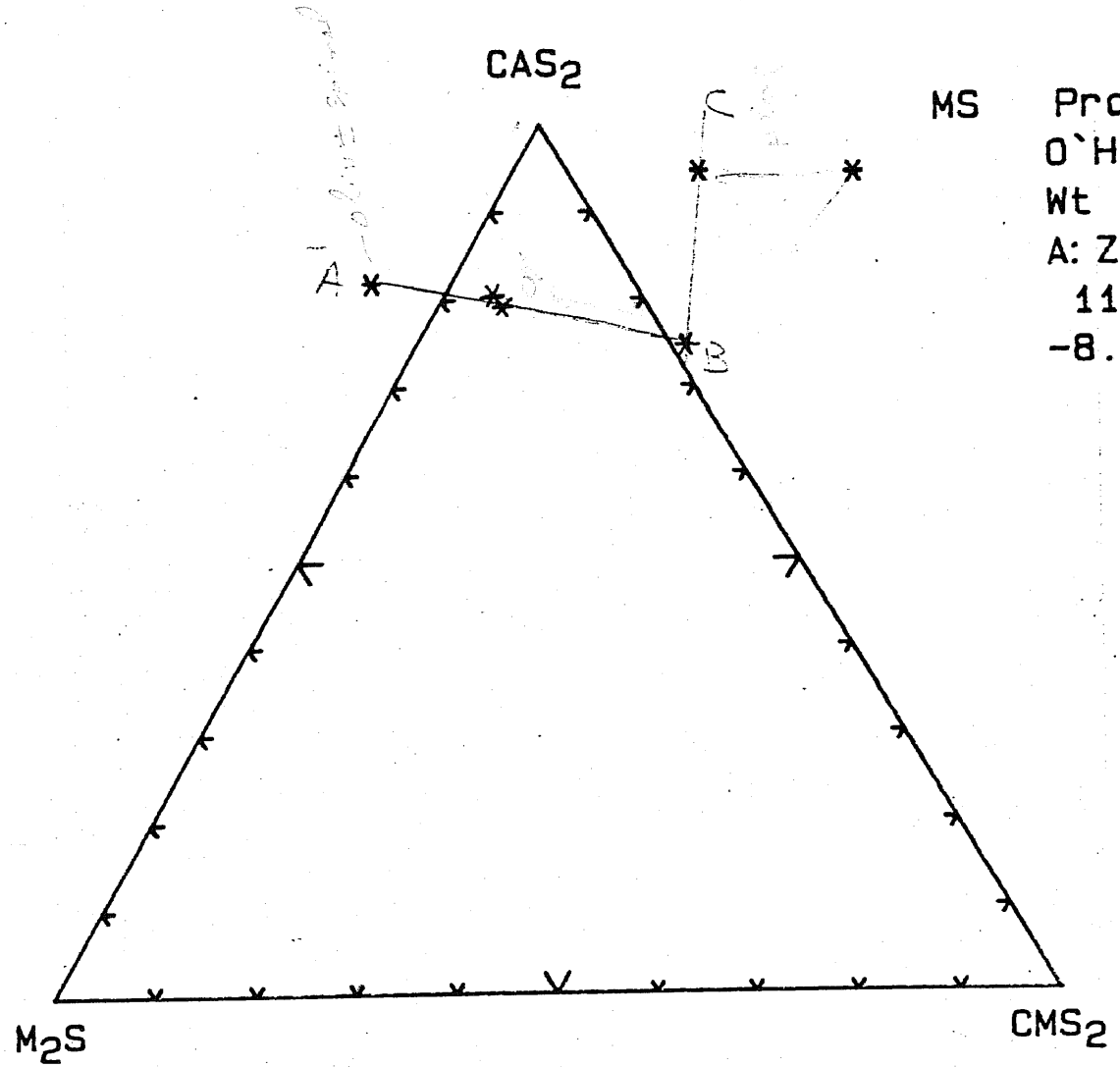

MS Proj
O`Hara 68
Wt %
A: ZAL23.ROC
1150
-8.16

92

CMAS plots of volcanic rocks from study area.

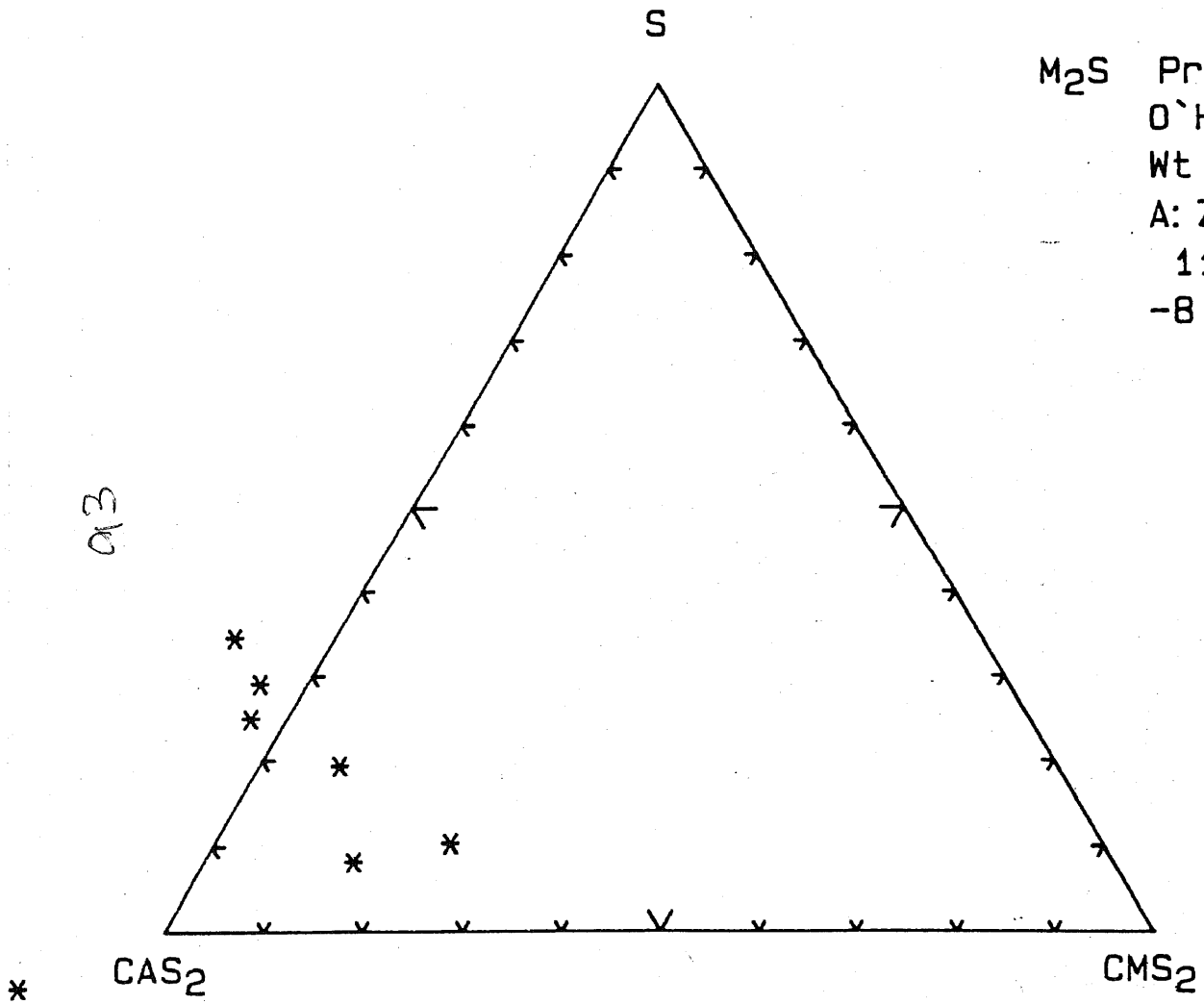

M_2S Proj
O`Hara 68
Wt %
A: ZAL23.ROC
1150
-8.16

a3

4.3 ROCK CHEMISTRY OF BASIC/ULTRABASIC ROCKS

Representative data including major element analyses and CIPW norms of the basic and ultrabasic rocks are shown in the (Table 4.3A). The data was obtained from the personal collection of S.Hamidullah, NCE in geology. The petrography of these analyses was performed by (Hamidullah et al,. 1976 and Baluch et al,. 1982).

On the AFM plot of Mccell (1973) majority of the analyses plot in the field defined for Mg-basalt and ultramafic rocks of the E.ld field region of eastern Australia. Three analyses plot along the MgO-FeO join, indicating iron enrichment whereas one sample plot along the trend defined for the calc - alkaline rocks (Fig.4.3a). On the AFM plot of Beard (1986) Barker and Aarth (1976), these data occur in the field of ultramafic cumulates (4 analyses), mafic cumulates (3 analyses) and non cumulates (3 sample)(4.3b). on the Al2O3-SiO2-MgO plot of Wilson(1971) the data cluster in the field of common layered ultrabasic and basic rocks (Fig.4.3c). The data straddle along the boundary between calcalkaline and tholeiitic field on Al2O3-FeO -MgO, Al2O3 vs An % and Feo/MgO vs SiO2 plots (see Fig. d-e-f).

OXIDE VS S.I. AND CMAS PLOTS

As expected on the basis of the petrographic data more or less linear trends, showing crystallization differentiation and the control of ferromagnesium minerals are shown by the majority of oxide vs S.I plots of the basic and ultrabasic rocks. MgO show

TABLE 4.3 THE COMPOSITION OF MAJOR ELEMENT AND C.I.P.W NORMS OF MAFIC/ULTRAMAFIC

File name A:CZAL22.KOC

Sample	AL1	AL2	AL4	AL6	AL7	AL3	AL4	AL5	AL8
Group #	1.00	1.00	1.00	1.00	1.00	3.00	1.00	1.00	1.00
Qual	1	1	1	1	1	0	1	1	1
Key	3	3	3	3	3	3	3	3	3
Ref	1	1	1	1	1	0	1	1	1
SiO_2	48.44	46.62	47.00	49.16	50.78	45.99	45.11	46.41	44.84
TiO_2	0.00	0.88	3.12	0.00	0.00	4.28	0.00	0.00	0.00
Al_2O_3	20.21	16.71	23.18	22.13	21.74	18.84	14.40	16.38	16.82
FeO	7.39	15.12	10.25	9.42	7.40	7.30	3.33	6.66	6.25
MnO	0.13	0.15	0.15	0.11	0.24	0.29	0.11	0.10	0.09
MgO	7.85	6.97	3.64	6.47	7.13	11.80	19.09	29.13	30.52
CaO	13.28	12.06	6.55	11.93	10.52	10.91	17.81	0.00	0.03
Na_2O	1.93	1.15	5.34	0.38	1.74	0.16	0.00	0.76	1.01
K_2O	0.26	0.00	0.39	0.00	0.05	0.05	0.00	0.11	0.00
P_2O_5	0.47	0.34	0.38	0.42	0.40	0.38	0.16	0.46	0.43
Total	100.00	100.00	100.00	100.00	100.00	100.00	100.00	100.00	100.00
S.I	45.160	29.990	18.540	39.780	43.680	61.430	85.150	80.540	80.770
Q	0.000	0.000	0.000	6.340	3.550	4.420	0.000	0.000	0.000
Or	1.420	0.000	2.250	0.000	0.300	0.300	0.000	0.590	0.000
Ab	14.810	8.880	39.780	2.960	13.710	1.350	0.000	6.010	8.380
An	41.430	36.950	28.840	52.620	46.100	49.560	36.590	2.810	2.600
Ne	0.000	0.000	2.010	0.000	0.000	0.000	0.000	0.000	0.000
C	0.000	0.000	2.880	0.770	0.600	0.000	0.000	14.970	15.770
Di	12.540	13.050	0.000	0.000	0.000	0.870	27.020	0.000	0.000
Hy	9.310	24.790	0.000	27.610	25.830	29.910	0.000	61.280	51.040
Ol	8.120	2.350	7.850	0.000	0.000	0.000	24.460	9.870	23.020
Mt	2.170	3.330	6.520	2.170	2.170	3.070	1.660	2.170	1.280
Il	0.000	1.520	5.700	0.000	0.000	7.980	0.000	0.000	0.000
Ap	1.000	0.720	0.860	0.900	0.860	0.860	0.350	1.000	0.970
CDS	0.000	0.000	0.000	0.000	0.000	0.000	3.180	0.000	0.000
FeO#	7.39	15.12	10.25	9.42	7.40	7.30	3.33	6.66	6.25
Mg#	0.548	0.344	0.287	0.438	0.522	0.647	0.867	0.832	0.847
den	2.66	2.79	2.65	2.68	2.63	2.74	2.74	2.74	2.75

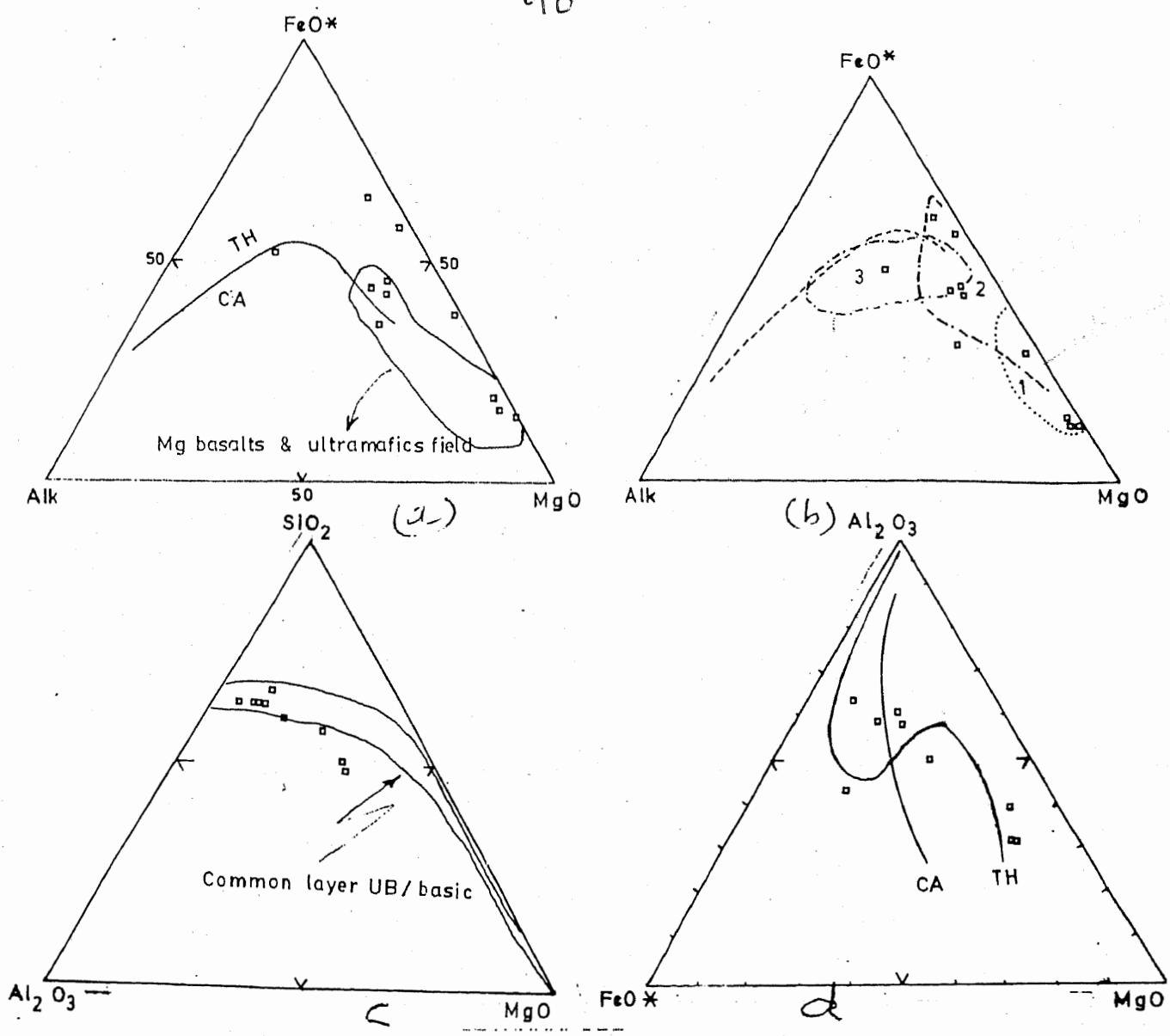

Fig. 4.3a. Plot of AFM for Allai-Kohistan mafic/ultramafic rocks with boundaries from Mccell (1973) and indicate calc-alkaline (CA) tholeiitic (TH) fields of Irvine and Bargar (1971).

Fig.4.3b. MgO-FeO-Na20+K20 diagrams of the analyzed rocks indicating (1) fields of ultramafic cumulates (2) mafic cumulates (3) non-cumulates (after Beard, 1986).

Fig.4.3c. Plot of Al203-Si02-MgO modified for the Allai-Kohistan mafic/ultramafic rocks, field adopted from Wilson (1971).

Fig.4.3d. Al203-FeO-MgO triangular diagram for the Allai-Kohistan mafic/ultramafic rocks. Trends are after Besson and Fonteilles (1974).

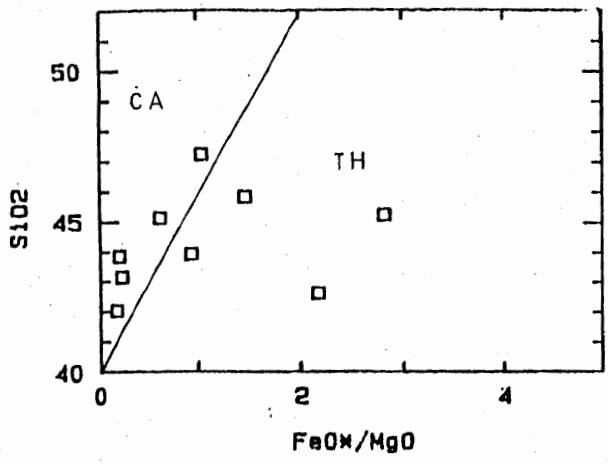

(f)

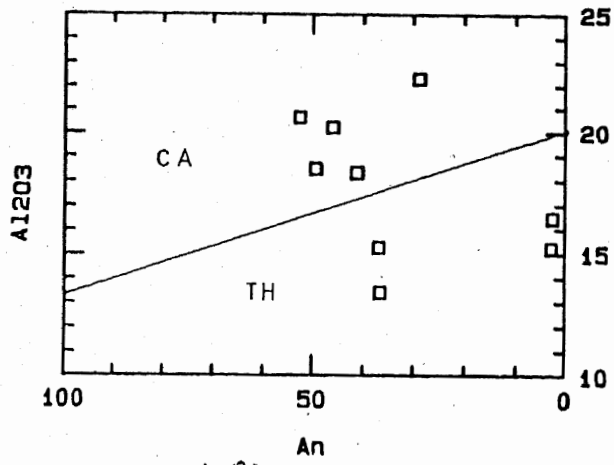

(e)

Fig.4.3e. Al2O3 vs An% plot for the Allai-Kohistan mafic/ultramafic rocks with boundaries of Irvine and Bargar (1971).

Fig.4.3f. FeO*/MgO against SiO2 plot for the Allai-Kohistan mafic/ultramafic rocks with distinction between calc-alkaline (CA) and tholeiitic (TH) fields of Miyashiro (1974).

a sharp decrease in the initial stage of fractionation at S.I > 75, indicating the sole control of olivine ± pyroxene. At S.I < 75 the slope of the trend becomes gentle, probably indicating pyroxene dominating olivine on the liquidus. On the Ca vs S.I plot the data of the ultramafic rocks (S.I > 55) shows various combinations of phases on the liquidus i.e. (i) Ca poor ultramafic rocks (Table 4.3A), where very low CaO (0.0-0.3 wt %) indicating the accumulation of olivine/ orthopyroxene ± spinel, (ii) Ca rich ultramafic with a considerable clinopyroxene accumulation and (iii) ultramafic with Ca-midway between the two groups, indicating the crystallization and differentiation of olivine/orthopyroxene and clinopyroxene together. On the CaO vs S.I plot at S.I < 55 the general trend shows decreasing CaO , pointing to a major control of clinopyroxene in the basic rocks.

The increasing Al2O3 with decrease in S.I (Fig. 4.3g) , indicates that plagioclase fractionation has not played a dominant role in the evaluation of these rocks. The initial increasing SiO2 in ultramafic rocks is consistent with this view point, however, the scatter of the data in the basic rocks shows plagioclase fractionation on the SiO2 vs S.I plots. The overall increasing total iron with decreasing S.I. and a linear negative correlation on the FeO* vs S.I plot, indicate a strong iron enrichment in the residual liquid, Which manifest that (i) during the ferromagnesium minerals fractionation had a MgO/FeO* > 1 (Mg rich olivine, orthopyroxene and clinopyroxene) and (ii) spinel played no role in the evaluation history of these rocks.

The increasing total alkali with the decreasing S.I signify

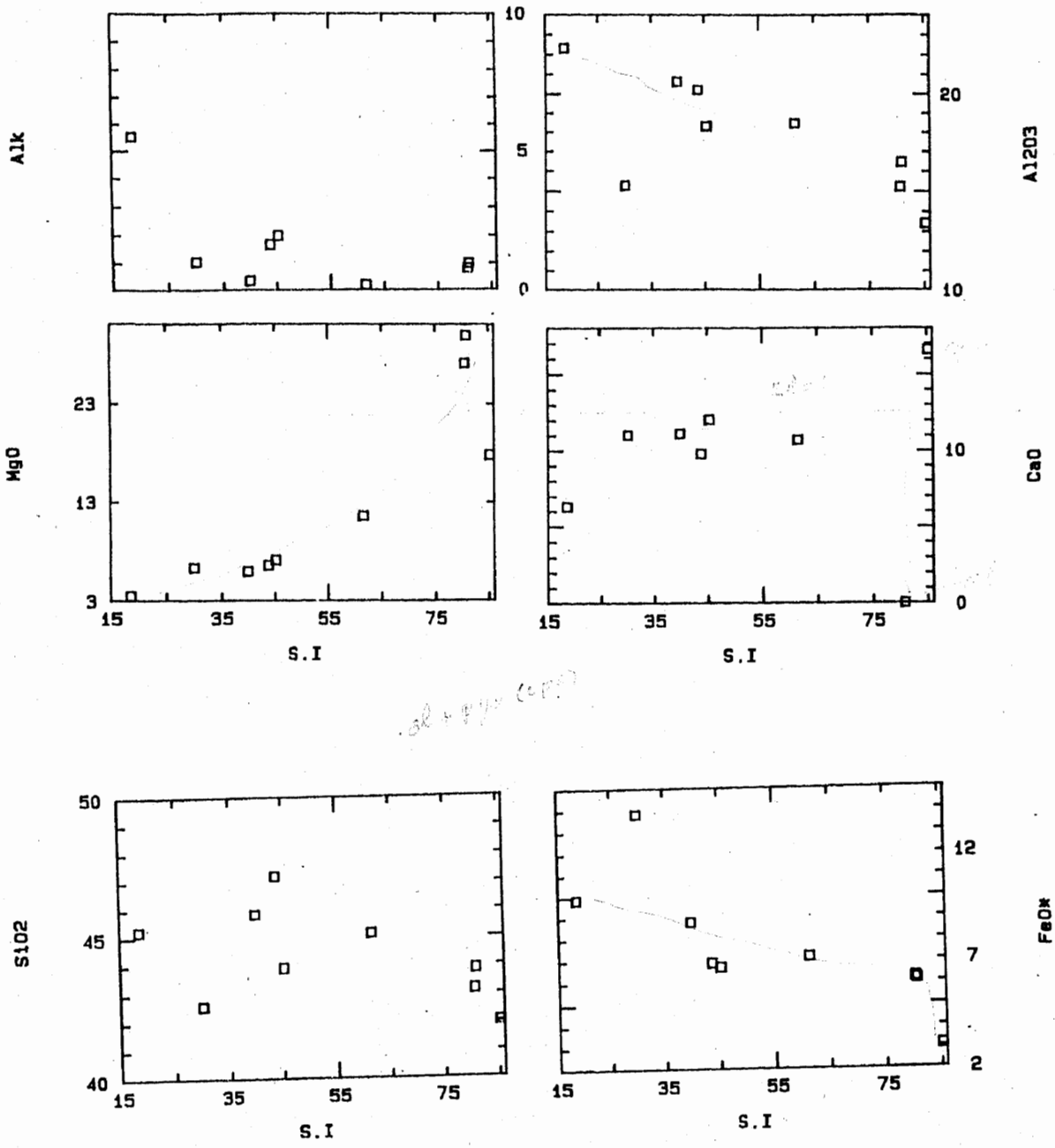

Major oxides Vs. Solidification index.

that the concentration of these elements in the residual liquid. The interpretation made for the oxide vs S.I plots are supported by the data plots in a projection from S plane into CAS2-MS2-CMS2 plane, indicating Ca poor ultramafics, plotting beyond the CAS2-M2S join of the triangular plots (outside the plot), and also reflect olivine and/or orthopyroxene fractionation. The Ca rich ultramafic, plotting in the middle of the plot, envisage equal role of clinopyroxene, plagioclase and olivine / orthopyroxene and finally the mafic rocks showing higher affinities towards the plagioclase apex, suggest the generally dominant role of plagioclase fractionation on the liquidus in these rocks. Similar interpretation can be obtained on the basis of data plots of these rocks in other projections.

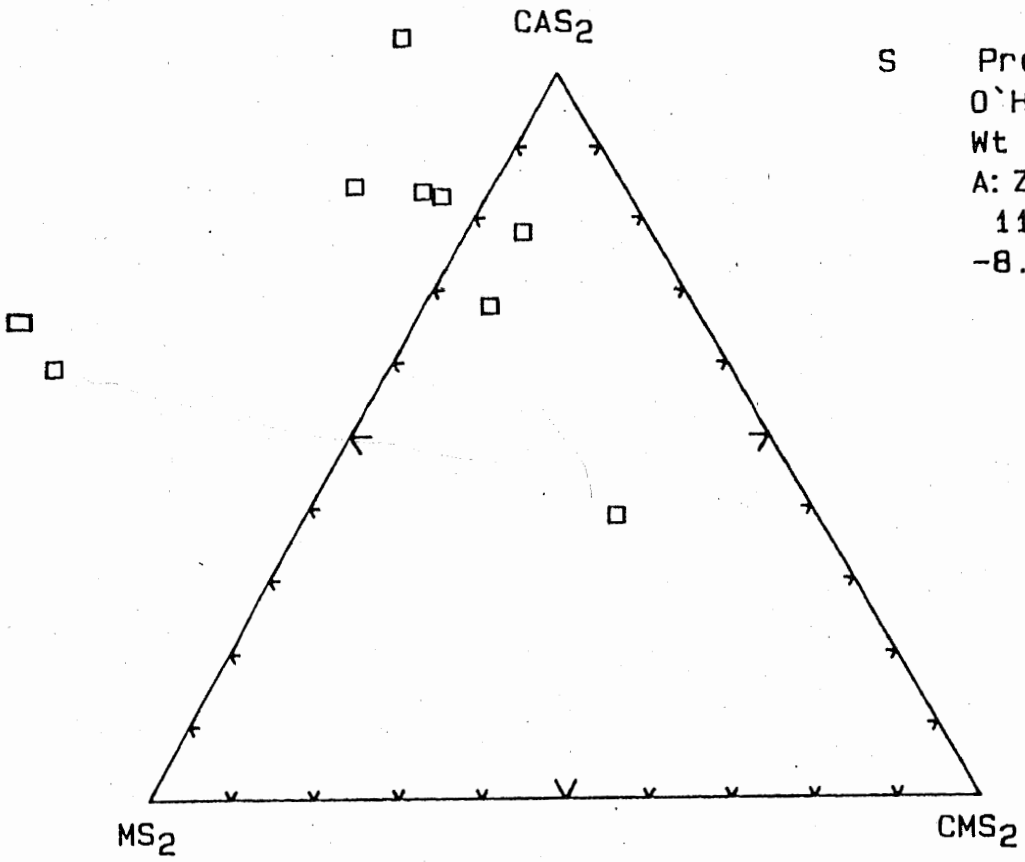

Fig.4.3h. CMAS plots of mafic/ultramafic rocks of Allai-Kohistan showing projection from S plane into CAS2-MS2-CMS2 planes of O' Hara (1976).

4.4 PETROCHEMISTRY OF GREEN SCHIST

The chemical analyses of five representative samples of the green schist are presented in the (Table 4.4A) The SiO2 of these analyses ranges from 44 to 48 %, reflecting their basic/ultrabasic nature. High TiO2(4.34 %) and Na2O(4.56 %) (Table 4.4A), is noted in these rocks. The general chemistry and their CIPW norms suggest these rocks probably, derived from igneous basic composition. The absence of corundum in the norms, the low content of SiO2 < 48%, the dominance of Na2O over K2O and the general average equal amount of MgO(9%) and CaO(9%) in these rocks also suggest that the green schist is a metamorphosed igneous basic rocks (Mason, 1966).The great abundance of chlorite and epidote in the green schist also furnish their igneous parentage (see also Miyashiro, 1973). On the classification diagram of(Cox et al.,1979) these rocks occupy the field of basalt(Fig.4.4a) The limited numbers of analyses presented in the (Table 4. 4A) are considered insufficient for drawing more petrogenetic interpretation, and more data is needed to perform further investigation.

TABLE 4.4 MAJOR ELEMENT AND C.I.P.W. NORMS DATA OF GREEN SCHIST FROM GANTAR

File name A:DZAL21.ROC

Sample	M10	M16	M34	M47	M48
Group #	8.00	9.00	10.00	11.00	12.00
Qual	1	1	1	1	1
Key	4	4	4	4	4
Ref	3	3	3	3	3
SiO_2	45.01	46.57	44.50	44.60	48.90
TiO_2	3.27	3.34	3.24	4.34	2.23
Al_2O_3	12.34	9.90	13.33	12.02	15.50
Fe_2O_3	6.01	5.02	10.55	10.36	8.18
FeO	6.00	5.01	2.73	4.40	2.94
MnO	0.25	0.38	0.29	0.22	0.24
MgO	11.00	11.50	6.25	12.00	6.25
CaO	10.85	8.00	13.44	7.85	8.20
Na_2O	4.56	2.61	4.50	3.42	4.50
K_2O	1.25	0.57	0.66	0.40	0.48
P_2O_5	0.80	0.73	0.81	0.91	0.52
H_2O+	0.40	3.39	1.31	1.31	2.50
H_2O-	0.09	0.02	0.00	0.00	0.09
Total	101.83	99.04	101.61	101.83	100.53
S.I	38.970	47.300	26.440	40.630	29.020
Q	0.000	1.270	0.000	0.000	0.000
Or	7.390	3.370	3.900	2.360	2.840
Ab	11.910	22.090	12.720	28.940	38.080
An	9.510	13.620	14.230	16.270	20.680
Ne	14.450	0.000	13.740	0.000	0.000
Di	30.890	16.630	37.910	13.200	13.380
Hy	0.000	21.600	0.000	3.030	1.630
Ol	12.090	0.000	2.330	17.450	10.050
Mt	6.920	7.020	6.870	8.470	5.410
Il	6.210	6.340	6.150	8.240	4.240
Ap	1.850	1.690	1.880	2.110	1.200
FeO#	11.41	9.53	12.23	13.72	10.30
Mg#	0.523	0.578	0.367	0.498	0.408
den	2.69	2.67	2.65	2.70	2.59

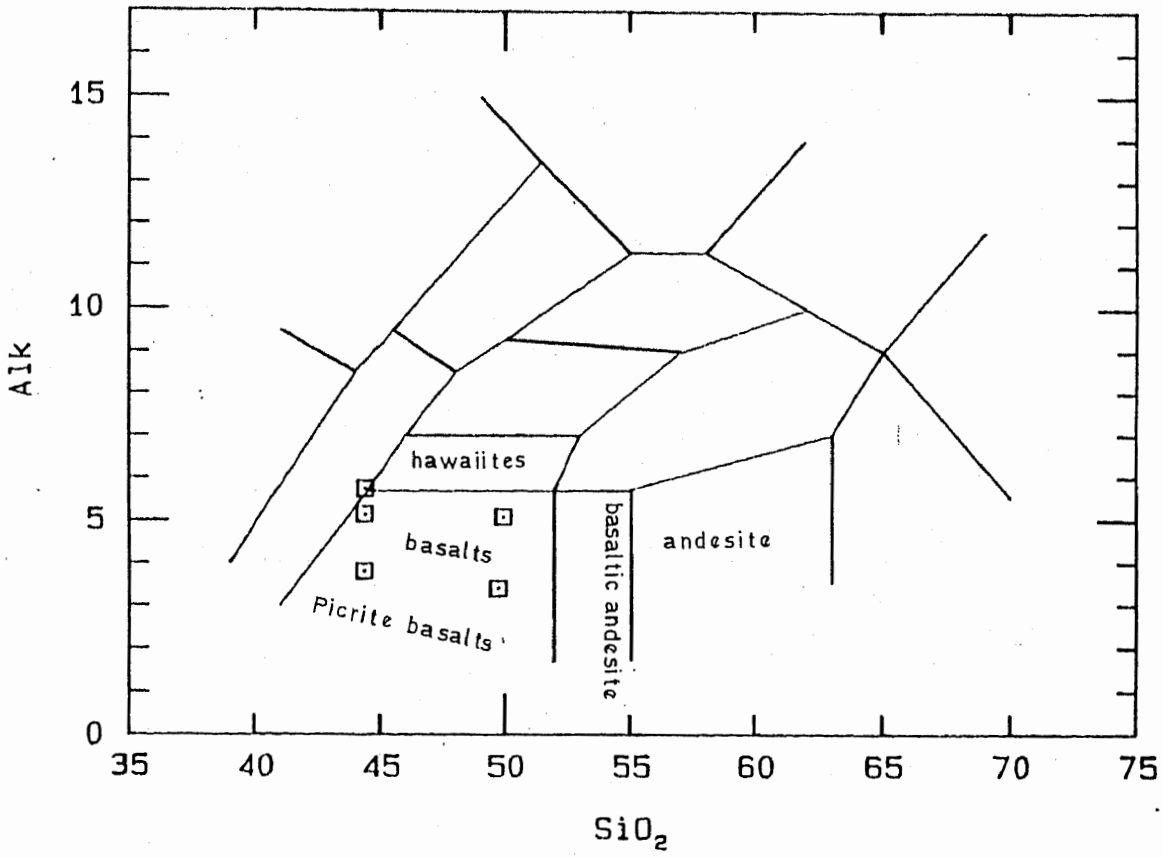

Fig.4.4a. Nomenclature of the normal volcanic rocks on the basis of SiO2 Vs Na2O + K2O diagram of the green schist of the studied area. Boundaries are after Cox et al. (1979).

CHAPTER 5 PETROGENESIS

The generally massive homogeneous, medium to course grained nature , the dominancy of hornblende and epidote assemblage, the correspondence of composition with those of the basic igneous rocks (Fig.4.1a-d), the continuous trend on oxide vs S.I. plots and CMAS plots indicating crystallization differentiation and the control of ferromagnesium minerals and plagioclase, and the non-alkaline basic characters shown on the affinity diagrams by the amphibolite (Fig4.1e-h), all indicate that the protolithic material of these particular rocks, was of basic igneous composition. The dominance of the well developed epidote and light green to deep green pleochroic hornblende and the intergrowing relationship of these minerals indicate that the amphiboles were subjected to epidote-amphibolite facies for a considerable duration. Hornblende are, however, compositionally zoned and though it was difficult to establish a close correspondence between the pleochroism color variation and composition from core towards margins, a general scheme of pleochroic colors varying from brownish green to green, greenish blue and light green to colorless margins, and of composition varying from tschermakite through tschermakitic hornblende, magnesio-hornblende, actinolitic hornblende to actinolite, all indicate a considerable wide range of pressure-temperature environment . The presence of highly altered/ cloudy plagioclase with only relics of fresh cores and the evidence of the development of well defined epidote crystals at the expense of this plagioclase, probably show that a metamor-

phism of relatively higher grade i.e. amphibolite facies, also played a role in the evolutionary history of these rocks, prior to the commencement of epidote amphibolite facies metamorphism. If this is the case, then (a) the brownish green tschermakite and the tschermakitic hornblende along with plagioclase must be representing crystallization during amphibolite grade metamorphism (b) magnesio-hornblende and actinolitic hornblende during epidote amphibolite facies. The alteration of hornblende to fibrous actinolite/ uralite and chlorite along margins, fractures and cleavages indicate further retrogression from epidote amphibolite facies into the green schist facies. These interpretations are consistent with the pressure/ temperature range obtained on the basis of Al2O3 Wt% parameter of hornblende i.e. tschermakite and tschermakitic hornblende (600°C corresponding to the upper limit of amphibolite facies, magnesio hornblende (560°C lower amphibolite facies) and actinolitic hornblende to actinolite (500°C) consistent with the upper green schist facies (see Miyashiro,1973 and Plyusnina,1982). Pressure estimates are obtained on these amphiboles manifesting 4-5 kb pressure corresponding with the absence of garnet in these rocks (Miyashiro,1973 p.259).

The oxides vs S.I. variation diagram and CMAS plots have shown that during the igneous crystallization, plagioclase and ferromagnesium minerals particularly clinopyroxene were the dominant phases on the liquidus. Also the affinity diagram show derivation from arc related magma transitional from tholeiitic to calc-alkaline character (see also Jan,1991). All these fea-

tures signify that the evolutionary history of amphibolites encompasses (a) generation of basic magma of transitional character between calc-alkaline and tholeiitic in arc related environment, (b) crystallization differentiation with dominant control of plagioclase and clinopyroxene on the liquidus and (c) the amphibolite grade metamorphism at 600°C temperature followed by retrogression to uplifting into epidote amphibolite facies at 560°C and finally to green schist facies 500°C with a maximum pressure 4-5 kb.

The presence of chlorite and epidote in the epidote amphibolite and green schist, the general correspondence of the temperature of crystallization obtained for actinolites in both of these rocks (see section 3), the transitional character between abyssal tholeiite and island arc environment shown by the epidote amphibolite (see Fig 4.1j), probably points towards some genetic relationship between these amphibolites and ophiolitic melange zone rocks of MMT. This is also supported by the occurrence of the clinopyroxene data of meta norite at Kalalota in the overlapping field of the deep sea pyroxene and island arc pyroxene (Papike, 1982), similarly the continuous compositional variation in the epidote amphibolite envision the situation where more distinct mineral species occurred together under a fixed set of physical condition (Robinson and Spear, 1982). However the general scarcity of such rocks in the MMT elsewhere is against such a view point and therefore a realistic approach of the interpretation of these rocks will be only possible, if data on trace element and isotopic abundance is obtained for these rocks.

The general correspondence of the hornblende pegmatite with

the amphibolite, on the basis of chemistry, indicate a similar origin for the two types. However, elsewhere at Mahak, (Hamidullah et al. Hussain, 1991) hornblendite and hornblende pegmatite are present, for which these workers have suggested the metasomatic development after amphibolites. The lower pressure estimates of (2 kb) for the amphiboles of hornblende pegmatite for Gantar, support this latter view.

The petrography and field relationship of the lavas from Allai Kohistan have been described by (Hamidullah et al., 1976; Shah and Majid, 1986 and Shah et al., 1991). The chemistry of these rocks shows the crystallization differentiation of plagioclase and ferromagnesium minerals like pyroxene ± olivine from a low-K-tholeiite magma. Though the epidote amphibolite from Gantar and Kalalota show transitional character between calc-alkaline and tholeiite, Shah (1986) and Shah et al. (1991) have presented a low-K tholeiitic affinities for the epidote amphibolite of the Shergarh Sar, which are more closely associated with the lavas in the field. Banded amphibolite are present in the Allai Kohistan and several model of origins have been suggested for such rocks by different workers (Shah and Majid, 1986 and Jan, 1988,1991). It is therefore, one of the several possibilities, that the banded amphibolite may be represented metamorphic equivalent of these lavas.

The mafic ultramafic rocks (data provided by S. Hamidullah) reflects character of ophiolitic cumulates and non-cumulates(Fig.) On the basis of chemical data (Table), a dominant

control of olivine/ orthopyroxene followed by clinopyroxene and plagioclase , shown by their CMAS and oxides vs S.I. plots, is typical of the gabbros and ultramafic rocks of oceanic characters.The presence of ilmenite and magnetite suggesting simultaneous crystallization with ferromagnesium minerals, reflects relatively high high oxygen fugacity during crystallization. Weather these mafic rocks generally do or do not correspond to the gabbro and norites of the Gantar and Kalalota has not been properly investigated. More field and chemical data is needed for their genetic relationship.

The occurrence of mafic - ultramafic rocks, blue schist and green schist (probably metamorphosed from basic rocks), pillow lava associated with the meta chert and lime stone , accounts for "normal sequence type" ophiolite of Miyashiro (1973). This normal sequence which is tectonically sheared, with dislocated/ thrusted contacts, and their intermingling nature also reveals multiple episodes of severe deformation along the southern megashear (MMT). Moreover, the ophiolitic assemblage of these rock suggest the remanent of tethyan oceanic crust.

As mentioned earlier (see section ( ), that the abundance of chlorite and epidote, low silica, the dominance of Na2O over K2O and the absence of corundum in the norms manifest the igneous parentage for the green schist. (see also Mason,1966 and Miyashiro, 1973).

The characteristic development of blue schist in the under lying thick slabs of ophiolite , pressure- temperature range in amphiboles and lack of compositional gap in the calcic amphiboles signify the subduction related prograde metamorphism

followed by retrogression / obduction.

CHAPTER 6 CONCLUSION

On the basis of study performed, the following major conclusions are derived :

o- The thesis area has been broadly divided into three petro-tectonic units from North to South (a) The Kohistan are sequence. (b) The Indus suture melange zone. (c) The Indo-Pakistan sub-continental plate (Salkhalas):

The following rocks units are observed in the study area:

A) Kohistan Arc Sequence:

(i) amphibolite (ii) epidote-amphibolite (iii) hornblende-pegmatite

B) Melange zone:

(i) green schist (ii) blue schist (iii) mafic-ultramafic rocks (iv) pillow lavas (v) meta-gabbro/norite

C) Salkhalas:

(i) quartz-muscovite-chlorite-carbonate schist (ii) quartz-actinolite schist (iii) calcareous schist (iv) graphitic schist (v) siliceous marble.

o- Five generations of calcic amphiboles including tschermakite, tschermakitic-hornblende, magnesio-hornblende, actinolitic-hornblende and actinolite,indicating continuous compositional variation, are observed in the epidote-amphibolites.

o- The pressure temperature estimates indicate that tschermakitic-hornblende probably have crystallized at a range from 550-600°C and actinolite at a temperature (500 -550 °C) under a PH2O 4-5Kb for calcic amphibole, while hornblende-pegmatite on the other hand indicate a low PH2O of 1-2Kb.

o- Amphibolite of the Kohistan arc are derived mainly from the tholeiitic-calc-alkaline magma through fractionation of ferro-magnesium minerals together with plagioclase, and was subjected to a metamorphism of amphibolites facies followed by retrogression into epidote amphibolite facies and green schist facies.

o- The lavas indicate close correspondence with the non-spilitic low-K-tholeiite, and reflect fractionation trend controlled by ferro-magnesium minerals and plagioclase similar to those shown by amphibolites, however these lavas indicate tholeiitic affinities rather than transitional character displayed by amphibolites.

o- The presence of chlorite and actinolite, the dominance of Na2O over K2O, the absence of corundum in the norms and low silica signify the derivation of green schist from an igneous parent.

o- The transformation of the blue schist assemblages to that of green schist assemblages in the melange zone indicate retrogression under the possible obducting environment.

o- The occurrence of mafic/ultramafic rocks, meta-gabbro/norites, blue schist, pillow lava and other basic rocks (metamorphosed to green schist) reflects ophiolitic sequence, being dislocated by tectonic deformation.

o- The cumulate nature of mafic/ultramafic rocks and the ophiolitic character shown by clinopyroxene of meta-norite indicate oceanic (tethyan) character for these rocks.

o- The over all types of metamorphism represented by various mineral assemblages in the area are (a) amphibolite facies (b) epidote-amphibolite facies (c) green schist facies and (d) blue schist facies.

o- The banded variety of amphibolite may be metamorphosed from volcanic rocks and non banded variety metamorphosed from gabbroic rocks.

Ahmad,W. and Hamidullah, S. 1987. Island Arc signatures from the Waziristan igneous complex N.W.F.P Pakistan. Geol.Bull.Univ. Peshawar. 20, 161-180.

Atkins,F.B. 1969. Pyx of the Busveld Intrusion, South Africa. J.Petro.10, 222-49 .

Besson,M. and Fonteilles,M.,1974. Relations entre les comportements contrastes delalumine et du fer dans les differentiations des series thalciitiques et calo-alkcalines. Bull. Soc.fr. Mineral. cristtall.97,445-449.

Barker,F. and Aarth,J.G.,1976. Generation of trondhjemetic-tonalitic liquids and Archean bimodal trondhjemite-basalt suites. Geology 4,pp.596-600.

Bard,J.P. (1970) composition of Hornblende, formed during the Herecynian Progressive Metamorphism of Aracena metamorphic belt SW (Spain) contr. mineral and petrol. 28, 117-134.

Bard J. p., 1983. Metamorphic evolution of an obducted island arc: example of the Kohistan sequence (Pakistan) in the Himalayan collided range. Geol. Bull. Univ. Peshawar 16, 105-184.

Binns,R.A. (1965a) The mineralogy of metamorphosed basic rocks from the Willyama complex, Broken Hill district, New South Wales. Part-I. Hornblende-Mineral. Mag.,35, 306-326 London.

Brown,G.M. 1967. Mineralogy of basaltic magma. In Hess,H.H, and Poldervaart, A.(Fds) Basalts, the Poldervaart treatise on rocks of Basaltic composition Newyonc, London, and Sydney, Interscience Publishers.

Bangash, I.H. 1991. Petrology and Geochemistry of the Southern amphibolite belt rocks from Mahak and surrounding area, Swat, Northern Pakistan. Unpublished M.Phil. thesis. pp 118.

Brown,E.H. (1977) The crossite content of Ca-amphibole as a guide to pressure of metamorphism. J.Petrol.18, 53-92 Oxford.

Baluch,W.K., Aslam, M., Begum, I., Shah, A., 1982. Geology of

Shergarh Sar Complex Allai-Kohistan, Hazara. Unpublished M.sc. Thesis. Univ. Peshawar.

Coleman,R.G. and Papike, J.J., (1968) Alkali Amphiboles from the Blue-schist of Cazadero, California Jour. Petrol.9, 105-122.

Cooper,A.F., (1972) Progressive metamorphism of metabasic rocks from the Haast schist group of Southern New Zealand. J. Petrology.,13, 457-92 .

Coward, M. P., Jan, M. Q., Rex, D. Tarney, J., Thirlwall, M., and Windley, B. F., 1982. Geotectonic framework of the Himalayas of N. Pakistan: J. Geol. soc. London 139, 299-308.

Coward,M.P.,Windley,B.F.,Broughton,R.D.,Luff,I.W.,Petterson,M.G.,Pudsey C.J.,Rex,D.C.
& Asif Khan,M.,1986. Collision Tectonics in the NW Himalayas.Geol. Soc., Sp.Pub.no.19,pp.203-219.
London,

Cox, K.G., 1962. A green beryl (emerald) near Mingora, swat state. Geol. Bull. Punjab Univ. 2, 51-52.

Cox, K.G., Bell, J.D., and Pankhurst, R. J. 1979. The Interpretation of Igneous Rocks. William Clowes Limited. London. pp 450.

Coleman, R.G. 1977. Ophiolites. Springer-Verlag Berlin. Heidelberg. Germany. pp 229.

Corwin, C., Fpdpr.F.V. and Roisenberg, A. 1986.
Silicate-phase composition in the Serra Geral (Parana) Continental flood basalts province, Southern Brozil, Nelles Jahrbuch mins. Abh 154,1,57-73.

Deer,W.A., Howie,F.A. and Zussman,J. (1966) An introduction to the rock-forming minerals Longman. Hong Kong (168-169).

Desio, A. and Shams, F.A.,1980. The age of the blueschists and the Indus Kohistan suture line, northwest Pakistan. Acad. Naz. Dei Lincei 8, 74-79.

Davidson and Mathison, C.I., 1974. Aluminous orthopyroxenes and associated cordirites, garnets and biotites from granulites of the Quairaching District, Western Australia. N.J 6. Miner. Mh.,6, 272-87.

Evans, B. W. & Trommsdorff, V. 1972. Der Einfluss des Elsens and

die Hydratistierung von Duniten. Schweiz. Min. Pet. Mitt. 52,251-256.

Engel,A.E.J. and Engel,C.G. (1962). Hornblende formed during progressive metamorphism of amphibolites NorthWest Adorondack Mountains, Geol.s.e, Am.73, 1499-1514 NewYork.

Ernst,W.G. (1972) Ca-Amphibole Paragenesis in the Shirataki District, Central Shikoku, Japan. Geo.soc of America Memair135, 73-94.

Ernst,W.G. (1979) Coexisting sodic and calcic amphiboles from high pressure metamorphic belt and the Stability of barroisitic amphibole. Min. Mag. 43,269-78 .

Gansser,A.,1980. The significance of of the Himalayan suture zone. Tect. Phys.,vol.62,no.1/2,pp.13-35.

Giret,A.,Bonin,B. and Leger,J.M. (1986) Amphibole compositional trends in oversaturated alkaline plutonic ring-complexes. Canadian Mineral. 18,481-495.

Grapes,R.H., Seijihashimoto and Sumiomiyasashita (1977) Amphiboles of a metagabbro-Amphibolite sequence, Hidaka Metamorphic Belt, Hokkaido J. of Petrol. 18,paot 2, 285-318.

Hamidullah,S. and Bowes,D.R. (1987) petrogensis of the Appinites suite Appin District, Western Scotland. Acta Universitaties Carolinae Geologica 4, 295-396.

Hamidullah S. (1983) petrogenetic studies of the appinite suite Ph.D. dissertation, Glasgow University, 397p.

✓ Hamidullah,S., Haq, I., Jehanzeb, and Khan, F., 1977. Mineralogy and petrology of the Shergarh Sar complex, Allai- Kohistan, Hazara. Unpublished M.sc. Thesis. Univ. Peshawar.

✓ Hamidullah, S. Hussain, J, & Reuber, I. 1992- Petrochemistry of the amphibolite belt rocks of the Mohmand and its surrounding. Geol. Bull. Univ. Pesh. Vol 23, (in press)

Himmelberg,G.,R., and Ford A.B. (1976) pyroxene of the Dufek Intrusion Antarctica: Jaurnal of petrol.17 part.2, 219-243.

Howie,R.A., 1965. The pyroxenes of metamorphic rocks. In controls of metamorphism, W.S. Pitcher and G.W. Flinn, ed) Oliver and Boyd, Edinburgs. 319-26

Irvine, T. N. and Baragar, W.R.A., 1971. A guide to the classification of the common volcanic rocks. Can J. Earth Sci. 8, 523-49.

Jan, M. Q.and Kempe, 1973. The petrology of the basic and intermediate rocks of Upper Swat, Pakistan. Geol. Mag., vol.110, pp. 285-300.

Jan, M. Q.,1979. Petrology of the obducted mafic and ultramafic metamorphites from the southern part of the Kohistan island arc sequence. Geol. Bull. Univ. Peshawar 13, 95-107.

Jan, M.Q. and Tahirkheli, R.A.K.,1979. A preliminary geological map of Kohistan and the adjoining areas, northern Pakistan.Geol. Bull. Univ. Peshawar (Special issue), vol.11.

Jan, M.Q., & Howie, R.A., 1980. Ortho- and clinopyroxenes from pyroxene granulites of Swat Kohistan, N. Pakistan. Min. Mag.,vol. 43, pp. 715-726.

Jan, M.Q., Khan, M.J. 1988. Relative abundances of Minor and Trace Elements in Mafic Phases from the Southern Part of the Kohistan Arc.Geol. Bull. Univ. Peshawar 21, 15-25.

Jan, M.Q., 1988. Geochemistry of amphibolites from the southern part of Kohistan arc, N. Pakistan. Min. Mag. vol.52, pp. 147-159.

Jan, M.Q., 1985. High-P Rocks along the Suture Zone around Indo-Pakistan Plate and Pjase Chemistry of Blueschist from Eastern Ladakh. Geol. Bull. Univ. peshawar 18, 1-40.

Jan, M.Q., Khattak, M.U.K., Parvez, M.K., and Windley, B.F., 1984. The Chilas stratiform complex: Field and mineralogical aspects. Geol. Bull. Univ. Peshawar 17, 153-169.

Jan, M.Q., 1990. Petrology and geochemistry of southern amphibolites of the Kohistan arc, N. Pakistan. In: Geology and Geodynamics Evolution of the Himalayan collision zone (K. K. Sharma, ed.). Phys. Chem. Earth, vol. 17, pp.71-92.

Kushiro,H., (1955), Ion substitution in ;the diopside-ferropigeorite series of CPx: Am.Mineralogist, 40,70-93.

Kamineni,D.C. (1986). A petrochemical study of calcic-amphibloe from the East Bull lake anothosite-gabbro layered complex, Dis-

trict of Algoma, Ontano. Contrib Mineral petro 93,471-481.

Kazmi, A.H. 1984. Petrology of the Bobai volcanics, NE Baluchistan. Geol. Bull. Univ. Peshawar. 17, 43-51.

Kazmi, A.H., Lawrence, R.D., Dawood, H., Snee, L. W. and Hussain,S.S.,1984. Geology of the Indus suture zone in the Mingora- Shangla area of Swat, N.Pakistan.Geol. Bull. Univ. Peshawar,vol.17,pp.127-144.

Kostyuk E.A. amd Sobolev, V.S. (1969) paragenetic types of calciferous amphiboles of metamorphic rocks Lithos 2, 67-82.

Laird,J. and Albee, A.L. (1981b) pressure, temperature, and time indicators in mafic schist:Their application to reconstructing the polymetamorphic history of Vermont. Amer. J.sci 281,127-175.

Leak, B.e. (1965) the relationship between possible octahedral aluminum and maximum possible octahedral aluminum in natural calciferous and subcalciferous amphiboles Am. Mineralogist 50,834-851.

Leake B.E. (1978): Nomenclature of amphiboles. Canadian Mineral. 16,501-520.

Leake,B.E. (1971) on aluminous and edenitic hornblendes Mineral Mag., 38, 389-407.

Lebas,M.J.(1962). The role ;;of Aluminum in igneous CPx with relation their percentage. Amer Jr.sce.260-267-288.

Leterrier,J., Maury,RC., Thonon,P., Girard,D,and Marchal,M. (1982). Identification of the magmatic affinities of paleo-volcanic series. Earth plan Sci letters 59, 139-154.

Lovering ,J.F. (1070) Green schist amphibolites from Haast River, New Zealand, Contr. Miner, petrol.27, 11-24.

Majid,M., and shah, M.T. 1985. Mineralogy of the Blueschist Facies metagraywacke from the Shergarh Sar Area, Allai-Kohistan, N.Pakistan. Geol. Bull. Univ. Peshawar. 18, 41-52.

Mason, B. 1958. Principles of Geochemistry. John Wiley & Sons, Inc. U.S.A. pp 329.

Mischm, P., and Rice,J.M. (1975). Miscibility of Tremolite and Hornblende in progressive Skagi Metamorphic suite. North Cascades, Washington. Journal of petrology,. 16, part-1 (1-21)

Miyashiro A. (1973). Metamorphism and metamorphic belts. Unwin Brothers, Surrey. (254-255).

Miyashiro, A., (1958). Regional metamorphism of the Gosaisyo-Takanuki in the Central Abukuma Plateau. J.Fac. Sci. Univ. Tokyo, Sect.11,11, 219-72 .

Miyashiro, A., 1974. volcanic rock series in Island arc and active continental margin. Amer. J. sci. 174. 321-355.

Miyashiro, A.,1975. Classification, characteristics and origin of ophiolites. Jour. Geol.vol.83,pp.249-281.

Miyashiro, A., 1977. Subduction zone ophiolites and Island arc ophiolites. S. k. saxena and Bhattachargi, S. (ed.) "Enetgetics of geological processes" Springer-Verlag (N.Y.).

Morimoto,N., Fabries,J., Ferguson,A.K., Ginzburg, I.V., Ross,M., Siefert,F.A., Zussman,J.,Aoki, K. and gottarioi, G. (1988). Nomenclature of pyroxene, American minerologist, 73.1123-1133.

Nisbet, E.G., and Pearce,J.A. (1977). CPx composition in mefic lavas from different tectonic settings. Contrib. Mineral Petrol 63, 149-160.

O' Hara, M.J. 1976. Data reduction and projection schemes for complex composition . Experimental petrology, 103-126. N.E.R.C. publication series D,6; Manchester.

Papike J.J. (1982). Pyroxene, Reviews in mineralogy. Mineralogical soe. of America 7, 495-525.

Papike,J.J., Cameron,K.L. and Baldwin,K. (1974). Amphiboles and Pyroxene>: characterization of other than quadrilateral components and Estimetes of Ferric iron from Microprobic data. Geol. soc. Amer. Abstr. Programs 6, 1053-1054-(?).

Perchuk,L.L. (1966) Temperature dependence of the coefficient of distribution of Calcium between co-existing amphibole and plagioclase: doklady Akad. Nauk SSSR, 169, 1436-1438.

Plyusnaina,L.P. (1982) Geothermometry and Geobarometry of Plagioclase-Hornblende bearing assemblages. Contrib. Mineral Petrol 80: 140-146

Poldevaart, A. and Hess, H.H. 1951. Pyroxene in the crystallization of basaltic magmas. Jour. Geol. 59, 472-489.

Raase P. (1974) Aland Ti contents of hornblende, indicators of pressure and temperature of metamorphism-contrib. Mineral. Petro., 45,231-236.

Robinson,P. and Spear, F.,S. (1982) Amphiboles: petrology and experimental phase relations. Minerological S.C. of America 9B,43-45.

Rex, A.J., Tirrul, R., Rex, D.C., Barnicoat, A., Windley, B.F. (1989) Metamorphic, magmatic, and tectonic evolution of the central Karakoram in the Biafo-Baltoro-Hushe regions of Northern Pakistan. GSA, Special paper 232. pp 47-73.

Robinsom, P., Schumacher,J., C. and Spear, F.,S. (1982) Amphiboles: petrology and experimental phase relations mineralogical S.C. of America 9B, 6-9.

Rodolico,F., 1931, Notesualcuni minerali dill, Albamia Sctten-trionale: Periodico Mineralogia,2, 5-12.

Searle, M.P., Rex, A.J., Tirrul,R.,Rex, D.C., Barnicoat,A. and Windley,B.F.,1989. Metamorphic, magmatic and tectonic evolution of the central Karakoram in the Biafo-Baltoro-Hushe regions of northern Pakistan. Geol. Soc. Amer. (Special paper 232).

Shido, F., (1958) plutonic and metamorphic rocks of the Nakoso Iritono districts in the Central Abukuma plateau. J.Fac.sci. Univ. Tokyo, Sect. 11,12, 85-102.

Schwarzer,R.R. & Rogers,J. J. W., 1974. Aworld wide comparison of alkali olivine basalts and their differentiation trends. earth planet. Sci. letters 23, 186-296.

Spear,F.S. (1980) Nasi ca Al exchange equilibrium between plagioclase and amphibole contrib mineral. petrol. 72,33-41.

Speer, J.A., Becker, S.W., and Farrar, S.S. (1980). Field relations and petrology of the post metamorphic, coarse-grained granitoids ;and associated rocks of ;the southern Appalachian Piedmont. In wories, D.R. ed., Proceedings: The caledonides in the U.S.A., Virginia Polytechnic Institute and state University. Memoir No. 2, 137-148.

Tarney,J.,1977. Petrology, mineralogy and geochemistry of the Falk Land Plateau basement rocks. Initial rep. Deep sea Drill. Proj.36,pp.893-921.

Thomson, M.L., Fleet,M.E. and Barnett,R.L. (1981) Amphiboles from the Fenzy Lake Ultramafic Complex, Southern Cenebec. Canadian Mineralogist 19, 469-477.

Tahirkhali,R. A. K., 1979. Geology of Kohistan and adjoining Eurasian and Indo-pakistan continents, Pakistan. Geol. Bull. Univ. Peshawar 11, 1-30.

Shah, M.T. 1986.Petrochemistry of the rocks from Shergarh Sar area Allai-Kohistan, Northern Pakistan. M.Phil. unpublished thesis. pp 218.

Velde.B., 1967. Phentite micas: synthesis, stability and natural occurance. Amer. Jour. Sci. 886-913.

Wilson, A.F. 1971. Some geochemical aspects of the Sapphirine-bearing Pyroxenites and related highly metamorphosed rocks from the Archaeam Ultramafic belt of south Quairading, Westren Australia. Geological Society of Australia. pp 401-411.

Winkler, H.G.F. 1974. Petrogenesis of Metamorphic Rocks.Springer-Verlag New York. pp 334.

Wood,R.M., (1980) Compositional zoning in sodic amphiboles from the blueschist facies. Mineralogical magazine, 43, 741-52 .x

Wilson A.F. 1960. Co-existing pyroxene: Some causes of variation and anamolies in the optically derived compositional tie-lines with the particular reference to charnockitic rocks. Geol.Mag.,97, 1-17.

Yousafzai, I. J., Bangash, M.A., Shah, A.A., and Ahmad, B., 1976. Petrography of the ultramafic and related rocks of Pashto and

Barai area, North-East of Shergarh Sar, Allai- Kohistan, hazara. Unpublished M.sc. Thesis. Univ. Peshawar.

Yoder, H.S., 1969. Calc-alkalic andesites. Experimental data bearing on the origin of their assumed characteristics. In "proceedings of the Andesite Conference", A.R. McBirney (ed.), Oregon Dept. Geol. Mineral. Ind. Bull. 65, 77-84.